ABSTRACT

Title of Thesis:	HARMONIZATION OF LIFE CYCLE CLIMATE PERFORMANCE AND ITS IMPROVEMENT FOR HEAT PUMP APPLICATIONS
	Sarah Troch, Masters of Science, 2016
Thesis Directed By:	Research Professor Yunho Hwang, Ph.D. Department of Mechanical Engineering

ABSTRACT

Life Cycle Climate Performance (LCCP) is an evaluation method by which heating, ventilation, air conditioning and refrigeration systems can be evaluated for their global warming impact over the course of their complete life cycle. LCCP is more inclusive than previous metrics such as Total Equivalent Warming Impact. It is calculated as the sum of direct and indirect emissions generated over the lifetime of the system "from cradle to grave". Direct emissions include all effects from the release of refrigerants into the atmosphere during the lifetime of the system. This includes annual leakage and losses during the disposal of the unit. The indirect emissions include emissions from the energy consumption during manufacturing process, lifetime operation, and disposal of the system. This thesis proposes a standardized approach to the use of LCCP and traceable data sources for all aspects of the calculation. An equation is proposed that unifies the efforts of previous researchers. Data sources are recommended for average values for all LCCP inputs. A

residential heat pump sample problem is presented illustrating the methodology. The heat pump is evaluated at five U.S. locations in different climate zones. An excel tool was developed for residential heat pumps using the proposed method. The primary factor in the LCCP calculation is the energy consumption of the system. The effects of advanced vapor compression cycles are then investigated for heat pump applications. Advanced cycle options attempt to reduce the energy consumption in various ways. There are three categories of advanced cycle options: subcooling cycles, expansion loss recovery cycles and multi-stage cycles. The cycles selected for research are the suction line heat exchanger cycle, the expander cycle, the ejector cycle, and the vapor injection cycle. The cycles are modeled using Engineering Equation Solver and the results are applied to the LCCP methodology. The expander cycle, ejector cycle and vapor injection cycle are effective in reducing LCCP of a residential heat pump by 5.6%, 8.2% and 10.5%, respectively in Phoenix, AZ. The advanced cycles are evaluated with the use of low GWP refrigerants and are capable of reducing the LCCP of a residential heat by 13.7%, 16.3% and 18.6% using a refrigerant with a GWP of 10. To meet the U.S. Department of Energy's goal of reducing residential energy use by 40% by 2025 with a proportional reduction in all other categories of residential energy consumption, a reduction in the energy consumption of a residential heat pump of 34.8% with a refrigerant GWP of 10 for Phoenix, AZ is necessary. A combination of advanced cycle, control options and low GWP refrigerants are necessary to meet this goal.

HARMINIZATION OF LIFE CYCLE CLIMATE PERFORMANCE AND ITS IMPROVEMENT FOR HEAT PUMP APPLICATIONS

By

Sarah Virginia Troch

Thesis submitted to the Faculty of the Graduate School of the
University of Maryland, College Park, in partial fulfillment
of the requirements for the degree of
Master of Science
2016

Advisory Committee:
Professor Yunho Hwang, Chair
Professor Jelena Srebric
Associate Professor Bao Yang

Acknowledgements

I would like to thank the Center for Environmental Energy Engineering for giving me the opportunity to conduct this research. I would also like to thank my advisor Dr. Yunho Hwang and Dr. Hoseong Lee for the invaluable assistance and encouragement during my research. Finally I would like to thank my family for their support.

Table of Contents

List of Tables

List of Figures

Nomenclature

Abbreviations:

LCCP	Life Cycle Climate Performance
TEAP	Technology and Economic Assessment Panel
UNEP	United Nations Environment Program
IIR	International Institute of Refrigeration
IPCC	Intergovernmental Panel on Climate Change
EIA	United States Energy Information Administration
AHRTI	Air-Conditioning, Heating, and Refrigeration Technology Institute
AHRI	Air-Conditioning, Heating, and Refrigeration Institute
AR4	IPCC Fourth Assessment Synthesis Report
AR5	IPCC Fifth Assessment Synthesis Report
AREP	Alternative Refrigerants Evaluation Program
ASHRAE	American Society for Heating, Refrigeration and Air Conditioning Engineers
ISO	International Organization for Standardization
ORNL	Oak Ridge National Laboratory
VCC	Vapor Compression Cycle
GWP	Global Warming Impact

TEWI	Total Equivalent Warming Impact
HVAC&R	Heating, Ventilation, Air Conditioning and Refrigeration
HP	Heat Pump
MAC	Mobile Air Conditioning
VI-FT	Flash Tank Vapor Injection
VI-IHX	Internal Heat Exchanger Vapor Injection
SLHX	Suction Line Heat Exchanger
EEV	Electronic Expansion Valve
TXV	Thermal Expansion Valve
MFR	Mass Flow Rate

Parameters/Variables:

C	Refrigerant Charge (kg)
L	Average Lifetime of Equipment (yr)
ALR	Annual Leakage Rate (% of Refrigerant Charge)
EOL	End of Life Refrigerant Leakage (% of Refrigerant Charge)
GWP	Global Warming Potential (kg CO_{2e}/kg)
Adp. GWP	GWP of Atmospheric Degradation Product of the Refrigerant (kg CO_{2e}/kg)
AEC	Annual Energy Consumption (kWh)

EM	CO_2 Produced/kWh (kg CO_{2e}/kWh)
m	Mass of Unit (kg)
MM	CO_{2e} produced/Material (kg CO_{2e}/kg)
mr	Mass of Recycled Material (kg CO_{2e}/kg)
RM	Ratio of CO_{2e} Produced and Recycled Material (kg CO_{2e}/kg)
RFM	Refrigerant Manufacturing Emissions (kg CO_{2e}/kg)
RFD	Refrigerant Disposal Emissions (kg CO_{2e}/kg)
h	Enthalpy (kJ/kg)
u	Velocity (m/s)
v	Specific Volume (m^3/kg)
W	Work (kW)
X	Quality (-)
P	Pressure (kPa)
$\dot{m}$	Mass Flow Rate (kg/s)
$\dot{V}$	Volumetric Flow Rate (m3/s)
Q	Capacity (kW)
T	Temperature (°C)
TA	Approach Temperature (K)

Greek Symbols:

η	Efficiency
ε	Effectiveness

Subscripts:

1,2,3…	State Points
ref	Refrigerant
air	Air
amb	Ambient Conditions
Room	Room Conditions
co/cond	Condenser
ev/evap	Evaporator
high	High Pressure Condition
low	Low Pressure Condition
sub	Subcooling
sup	Superheating
ideal	Ideal Conditions
m	Ejector Motive Nozzle
s	Ejector Suction Nozzle
dis	Ejector Diffuser
mix	Ejector Mixing Section

Chapter 1 : Introduction

This thesis explores the development of a harmonized Life Cycle Climate Performance (LCCP) metric and its applications to advanced vapor compression cycle options. The development process to create a guideline for the International Institute of Refrigeration is discussed. An Excel based tool was developed for residential heat pumps. Different advanced cycle options for vapor compression cycles were evaluated and applied to LCCP.

1.1 Climate Change

Climate change is an increasingly important global concern with far reaching effects. The heating, ventilation, air conditioning and refrigeration (HVAC&R) industry is spending a large amount of effort in reducing the environmental impacts of HVAC&R systems. Electricity usage constitutes the largest factor in LCCP comparisons. According to the United States Energy Information Administration (EIA), the world residential energy use will increase by 1.5% per year from 1,500 GWh in 2010 to 2,400 GWh in 2040, while the commercial energy use will increase by 1.8% per year [1]. This increase reflects the growing use of electricity worldwide. On average, households in developed countries use 53% of their energy consumption for space heating and cooling [1]. The overall usage of electricity has increased with the number of appliances and the increased prevalence of HVAC systems in all buildings. A careful accounting of the related emissions is vital in slowing the current and future emissions of greenhouse gases.

Discussions about the climate impact is often limited to the GWP of the

fluids used; but this is far too restrictive, as it does not take into account the real emissions of fluids, and ignores indirect emissions, especially the ones related to energy use over the life time of the equipment. Focusing solely on GWP can lead to irrational and counterproductive decisions. This is why it is so important to use more comprehensive indicators of the real Green House Gases emissions of systems over their life time.

1.2 Life Cycle Climate Performance

Life Cycle Climate Performance is an evaluation method by which HVAC&R systems can be evaluated for the global warming impact over the course of their complete life cycle. It is calculated as the sum of direct and indirect emissions generated over the lifetime of the system "from cradle to grave". Direct emissions include all effects from the release of refrigerant into the atmosphere during the lifetime of the system. This includes annual leakage and losses during the disposal of the unit. The indirect emissions include emissions from the manufacturing process, energy consumption and disposal of the system [2-11].

LCCP was first proposed by the Technology and Economic Assessment Panel (TEAP) of the United Nations Environmental Program (UNEP) [10] in 1999 to calculate the "cradle to grave" climate impacts of the direct and indirect greenhouse gas emissions. This methodology was then applied by the government and industry researchers in several facets such as evaluating potential refrigerants to replace HCFCs [5].

1.3 Current Metrics

The Total Equivalent Warming Impact (TEWI) is a known metric that measures the global warming impact of a HVAC&R system by quantifying the amount of greenhouses gases it emits during its usage phase, from commissioning to end of life. It takes into account the direct and indirect emissions over this period. The direct emissions result from the leaks, and the fluid that is not recovered at the end of life ("EOL"). The indirect emissions result from the energy use over the same period.

LCCP is a more comprehensive evaluation than TEWI. TEWI does not account for the energy embodied in the product materials, greenhouse gas emissions from chemical manufacturing and end-of-life disposal of the unit [5-10]. LCCP can also account for minor emission sources that are not accounted for in TEWI such as transportation leakage, manufacturing leakage, and refrigerant manufacturing emissions [3-10].

LCCP is a more comprehensive accounting tool than TEWI. TEWI does not consider the energy embodied in product materials, greenhouse gas emissions during chemical manufacturing, and end of life disposal of the unit. The small sources of emissions generated over the course of the lifetime of the unit are explicitly accounted for in LCCP. This allows for a more holistic picture of the environmental impact of the unit.

As more accurate methods of measuring greenhouse gas emissions are developed, it becomes more important to measure the minor emissions sources from the units. More environmentally friendly methods of electricity production are

becoming a larger percentage of the total production. As the emissions from energy consumption decrease, other factors in LCCP will become more influential.

LCCP method should be used when a more in depth analysis of the environmental impact of a unit is warranted. TEWI could be used when a quicker analysis of the unit is desired. A visual comparison of TEWI and LCCP is shown in Figure 1.

As of today, TEWI is the benchmark for the evaluation of total emissions. It offers a great improvement compared to assessments based solely on GWP. It has a well standardized calculation method. It is described, for instance, in the European standard EN-378 Refrigerating systems and heat pumps — Safety and environmental requirements [12]. The output of the calculation is the number of tons of equivalent CO_2 emitted by the system over its life time. It is also straightforward when evaluated "specific TEWI". That is the average kilograms of CO_2 emitted per kWh of cooling energy generated by the system (or of heating for a heat pump). The use of the specific TEWI allows for easy comparisons of various technologies used for similar applications.

Barriers to the use of LCCP include the difficulties in assessing some key input parameters such as the leakage rates, EOL fluid recovery, or the carbon foot print of the energy used. Therefore, some do not want to use it, claiming that it is too complicated to be practical. TEWI is also criticized because it is not comprehensive enough. It only covers the usage phase of the system, ignoring other phases of the cycle like manufacturing, transportation, or disposal. The developed guideline aims to

reduce the difficulty of finding key input parameters by provided current average values and reliable data sources for all parameters.

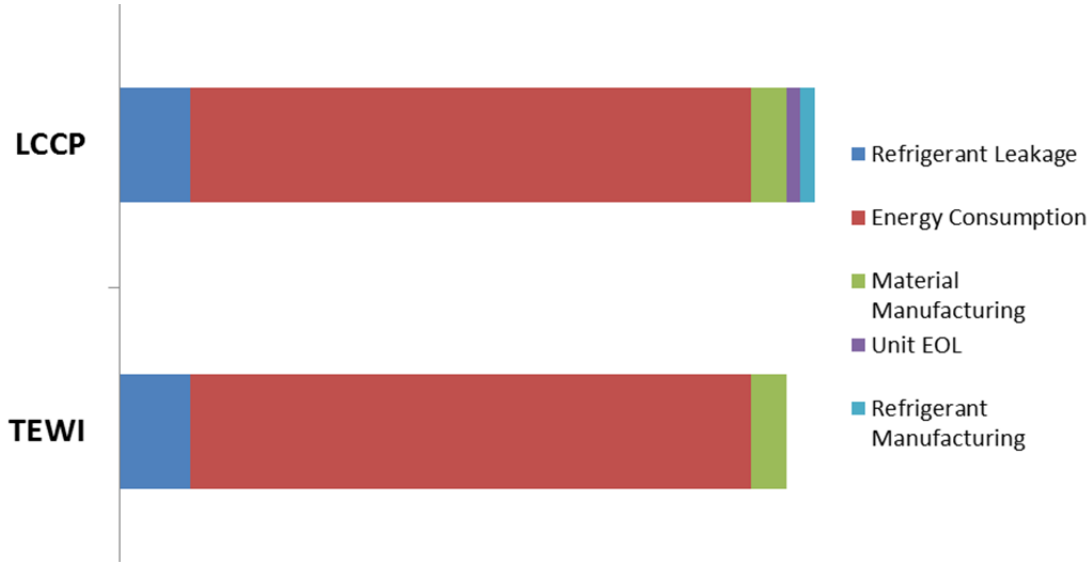

Figure 1: LCCP versus TEWI

1.4 Advanced Cycle Options

The basic vapor compression cycle is comprised of four components: compressor, evaporator, thermal expansion device and a condenser. This cycle has inherent thermodynamic losses when it is compared to the ideal reverse Carnot cycle. These losses are associated with single phase gas compression and isenthalpic compression needing finite temperature difference in heat exchangers [13]. Advanced cycle options attempt to reduce these losses in various ways. There are three categories of advanced cycle options: subcooling cycles, expansion loss cycles and multistage cycles. Subcooling cycles include suction line heat exchangers, thermoelectric subcoolers, and mechanical subcooling. Expansion loss recovery cycles include expander and ejector cycles. Multi-stage cycles include vapor or liquid injection cycles, two-phase refrigerant injection cycle and the saturation cycle. This

analysis focuses on the suction line heat exchanger cycle, the expander cycle, the ejector cycle and the vapor injection cycle [14].

Subcooling cycles increase the amount of subcooling the refrigerant is subjected to prior to entering the expansion valve. This type of system is commonly used to increase efficiency. This cycle ensures that subcooled liquid refrigerant is supplied to the expansion device inlet and superheated vapor refrigerant is supplied to the compressor inlet.

Expansion loss recovery cycles use different devices such as an ejector or a expander to recover work performed by the expansion device and transfer it back to the compressor or to produce power. The expander does this by recovering mechanical work or converting it into to electricity that can be used to power the compressor. The ejector lifts evaporated vapor at the lowest operating pressure of the cycle back into the compressor reducing the pressure ratio the compressor must reach.

Multi-stage cycles work to decrease the performance degradation that occurs when the temperature difference between the evaporation and condensation increases under the condition of either very low or very high ambient temperature [14].

Chapter 2 : Motivation and Research Objectives

2.1 Motivation

The importance of controlling and reducing greenhouse gas emissions has only increased since the dangerous effects were first formally recognized in the Kyoto Protocol [11]. This protocol placed restrictions on greenhouse gas emissions which included high global warming potential (GWP) refrigerants. This encouraged the development of alternative refrigerants that continues today with research into low GWP refrigerants and natural refrigerants.

LCCP is one method that has been developed to quantify the amount of emissions released during the unit's life time. Of those emissions, electricity usage constitutes the largest factor in LCCP comparisons. The United States Energy Information Administration (EIA) projects that the world residential energy use will increase by 1.5% per year 1,500 GWh in 2010 to 2,400 GWh in 2040 and commercial energy use will increase by 1.8% per year [1, 15]. This increase reflects the larger penetration of electricity around the globe. On average, households in developed countries use 53% of their energy consumption for space heating and cooling [15]. The overall usage of electricity has increased with the number of appliances and the increased prevalence of HVAC&R systems in all homes globally. A careful accounting of these emissions is vital in slowing the emissions of greenhouse gases today and into the future.

2.2 Research Objectives

The first research objective was to develop a guideline for the use and application of LCCP for the International Institute of Refrigeration (IIR). This guideline includes a unified method of application for LCCP and traceable data sources for all aspects of the equation. An equation was developed that combined the elements of previous researchers. Traceable data sources for each LCCP input were identified and included into the developed guideline. An Excel based tool was developed for residential heat pumps.

The second research objective was to evaluate the impacts of advanced vapor compression cycle options on LCCP. The cycles evaluated include the suction line heat exchanger, the expander cycle, the ejector cycle and the vapor injection cycle. The performance of each cycle was evaluated using the AHRI 210/240 Std. test conditions.

Chapter 3 : Literature Review

3.1 Life Cycle Climate Performance

LCCP was first proposed by the Technology and Economic Assessment Panel (TEAP) of the United Nations Environmental Program (UNEP) [10] in 1999 to calculate the "cradle to grave" climate impacts of the direct and indirect greenhouse gas emissions. The ADL reports in 1999 and 2002 [3] were the first to use this method to evaluate the performance of specific HFCs compared to other working fluid in various technologies. Spatz [6] studied the performance and LCCP of three replacement refrigerants for R-22. The direct effects of refrigerant leakage and end-of-life loss, and indirect effects of power consumption were included. This study demonstrated that the indirect effects dominate the calculation.

There are several LCCP and TEWI tools in existence. GREEN-MAC-LCCP was the first comprehensive excel based tool to use the LCCP methodology to evaluated mobile air conditioning (MAC) units [7,8]. This model is globally used by the automobile industry and publically available through the United States Environmental Protection Agency (U.S. EPA). It has become the standard evaluation tool in the MAC industry.

The Air Conditioning, Heating and Refrigeration Technology Institute (AHRTI) sponsored a project to develop an Excel based tool for residential heat pump applications [4, 9]. The tool included both detailed and simplified calculations for residential heat pumps. The model included direct and indirect impacts of refrigerant emissions, indirect impacts of energy consumption, energy to manufacture

and dispose of the system and refrigerants. The annual energy consumption calculation uses performance data as defined by AHRI Standard 210/240 [16]. Beshr et al. [17-18] developed a web based open source LCCP tool for all air conditioning and refrigeration applications. Both a web tool and desktop application with expanded capabilities were created. The tool includes 14 refrigerants and 47 cities built in with the option to add additional refrigerants and locations. The tool is designed to be easily modified to user preferences. The tool can be used with any system simulation software, load calculation tool, and weather and emissions data types. It is designed to evaluate existing units rather than for the designing of new units.

IPU Pack Calculation Pro is a commercially available tool which uses the TEWI and Life Cycle Cost (LCC) methodologies to evaluate refrigeration systems and heat pumps for various locations around the world. The current version of the tool is version 4.11 [19].

Hwang et al. [20] performed a comparison of R-290 and two HFC blends for walk-in refrigeration systems using LCCP. The LCCP of R-410A is lower than that of R-290 as long as the annual emission is kept below 10%. It was concluded that R-410A has less or equivalent environmental impact as compared to R-290 when safety (toxicity and flammability), environmental impact (climate change), cost and performance (capacity and COP) are considered [20]. Chen also used the LCCP methodology to compare the use of R-410A and R-22 in residential air conditioners [21]. Chen determined that R-410A showed significant improvements over R-22 and would significantly reduce the indirect emissions of the unit.

Beshr et al. performed a comparative study on the environmental impact of supermarket refrigeration using low GWP refrigerants [22]. The ORNL LCCP tool was used for this research. The study compared four different supermarket refrigeration systems in different climates with in the U.S. The parametric analysis showed that by using low GWP refrigerants the effect of the annual leak rate on the total system emissions decreases. The sensitivity analysis also showed that by using low GWP refrigerants, or more charge conservative systems, the effect of the hourly emission rate for electricity production on the total system emissions increases [22].

Li performed a LCCP assessment of a packaged air source heat pump for residential applications [23]. It was determined that the seasonal energy efficiency ratio (SEER) rating for the heat pump had the largest impact on the calculation. When the COP is improved by 5%, 10% and 15% as compared with the baseline 14 SEER R-410A, the corresponding LCCP is decreased by 4%, 8%, and 12%, respectively. To achieve the efficient $CO_{2\text{-eq.}}$ emission reductions, more attention should be paid for energy efficiency improvements [23].

3.2 Advanced Vapor Compression Cycle Options

Vapor compression cycle (VCC) is the basic cycle that is used in most air conditioning and refrigeration options. Many modifications have been developed to improve the performance of this cycle. Advanced VCC are categorized into three main groups: subcooling cycles, expansion loss recovery cycles, and multi-stage cycles. One cycle was evaluated in each category. For the subcooling cycles, the suction line heat exchanger cycle was evaluated. For the expansion loss cycles, the expander cycle and the ejector cycle was evaluated and for the multi-stage cycle, the

vapor injection cycle was evaluated. Each modified cycles offer different benefits and disadvantages with regards to cycle performance. The choice of cycle is dependent on the application of the specific system.

3.2.1 Suction Line Heat Exchangers

One method to improve cycle performance is to increase the amount of subcooling the refrigerant is subjected to prior to entering the expansion valve. Suction line heat exchangers (SLHX) or internal heat exchanger (IHX) as they are also called are a common method to achieve this. This type of system is commonly used to enhance the efficiency of the cycle. SLHXs are located between the condenser outlet and the expansion device inlet and between the evaporator outlet and the compressor inlet. Cold refrigerant from the suction line is used to cool the refrigerant at the condenser outlet [14]. Figure 2 shows a basic SLHX cycle from Park et al., 2015.

According to ASHRAE handbook [24] SLHXs are useful for improving system performance, subcooling liquid refrigerant to prevent the formation of flash gas at the expansion valve inlets, and evaporating any remaining liquid in the suction line before entering the compressor. The addition of a SLHX typically increases the heating capacity of the system. However, the increased temperature of the refrigerant entering the compressor adversely affects the compressor efficiency, which degrades the entire system performance [14].

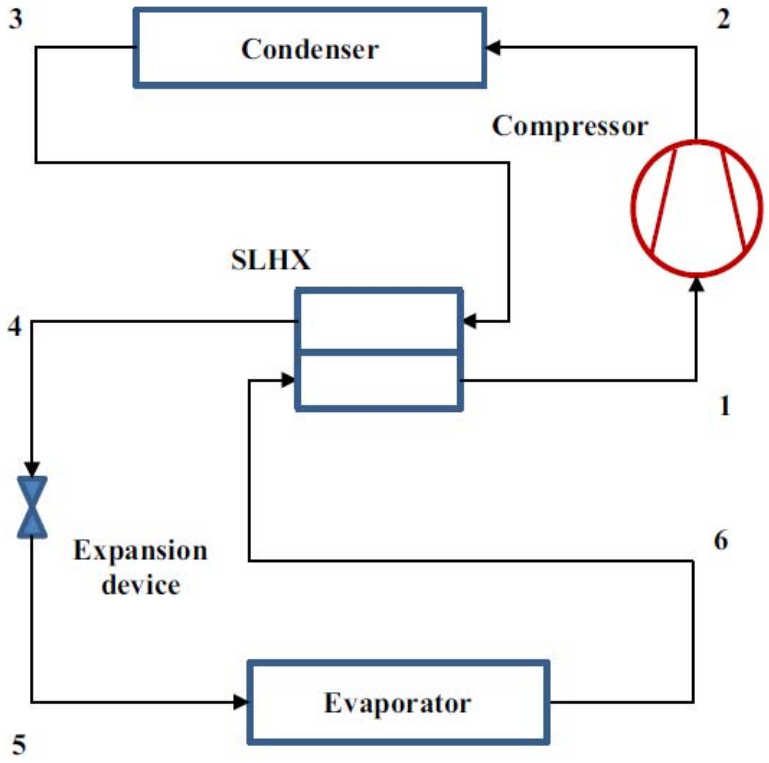

Figure 2: Basic SLHX Cycle [14]

Fluids with low specific heat do not benefit from the installation of a SLHX and performed better using the basic VCC. Fluids with higher specific heat had a lower COP in the basic VCC but their performance improved with the use of SLHX [25].

Hermes et al. [26] evaluated the refrigerant charge reduction in vapor compression refrigeration cycles with the use of liquid-to-suction heat exchangers. The condensing pressure was held fixed at 40°C, whereas the evaporating pressure was kept at -25°C (LBP applications) and also at 7°C (HBP applications). Charge reductions up to ~15% were observed for refrigerants R-134a, R-290, and R-600a in LBP conditions, whereas charge reductions by 5% were found for HBP applications. The system COP increased 6% for R-134a, 5% for R-290, 9% for R-600a, and

decreased -1% for R-22 and -6% for R-717. This study verified previous studies which determined that the potential benefits of SLHX are largely dependent on the properties of the fluids being used [26].

Fernandez et al. [27] performed a comparison of a CO_2 HPWH with a baseline cycle and two high COP cycles. The overall COP was maximized at higher ambient temperatures and at lower hot water temperatures. The overall COP was 30% higher for heating a full tank of cold water than reheating a warm tank water after standby losses. Performance enhancement of the two-stage cycle with internal heat exchanger was found only for standby loss reheating at low ambient temperatures and was 7.5%, while that of the SLHX cycle was up to 7.9% for initial tank water heating and around 3.4% for reheating a warm tank water [27].

Preissner [28] conducted a study on CO_2 VCC using scroll expanders and SLHX. Experimental tests were conducted on a CO2 system and an R-134a system. The COP improvement an outdoor temperature of at 45ºC was about 15 and 9 %, for CO2 and R134a respectively. Even though the performance of the CO2 cycle improved more than the R134a cycle, the CO2 system still falls short in performance by 8 to 23 % for the range of typical operating conditions [28].

Alabdulkarem et al. [25] performed testing, simulation and soft-optimization of a R-410A low-GWP alternatives in a HP system. A SLHX was used to match the capacity of R-410A. D2Y60 was the only refrigerant that showed significant improvement of performance. All other refrigerants tested negatively affected the performance of the cycle [25].

3.2.2 Expander Cycle

Another method of improving the performance of the VCC is to recover expansion losses. One common method is the use of an expander as the expansion device instead of the typical electronic expansion valve (EEV) or thermostatic expansion valve (TXV). The expander generates an isentropic process during the expansion of the refrigerant. This device can be seen as a compressor operating in reverse [14]. Figure 3 shows a conventional expander cycle.

The expander improves the VCC in two ways. The cooling capacity is increased through the isentropic expansion process and by utilizing the recovered expansion losses to assist the compressor which reduces energy consumptions. First law estimations show potential improvements of the COP in the order of 40% to 70% and 5%-15% increase in capacity [14].

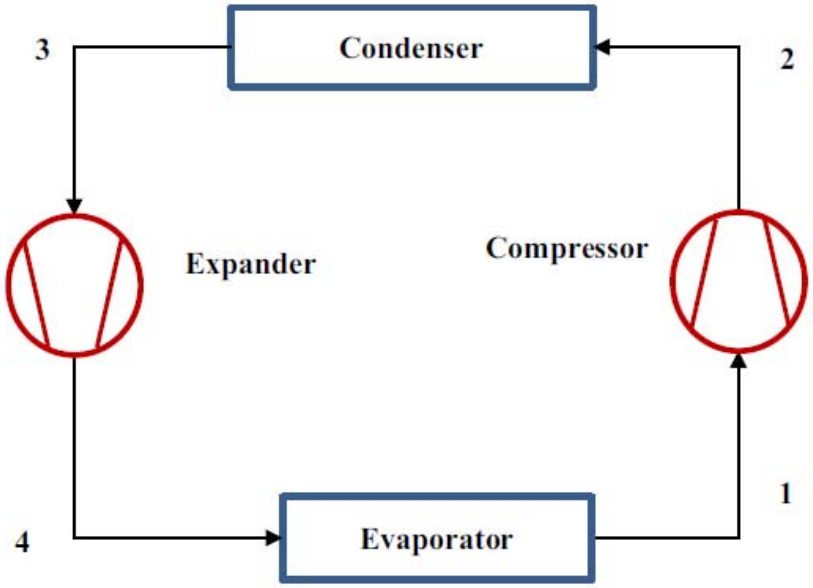

Figure 3: Expander Cycle [14]

The most dramatic savings were demonstrated by She et al. [29]. The performance of a conventional VCC, a mechanical subcooling system and a conventional expander cycle were compared to a modified expander cycle. The cycle showed 67%, 19.27% and 17.3% improvement of COP, respectively [29].

Moles et al. [30] conducted a theoretically performance evaluation of different single stage VCC configurations using R-1234yf and R-1234ze(E). The COP was increased between 9-20% over the basic VCC depending on the refrigerant being tested. The most efficient configuration was determined to be the use of an expander or an ejector as expansion device [30].

Yang et al. [31] performed an investigation of a transcritical CO_2 two-stage compression cycle with an expander. The proposed cycle was compared to a transcritical low pressure cycle, a single stage cycle and an optimal intermediate

pressure cycle with COP improvements of 11.32%, 9.65%, and 0.72%, respectively [31].

Preissner [28] modeled both a CO_2 cycle and an R-410A cycle with scroll compressor. The expander cycle was modeled with 100% efficiency. The cycle yielded the largest system improvements of 40 to 65 % for an outdoor temperature of 25 to 45ºC. The improvement for CO2 is two to three times as large as for R-134a.

3.2.3 Ejector Cycle

Another cycle that recovers expansion losses is the ejector cycle. When an ejector is used as an expansion device it operates as an energy converter that transforms expansion losses into kinetic energy and then back to an increased pressure which reduces the amount of work the compressor is required to perform. The ejector is mainly composed of a nozzle, mixing chamber and a diffuser. It is designed to mix the high pressure fluid from the condenser with the low pressure fluid from the evaporator. The fluid from the condenser flows through the ejector and out through the nozzle creating low pressure but high velocity at the nozzle outlet. This low pressure draws in the fluid from the evaporator to be mixed together in the mixing chamber. The combined fluid exits the diffuser, recovers pressure in some degree, and is sent back to the compressor. The separator protects the compressor by ensuring the only superheated vapor goes into the suction side of the compressor. A typical system configuration and P-h diagram is shown in Figure 4.

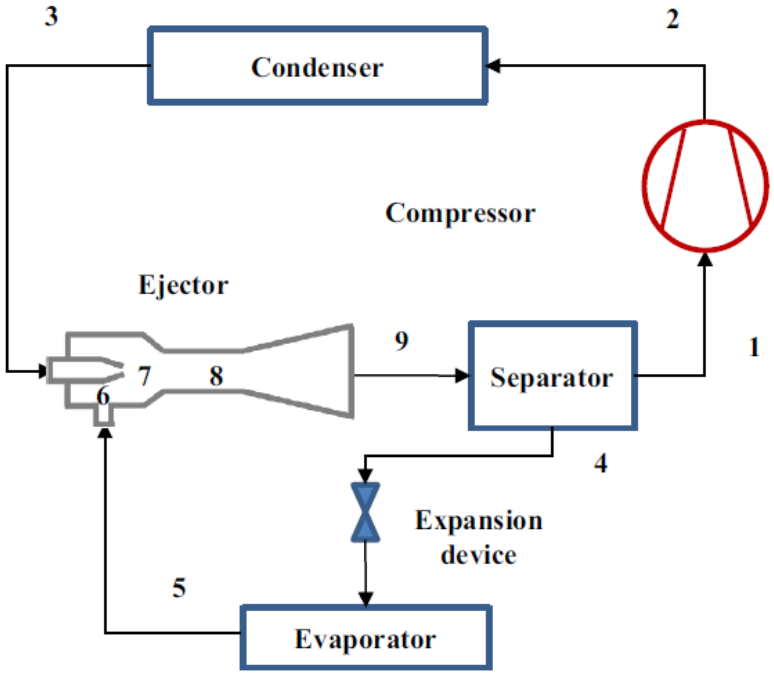

Figure 4: Typical Two-Phase Ejector Cycle Configuration [14]

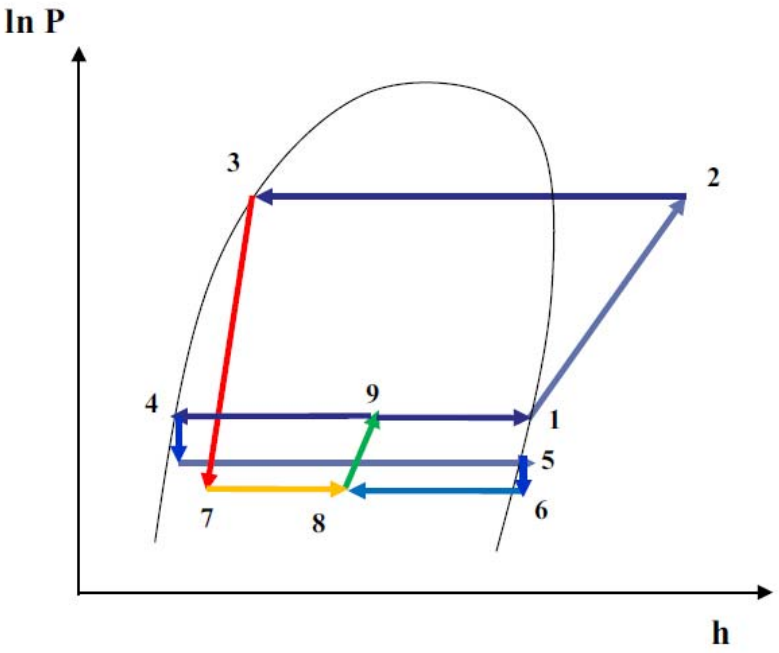

Figure 5: Two-Phase Ejector Cycle in P-h Diagram [14]

Naduvath [32] performed theoretically and experimental studies of single and two-phase ejectors for use in vapor compression refrigeration systems. Multiple ejector geometries and flow rates were evaluated. Energy savings as high as 21% were theoretically estimated using the single phase ejector while 29% savings were estimated using the two-phase ejector [32].

Wang et al. [33] performed comparative studies of ejector-expansion vapor compression refrigeration cycles for applications in domestic refrigeration-freezers by developing simulations and experimentally. Using a modified ejector cycle with a suction line heat exchanger, the COP and volumetric refrigeration capacity were improved by about 9.22% and 18.43%, respectively [33]. The simulation results show that various ejector cycles and modified ejector cycle outperform basic VCC in COP and volumetric refrigeration capacity by approximately 7.98%, 11.58%, 4.68%, 7.18%, 14.07% and 16.01%, 22.20%, 9.23%, 13.38%, 28.46% on average.

Li et al. [34] conducted a theoretical study on the ejector refrigeration cycle using R-1234yf as working fluid. The COP and VCC improvements of R-1234yf ejector cycle range from 8.47% to 23.29% and from 6.02% to 26.45%, respectively, as compared to the basic VCC.

3.2.4 Vapor Injection Cycle

The vapor injection cycle is one type of multi-stage advanced cycle. This type of cycle works to decrease the performance degradation that occurs when the temperature difference between the evaporation and condensation increases under the condition of either very low or very high ambient temperature [14]. There are two common types of vapor injection cycles: the vapor injection cycle with an internal

heat exchanger (VI-IHX) and a vapor injection cycle with a flash tank (VI-FT). Refrigerant in its vapor form is injected directly into the compressor. The source of this vapor differentiates the two types of cycles. The VI-IHX cycle uses an additional heat exchanger and expansion valve after the condenser to generate the vapor to be injected back into the compressor. The VI-FT cycle uses a flash tank to separate the different phases of refrigerant. The vapor is drawn off and injected into the compressor. The liquid flows through the expansion valve and into the evaporator. Cycle drawings are shown for both types of cycles in Figure 6 and Figure 8 from Wang et al. [35].

The benefits of the vapor injection cycle include [36]:

- Capacity improvements in severe climates
- System capacity can be varied by controlling the injected refrigerant mass flow rate resulting in energy savings
- The compressor discharge temperature is lower than a conventional cycle improving the working envelope of the compressor.

Flash tank cycles typically perform better than the internal heat exchanger cycles [36]. The superheat of the injected vapor of the VI-FT cycle is typically lower than that of the VI-IHX cycle. This results in a more efficient compression process which reduces the energy consumption of the system [36]. However, VI-IHX cycles have a much wider operating range.

Wang X. et al. [35] performed an experimental study of an 11 kW R-410A heat pump system with a two-stage vapor-injected scroll compressor. The vapor-injected scroll compressor was tested with the cycle options of both flash tank and

internal heat exchanger configurations. A cooling capacity gain of around 14% with 4% COP improvement at the ambient temperature of 46.1 °C and about 30% heating capacity improvement with 20% COP gain at the ambient temperature of -17.8 °C were found for the vapor-injected R-410A heat pump system as compared to the conventional system which has the same compressor displacement volume [35].

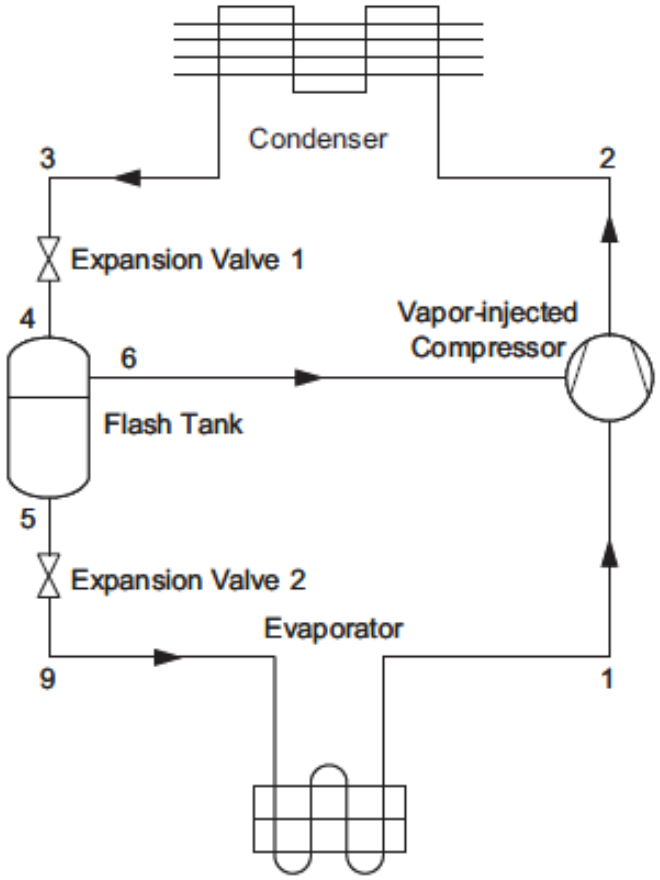

Figure 6: VI-FT Cycle Configuration [35]

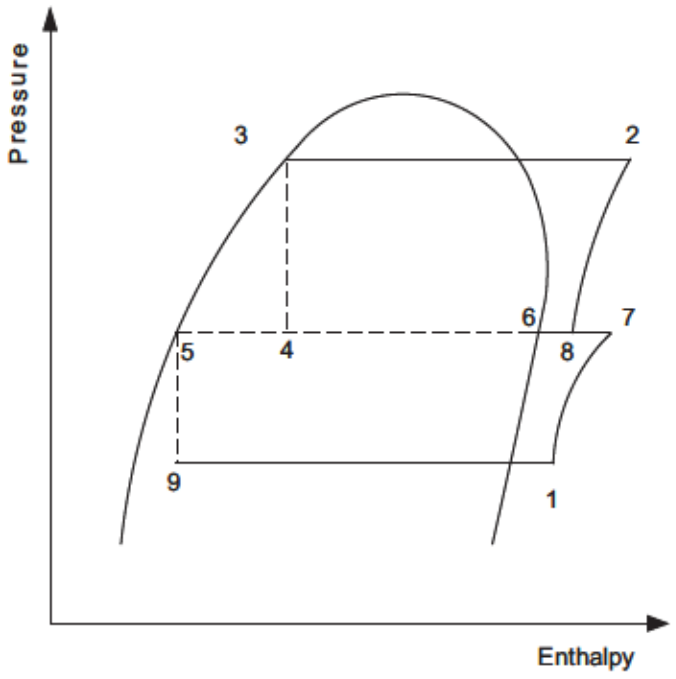

Figure 7: VI-FT Cycle in P-h Diagram [35]

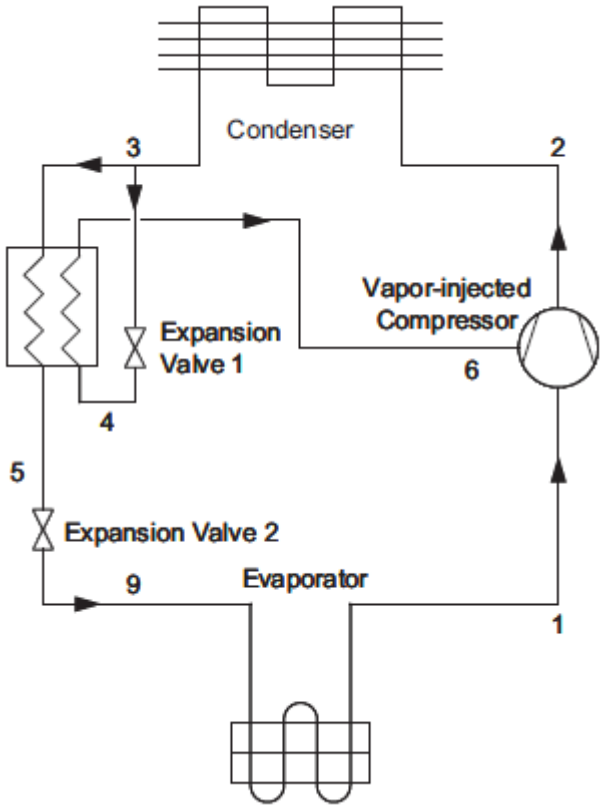

Figure 8: Vapor Injection Internal Heat Exchanger Cycle [35]

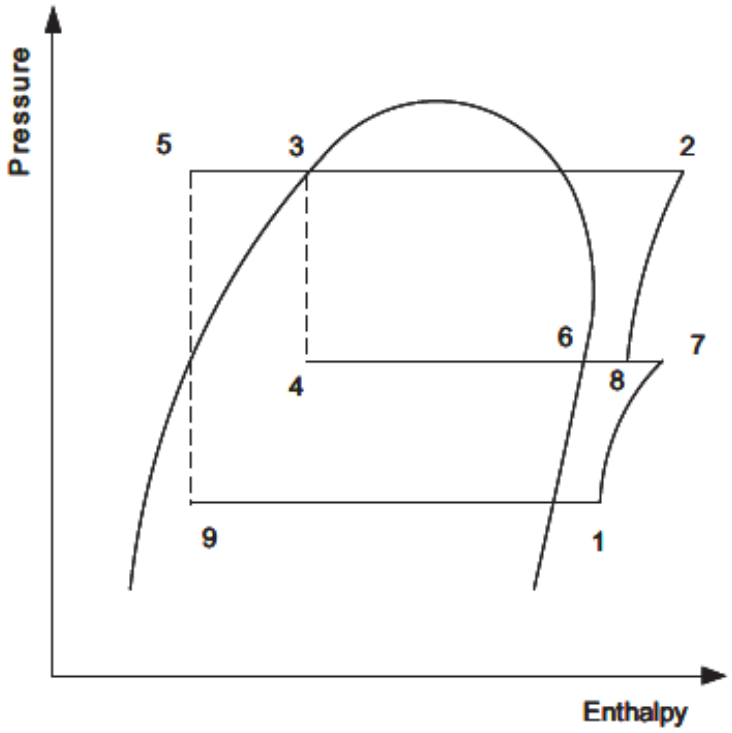

Figure 9: VI-IHX Cycle in P-h Diagram [35]

The use of vapor injection can dramatically improve the performance of the VCC. Most research surveyed showed increases in both COP and in heating capacity of the unit. The amount of the increased depended on the exact system design and the refrigerant used. Redon et al. [37] demonstrated that vapor injection can improve the COP by 30% over a single stage system in a subcritical two-stage vapor injection heat pump system. However, he also demonstrated that poor design choices could decrease COP by 10% [37]. Shuxue et al. [38] performed an experimental study of an enhanced vapor injection heat pump system using R-32. They demonstrated a 3% increase in COP and a 9% increase in heating capacity. Xu et al. [39] evaluated the performance of a vapor injection heat pump with R-410A and R-32. The HP's COP increased by 9% and the heating capacity increased by 10% when using R-32 compared to the cycle using R-410A. He et al. [40] performed an experimental study

evaluating the performance of a vapor injection high temperature heat pump. This study showed no significant increase in COP but a 7.7-22.6% increase in heating capacity. Baek et al. [41] evaluated the performance of a CO_2 HP at low ambient temperatures with vapor injection. The heating capacity and the COP increased 12.1% and 12.7% respectively when a subcooler vapor injection system was used as compared to a VI-FT cycle.

Chapter 4 : Development of Guideline for Life Cycle Climate Performance

The International Institute of Refrigeration (IIR) created a working group focusing on the Life Cycle Climate Performance methodology in 2012. The primary goal of the working group was to develop a guideline on the use of LCCP and to develop tools to assist in this process. The guideline provides a roadmap on how LCCP can be applied to different applications and provides traceable references for all components of LCCP calculation. This chapter discusses the process used to create the IIR guideline and the sources used.

4.1 LCCP Equation Development

The LCCP equation was developed from multiple prior LCCP studies. The common elements were combined and clarified. The LCCP equation is split into two main parts, direct and indirect emissions. The equations from previous research are shown in Table 1 and Table 2, respectively. The resulting equation is shown in Eqn. 1. Each component accounts for a different type of emissions released over the lifetime of the unit. The emission terms are in the units of kg CO_2e/kg.

Table 1: Direct Emissions Equations

Source	Direct Emissions Equation
GREEN-MAC-LCCP [7]	Direct Emissions = GWP (direct from MACs leaks) + GWP (direct from additional sources: (atmospheric reaction products of refrigerant)
AHRI LCCP [4]	Direct emission = (Ref. GWP + Adp. GWP) x (annual leakage x years of life time + refrigerant loss at EOL)
ORNL LCCP [17]	$Em_{direct} = Em_{ref,leak} + Em_{acc} + Em_{serv} + Em_{ref,EOL} + Em_{ref,prod} + Em_{reaction}$ $Em_{ref,leak}$ = charge*system lifetime*annual leakage rate*GWP Em_{acc} = charge*system lifetime*annual accident leak rate*GWP Em_{serv} = total number of services*charge*servicing leak rate*GWP $Em_{ref,EOL}$ = % of refrigerant lost at end of life*charge*GWP $Em_{ref,prod}$=ref. production and transportaion leak rate*charge*GWP

Table 2: Indirect Emissions Equations

Source	Indirect Emissions Equation
GREEN-MAC-LCCP [7]	Indirect Emissions = (manufacturing, transport & service leakage) + (EOL refrigerant emissions) + GWP (indirect from MAC operation) + GWP (indirect from additional sources: (chemical production of refrigerant & transport) + (MACs manufacturing & its vehicle assembly) + (EOL recycling processes)
AHRI LCCP [4]	Indirect Emissions = (Σ equivalent CO_2 kg/kWh x annual operating energy kWh) x years of life time + Σ (equivalent CO_2 kg/kg material x mass of materials kg) + Σ (equivalent CO_2 kg/kg material x mass of recycled materials kg)
ORNL LCCP [17]	$Em_{indirect} = Em_{sys,man} + Em_{ref,man} + Em_{sys,EOL} + Em_{elec} + Em_{ref,disp} + Em_{sys,trans}$ $Em_{sys,man}$ = mass of each material*CO_{2e} emissions of material production $Em_{ref,man}$ = charge*(1+system lifetime*annual leak rate - % of reused refrigerant)*CO_{2e} emissions for virgin refrigerant $Em_{sys,EOL}$ = energy of recycling of metals*mass of metals*CO_{2e} of metals + energy of recycling of plastics*mass of plastics*CO_{2e} of plastics Em_{elec} = system lifetime*$\sum_0^{8760} hourly\ energy\ consumed$*emission rate for electriciy production $Em_{ref,disp}$ = mass of material*energy of recycled material $Em_{sys,trans}$ = energy of transporting the unit

The common elements of each of the sources were combined to develop Equation 1.

$$LCCP = Direct\ Emissions + Indirect\ Emissions$$

$$Direct\ Emissions = C * (L*ALR + EOL)*(GWP + Adp.\ GWP) \quad (1)$$

$$Indirect\ Emissions = L * AEC * EM + \sum(m * MM) + \sum(mr * RM) + C * (1 + L * ALR) * RFM + C * (1-EOL) * RFD$$

Where C is the refrigerant charge (kg), L is the average lifetime of equipment (yr), ALR is the annual leakage rate (% of Refrigerant Charge), EOL is the end of life refrigerant leakage (% of Refrigerant Charge), GWP is the global warming potential (kg CO_2e/kg), Adp. GWP is the GWP of atmospheric degradation product of the refrigerant (kg CO_2e/kg), AEC is the annual energy consumption (kWh), EM is the CO_2 produced/kWh (kg CO_2e/kWh), m is the mass of unit (kg), MM is the CO_{2e} produced/material (kg CO_2e/kg), mr is the mass of recycled material (kg), RM is the CO_{2e} produced/recycled material (kg CO_2e/kg), RFM is the refrigerant manufacturing emissions (kg CO_2e/kg) and RFD is the refrigerant disposal emissions (kg CO_2e/kg).

The common elements in the direct emissions included the annual leakage of refrigerant from the systems. Atmospheric degradation products were accounted for in GREEN-MAC-LCCP [7] and AHRI research [4]. Additional small leaks are accounted for explicitly in the ORNL's tool [17] and GREEN-MAC-LCCP [7] and implicitly in the annual leakage rate by the AHRI tool [4]. In the equation developed for the IIR guideline, the annual leakage rate and atmospheric degradation products were explicitly accounted for. The minor leakages from transportation and service were assumed to be accounted for in the annual leakage rate to create a more concise

formula. The annual refrigerant leakage and the end of life leakage are accounted for in the (L*ALR + EOL) term. These terms are multiplied by the GWP of the refrigerant and the charge. The adaptive GWP term accounts for additional degradation products from the refrigerant that is not included in the GWP term. This should be included if the amount is known.

For the indirect emissions equation, all of the researchers included the emissions for the energy consumed by the unit, the manufacturing emissions from the materials and the refrigerants as well as the end of life disposal of the unit and the refrigerant. The indirect emissions equation developed for the IIR guideline accounts for all other emissions during the units lifetime. The L*AEC*EM term accounts for the emissions generated by the electricity consumption of the unit. This term is calculated using an annual load model, local weather data and local electricity production emissions rates. The $\sum$ (m*MM) term account for the emission generated by the manufacture of the material used in the unit. The unit's weight is multiplied by the percentage of composition of that material and then by the emissions rate to calculate to total manufacturing emissions. The average values for material manufacturing are located in the IIR guideline [42]. If the amount of recycled material used in the initial manufacturing process is know this is factored into the manufacturing emissions. The $\sum$(mr*RM) term accounts for the emissions generated when the material in the unit is recycled at the end of the unit's operational life. The C(1 + L*ALR)*RFM term accounts for the emissions generated when the refrigerant is manufactured. This includes the refrigerant needed to recharge the unit. The equation assumes that the unit is recharged annually. Average manufacturing values

for common refrigerants are included in the guideline. If the refrigerant is not there, the manufacturer's emissions data may be used or the weighted average of the refrigerant compositions may be calculated from the given values. The C*(1-EOL)*RFD terms account for emissions generated from the recovery of the refrigerant.

4.2 Direct Emissions

Direct emissions are comprised of the effects of refrigerant released into the atmosphere over the course of the lifetime of the unit. This includes:

- Annual refrigerant loss from gradual leaks
- Losses at end of life disposal of the unit
- Large losses during operation of the unit
- Atmospheric reaction products from the breakdown of the refrigerant in the atmosphere

These four categories are calculated using the rate of refrigerant leakage multiplied by the charge of the system and the global warming potential (GWP) of the refrigerant. The resulting equation is shown in Equation 2.

$$Direct\ Emissions = C * (L*ALR + EOL)*(GWP + Adp.\ GWP) \quad (2)$$

Where C is the refrigerant charge (kg), L is the average lifetime of equipment (yr), ALR is the annual leakage rate (% of Refrigerant Charge), EOL is the end of life refrigerant leakage (% of Refrigerant Charge), GWP is the global warming potential

(kg CO_2e/kg), and Adp. GWP is the GWP of atmospheric degradation product of the refrigerant (kg CO_2e/kg).

4.2.1 Global Warming Potential

Global Warming Potential (GWP) of a refrigerant is defined as an index used to compare the relative radiative forcing of different gases without directly calculating the changes in atmospheric concentrations. GWPs are calculated as the ratio of the radiative forcing that would result from the emission of one kilogram of a greenhouse gas to that from the emission of one kilogram of carbon dioxide over a fixed period of time [43].

The GWP values obtained from the United Nations Intergovernmental Panel on Climate Change's (IPCC) Fifth Assessment: Climate Change (AR5) are used for this assessment [44]. These values are calculated using a 100 year timeline for policy and consistency purposes. This timeline accounts for the majority of all effects caused by refrigerants. There are arguments for the use of a longer timeline; however, none of the previous research or studies used the longer timeline. The IPCC and most governments worldwide use the 100 year timeline. The AR5 values are the most commonly used values in research and in public policy internationally. The use of these values enables the researcher to compare them more easily to other research done around the world.

The types of refrigerants in use are constantly increasing as research into mixtures and alternate refrigerants expands the boundaries of known applications. The IPCC Assessments are not always able to include all of the refrigerants available.

Many are developed and come into use between the publishing of the most recent update. If the refrigerant is not included AR5, the manufacturer's GWP values may be used. To calculate refrigerant mixtures a weighted average of the component refrigerants should be used. Table 3 shows several common refrigerant GWP and Adp. GWP values. The refrigerant values that were not listed in AR4 [45] and AR5 [44] were obtained from the AHRTI report (Zhang, et al. 2011) [4]. These values were based on information from the manufacturer's and from publically available information.

Table 3: GWP Values

Refrigerant	**GWP[3, 23] (kg CO_2e/kg)**	**Adp. GWP (kg CO_2e/kg)**
CO_2	1	0
HFC-32	677	-
HFC-1234yf	<1	3.3 [46]
HFC-134a	1,300	1.6 [46]
R-290	3	-
HFC-404A	3,943	-
HFC-410A	1,924	-

4.2.2 Unit Lifespans

Average unit lifetimes are taken from AR4, AR5 reports and United Nation Environmental Protectorate (UNEP) Technical Options Committee 2002 report [44, 45, 47]. Units have become more reliable over the past decades and continue to improve. The values given are the averages for developed countries and include those units already in service. As older units are replaced, the average unit lifetimes will

increase. These values are displayed in Table 4 for various types of units.

Table 4: System Information

System Type	ALR (%)	EOL (%)	L (years)
Residential Packaged Units [3, 47]	2.5	15	15
Residential Split Units[3, 47]	4	15	15
Packaged Refrigeration[3, 47]	2	15	15
Supermarket - Direct System[3, 9, 47]	18	10	7-10
Supermarket - Indirect System[3, 9, 47]	12	10	7-10
Commercial Refrigeration – Stand-alone[44, 45, 47]	5	15	15
Commercial - Packaged Units [45,45,47]	5	15	10
Commercial - Split Units [44,45,47]	5	15	10
Chillers [44, 45, 47]	5	15	15
Marine [44, 45, 47]	20	15	15

4.2.3 Unit Annual Refrigerant Leakage Rates

Annual leakage rates are the sum of the gradual leakage of a system over the course of a year. These averages also include catastrophic leaks spread out over the lifetime of the unit. This term does not include refrigerant lost when the unit is disposed of. These rates vary widely for different types of systems, equipment design, workmanship when the unit was installed and various other factors.

The annual leakage rates chosen are a compilation of units currently in service. Annual leakage rates (ALR) shown in Table 4 are average values from developed countries in AR4, AR5, and UNEP Technical Options Committee 2002 report [44, 45, 47]. Rates have dropped considerably over the last decade and

continue to decrease. As further research and regulations are published these values will be updated.

4.2.4 Unit End-of-Life Leakage Rates

The end-of-life leakage rates include the amount of refrigerant that is lost when the unit is disposed of. The rates shown in Table 4 are averages for developed countries from AR4, AR5 and UNEP Technical Options Committee 2002 report [44, 45, 47]. These rates reflect regulations passed in developed countries to limit the amount of refrigerants that are released into the atmosphere. For example the U.S. limits the amount of refrigerant released from an appliance to 15% for units with a charge of 22.7 kg [48].

4.3 Indirect Emissions

Indirect emissions are comprised of the effects of the emissions generated by the use of the unit over the course of the lifetime of the unit. This includes:

- Emissions from electricity generation
- Emission from the manufacture of materials
- Emissions from the manufacture of refrigerants
- Emissions from the disposal of the unit

Each emissions factor is calculated separately. The resulting equation is shown in Equation 3. The data sources for each emissions type were identified. The manufacturing emissions were taken from industry associations averages from the European Union and the United States such as the International Aluminum

Association and the World Steel Association.

$$Indirect\ Emissions = L * AEC * EM + \sum(m * MM) + \sum(mr * RM) + C * (1 + L * ALR) * RFM + C * (1-EOL) * RFD \quad (3)$$

Where C is the refrigerant charge (kg), L is the average lifetime of equipment (yr), ALR is the annual leakage rate (% of Refrigerant Charge), EOL is the end of life refrigerant leakage (% of Refrigerant Charge), AEC is the annual energy consumption (kWh), EM is the CO_2 produced/kWh (kg CO_2e/kWh), m is the mass of unit (kg), MM is the CO_{2e} produced/material (kg CO_2e/kg), mr is the mass of recycled material (kg), RM is the CO_2e produced/recycled material (kg CO_2e/kg), RFM is the refrigerant manufacturing emissions (kg CO_2e/kg) and RFD is the refrigerant disposal emissions (kg CO_2e/kg).

4.3.1 Energy Consumption Calculation

The preferred method to calculate the annual energy consumption of the system is to use an annual load model in accordance with ISO and ASHRAE standards [49-51]. This model takes into consideration unit performance characteristics, unit load information, and local weather. A temperature bin method should be used to analyze the weather data. An example demonstrating this is shown in Chapter 5 for a residential heat pump.

The cooling and heating loads should be calculated using the International Organization for Standardization (ISO) Standard [49] or ANSI/AHRI Standard for the type of system being evaluated. Most of the standards are available in SI and IP units. For air conditioning, heating, refrigeration units, and chillers whose performance is dependent on the ambient weather conditions, a minimum of four temperature bins

for cooling and four bins for heating should be used. The load should be calculated for each bin, and then added to determine the total energy consumption per year. For units whose energy consumption is not dependent on ambient weather conditions, the calculation procedure in the respective standard should be used and summed for the unit's lifetime. Once the total energy consumed is calculated, this should be multiplied by the electricity generation emissions rate for the area to obtain the indirect CO_{2e} emissions from power consumption. A sample calculation for a residential heat pump using ANSI/AHRI Standard 210/240-2008 [16] is shown in Chapter 5.

Standby power or compressor crankcase heaters may also consume a significant amount of energy. These devices should be considered in climates where the compressor is off or in standby for a significant amount of time such, as Canada or Scandinavia. The methodology to account for this energy consumption is stated in some standards such as European standard EN-14825 [52].

The temperature bin method was chosen for its relative ease of calculation and its use in previous LCCP research. The ORNL LCCP tool [10, 17], AHRI LCCP tool [4] and GREEN-MAC-LCCP [7] use this method to evaluate the chosen climate data. This method provides a way to represent climate severity and its effects on different HVAC units. This method is also more accurately represents units whose performance varies with outdoor temperature and occupancy. Table 5 shows the standard temperature bins used for residential units from the AHSI/AHRI Standard 210/240 as an example. These bins were used for all further work in the LCCP guideline.

Table 5: Residential Heat Pump Standard Temperature Bins for the United States [16]

Bin Number	Cooling Bins (°C)	Representative Temperature
1	18.3-21.0	19.4
2	21.1-23.8	22.2
3	23.9–26.6	25
4	26.7-29.3	27.8
5	29.4–32.1	30.6
6	32.2-34.9	33.3
7	35–37.7	36.1
8	37.8-40	38.9
Bin Number	**Heating Bins (°C)**	**Representative Temperature**
9	15.6-18.2	16.7
10	12.8-15.5	13.9
11	10-12.7	11.1
12	7.2-9.9	8.3
13	4.4-7.1	5.6
14	1.7-4.3	2.8
15	(-1.1)-1.6	0
16	(-3.9)-(- 1.2)	-2.8
17	(-6.7)-(-4.0)	-5.6
18	(-9.4) - (-6.6)	-8.3
19	(-12.2) - (-9.5)	-11.1
20	(-15) - (-12.3)	-13.9
21	(-17.8)-(-15.1)	-16.7
22	(-20.6) - (-17.9)	-19.4
23	(-23.3) - (-20.7)	-22.2
24	(-26.1) - (-23.4)	-25
25	(-28.3) - (-26.2)	-27.8
26	(-28.4) and Below	-30.6

4.3.2 Climate Data

The climate data is used to determine the load on the unit. This data should be broken down by hours through the year. Each hour should reflect the average over a

number of years to reflect the climate severity rather than any weather abnormalities. This method eliminates out irregularities from year to year. Multiple sources for accurate climate data exist. The International Weather for Energy Calculations datasets (IWEC), 2013 and the National Renewable Energy Laboratories (NREL) – Typical Meteorological Year database (TMY3), 2015 [53-55] should be used whenever possible. The International Energy Agency (IEA) and the U.S. Department of Energy (U. S. DOE) provide lists of alternative sources if the location being modeled is not included in the IWEC datasets or TMY3 [56, 57]. These databases are categorized by the closest city to where the data was collected. The climate region of the locations should be taken into consideration when selecting a location.

4.3.3 Electricity Generation Emissions

The emissions created by the generation of electricity are the primary factor in the LCCP calculation. Emissions rates should be measured in kg CO_2e/kWh. The LCCP methodology assumes that the unit being evaluated uses the electric grid for 100% of the required power. Electricity generation emissions rates vary dramatically across the world and within countries. The rates depend on the type of generation that is used in the region. Where hydro power is prevalent, the emissions rates are much lower than where coal power plants are the primary source of generation. The emission rate chosen should be the most localized rate for the location in question. If the local or regional rate is not available the country average should be used. The North American Electricity Reliability Corporation (NERC) and the IEA provide current electrical power generation emissions [58, 59]. NERC measures the emissions for North America in five zones or interconnections. Within each interconnection it is

extremely difficult to determine from which power plant the energy consumed was generated; therefore, the interconnection average should be used. The interconnections are shown in Figure 10. The International Energy Agency measures emissions on a country basis. A range of emissions values for various countries are shown in Figure 11.

The emission rate to be chosen depends on the purpose of the calculation. For a specific user, who wants to minimize a specific application's emissions, the local rates can be used. In general, it is relevant to use a common rate over an area where the electrical networks are interconnected. For example, the average for the European Union is 0.454 kg CO_2e/kWh [60]. If the purpose is to compare products intended to be sold worldwide, the global average value (0.623 kg CO_2e/kWh) [60].

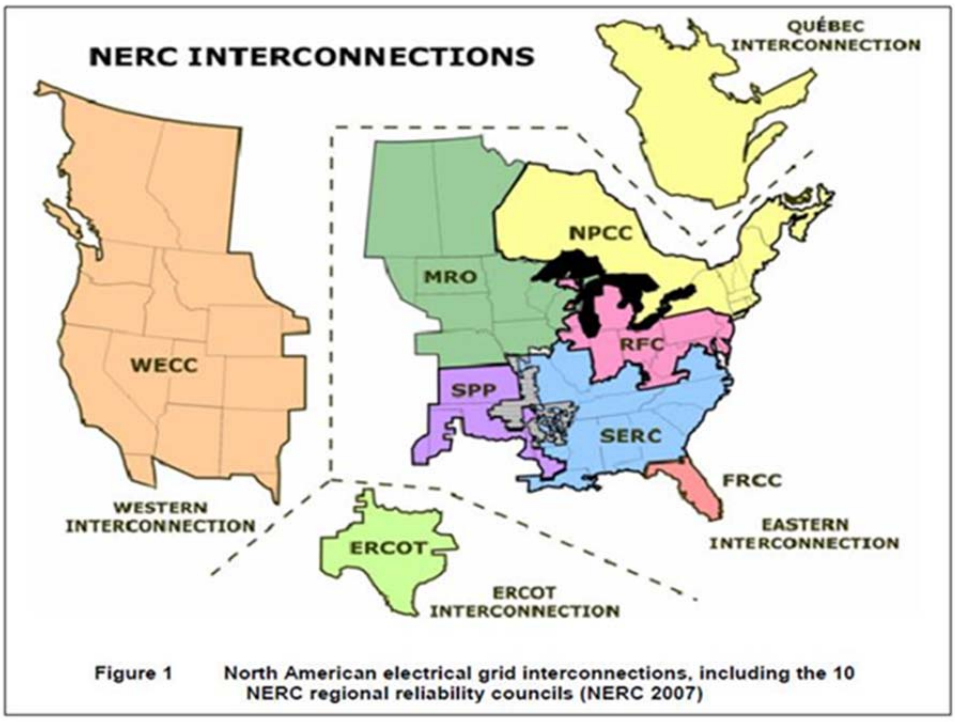

Figure 10: NERC Interconnections [58]

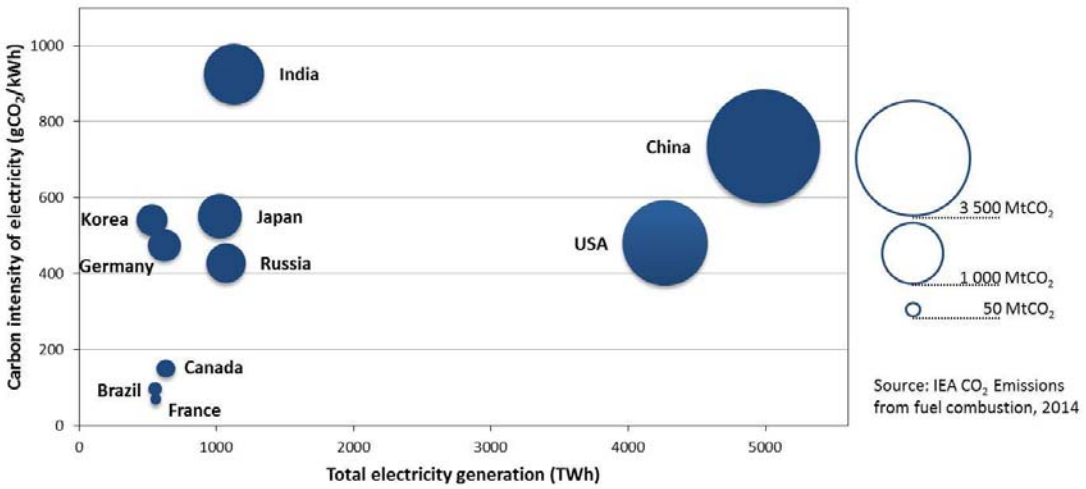

Figure 11: Carbon Intensity of Electricity Generation [59]

4.3.4 Comparing LCCPs for Different Refrigerants

When comparing solutions using different refrigerants, care must be taken to make an "apple to apple" comparison. For instance, inter-comparisons are only meaningful between systems having similar capacities. It is often difficult to have precisely the same capacity at the same conditions with different technologies. In that case, the use of "specific LCCP" provides a more relevant comparison.

4.3.5 Effects of Refrigerant Leakage on Energy Consumption

The baseline equation as written in the guideline assumes that the system is recharged to its optimal refrigerant change annually and that the effects to the energy consumption on the system are minimal. However, refrigerant leakage will have a negative impact on the performance of HVAC&R units over their lifetime. This performance degradation may be considered when calculating the energy consumption of the unit. The performance degradation can be determined using unit test data or data from previous research.

4.3.6 Material Manufacturing Emissions

Material manufacturing emissions were gathered from various industry sources in the United States and the European Union. These sources included trade associations, governmental departments, and previous research efforts. The four most common materials in the manufacture of HVAC&R units are included in the LCCP guideline.

4.3.6.1 Percentage of Composition

The average percentage of the composition of a residential heat pump is shown in Table 6 [4, 10, 17]. Each type of unit will have different breakdown of percentages. These percentages should be used to calculate the manufacturing emissions for the unit. These values were taken from both the AHRI LCCP tool and the ORNL LCCP tool [4, 10, 17].

Table 6: Residential Heat Pump Percentage Composition

Material	Percentage of Unit Composition
Steel	46% [4, 10, 17]
Aluminum	12% [4, 10, 17]
Copper	19% [4, 10, 17]
Plastics	23% [4, 10, 17]

4.3.6.2 Steel

Steel is another essential component in HVAC&R units. According to the International Energy Agency, the iron and steel industries generate approximately 6.7% of the total carbon dioxide emissions annually. In the last fifty years, the steel making process has become much more energy efficient reducing the energy

consumption by 60% [60]. A public record search was conducted for virgin steel manufacturing emissions globally. The results are shown in Table 7. These values were much more consistent than those of the aluminum. The values ranged from 1.6 kg CO_2/kg to 2.95 kg CO_2/kg. From the values shown below, a worldwide average was chosen from the most recent sources of 1.8 kg CO_2/kg [60]. This value is from the World Steel Association's position paper [60]. A global value is necessary because 47% of all steel produced annually is manufactured in China, 27% is manufactured in developing nations and just 26% is manufactured in developed regions.

Table 7: Steel Manufacturing Emissions

Source	**Emissions Value**
GREEN-MAC-LCCP [7]	2.3 [kg CO_2/kg]
AHRI LCCP [4]	2.02 [kg CO_2/kg]
ORNL LCCP [10,17]	2.3 [kg CO_2/kg]
IPCC TEAP Report 2009 [62]	2.95 [kg CO_2/kg] 1.60-2.78 [kg CO_2/kg] AVERAGE: 2.57
Manufacture of Trains (Simonsen, 2009) [63]	1.71 [kg CO_2/kg]
The Low Carbon Future of the European Steel Sector (Sept. 2012) [64]	1.6 [ton CO_2/ton Steel]
Steel's Contribution to a Low Carbon Future (World Steel Association) [61]	1.8 [kg CO_2/kg]
Emission Mitigation of CO2 in Steel Industry (2006) [65]	BOF: 2.15 [CO_2/ton] EAF: 0.5663
A Brief Overview of Low CO2 Technologies for Iron and Steel Making (2010) [66]	World Ave: 2200 kg CO_2/ ton Developed: 1800 kg CO_2/ton
Methods for Estimating GHG Emission Reductions from Recycling (CA. EPA) [67]	2.1 [$MTCO_2e$/short ton]

4.3.6.3 Aluminum

One of the four most prevalent materials in HVAC equipment is aluminum. This material is very energy intensive to manufacture from primary sources. More

than half of the energy used in non-ferrous metals is for primary aluminum production. Worldwide production of electricity required 1.9 EJ of electricity in 2006, about 3.5% of global electricity consumption [68]. Aluminum production can be split into primary aluminum production and recycling. Primary production is about 20 times as energy intensive as recycling and represents the bulk of energy consumption [69]. A public records survey was conducted for aluminum production emissions. The resulting values are shown in Table 8. The values varied dramatically from different sources and different production methods. A median value of 12.6 kg CO_2/kg from the U. S. Energy Requirements for Aluminum Productions Report prepared for the U.S. Department of Energy was chosen from the available sources [68]. This value averages all of the different methods of primary production. This value closely matches the emissions measured by the International Aluminum Institute.

Table 8: Aluminum Manufacturing Emissions

Source	Emission Value
GREEN-MAC-LCCP [7]	1.6 [kg CO_2e/kg]
AHRI LCCP [4]	10.6 [kg CO_2e/kg]
ORNL LCCP [10,17]	1.6 [kg CO_2e/kg]
IPCC TEAP Report 2009 [62]	5.96 [kg CO_2e/kg] 170 [MJ/kg]
U.S. Energy Requirements for Aluminum Production BCS Report prepared for DOE, Feb 2007 [68]	12.6 kg [kg CO_2e/kg]
Manufacture of Trains (Simonsen, 2009) [63]	16.9 [kg CO_2e/kg]
Energy and Environmental Profile of U.S. Aluminum Industry (1997) [69]	15.18 [kWh/kg] Most Efficient: 13 [kWh/kg]
International Aluminum Institute, LCI, May 2000 [70]	12,700 [kg CO_2/ton]
Aluminum the Element of Sustainability. The Aluminum Association, 2011 [71]	2.2 [ton CO_2e/ton]
Methods for Estimating GHG Emission Reductions from Recycling (CA. EPA) [67]	14.1 [MTCO_2e/short ton]

4.3.6.4 Copper

Copper contributes approximately 19% of the contents of a residential heat pump. It is also an essential component in many other sectors. Copper is produced globally with the majority mined in Latin America at 42% of the global total [72]. A public records search was conducted to determine the virgin manufacturing emissions values of copper. The results are shown in Table 9. The values ranged from 2.04 kg CO_2/kg to 4.7 kg CO_2/kg. A median value of 3.0 kg CO_2/kg was chosen from the available sources [73].

Table 9: Copper Manufacturing Emissions

Source	Emissions Value
GREEN-MAC-LCCP	3.3 [kg CO_2e/kg]
AHRI LCCP	4.04 [kg CO_2e/kg]
IPCC TEAP Report 2009 [62]	100 [MJ/kg]
Streamlined Life-Cycle Greenhouse Gas Emission Factors for Copper Wire, EPA June 2005 [74]	2.04 [ton CO_2e/ton] Recycled: 1.64[ton CO_2e/ton] Average: 2.02
Copper (International Copper Association, 2000) [75]	25 [MWh/ton] 4770 [kg CO_2/ton]
The Environmental Profile of Copper Products (European Copper Institute) [73]	3.0 [kg CO_2e/kg]

4.3.6.5 Plastics

Plastics are an integral part of HVAC&R units. A public record search was conducted to determine an average emission value for the manufacture of plastics. The results are shown in Table 10. The values ranged from 1.4 kg CO_2e/kg to 3.8 kg CO_2e/kg. A median value of 2.8 kg CO_2e/kg was taken from the Franklin Associates report prepared for the American Chemistry Council [76]. This study averaged the emissions from all types of commonly used plastics in commercial applications.

Table 10: Plastics Manufacturing Emissions

Sources	Emissions Value
GREEN-MAC-LCCP	3.0 [kg CO_2e/kg]
AHRI LCCP	1.8~3.8 (average 2.8) [kg CO_2e/kg]
ORNL LCCP	3.0 (kg CO_2e/kg)
"Cradle to Grave Life Cycle Inventory of Nine Plastic Resins and Four Polyurethane Precursors," Franklin Associates report prepared for the American Chemistry Council, July 2010) [76]	2.8 (kg CO_2e/kg)
Plastics (EPA) [77]	1.95 ($MTCO_2$e/short ton)
Methods for Estimating GHG Emission Reductions from Recycling (CA. EPA) [67]	1.4 [$MTCO_2$e/short ton]

4.3.7 Recycled Material Manufacturing Emissions

In many cases recycled materials are used in the manufacture of HVAC&R units rather than pure virgin materials for economic and environmental reasons. Most recycled materials require considerable less energy to manufacture. Most recycled materials use a certain portion of virgin materials and recycled materials. The percentages of recycled materials used and its respected production energy are shown in Table 11.

Many materials today are manufactured with a mixture of virgin and recycled materials. The average values of virgin material to recycled materials are shown in Table 12. The emissions values for recycled materials were then taken and weight to develop the mixed manufacturing emissions shown in Table 11 [61-77].

Table 11: Recycled Material Manufacturing Emissions

Material	**Percentage of Mixed Material Composition**	**100% Recycled Material Manufacturing Emissions**
Steel [60-66]	29%	0.54 kg CO_2e/kg
Aluminum [67-70]	67%	0.63 kg CO_2e/kg
Copper [70-74]	40%	2.64 kg CO_2e/kg
Plastics [75,76]	7%	0.12 kg CO_2e/kg

Table 12: Material Manufacturing Emissions

Material	**Virgin Manufacturing Emissions (kg CO_2e/kg)**	**Mixed Manufacturing Emissions (kg CO_2e/kg)**
Steel	1.8 [64]	1.43 [64]
Aluminum	12.6 [68]	4.5 [68]
Copper	3.0 [73]	2.78 [73]
Plastics	2.8 [76]	2.61 [76, 77]

4.3.8 Refrigerant Manufacturing Emissions

Refrigerant manufacturing emissions rates are shown in Table 13 for selected refrigerants. These values were gathered from various studies and manufacturer's information [7, 79-82]. These values are averages of the available sources. They will be updated as more efficient methods of manufacturing are developed.

Table 13: Refrigerant Manufacturing Emissions

Refrigerant	**Manufacturing Emissions (kg CO_2e/kg)**
HFC-32 [7, 82]	7.2
HFC-1234yf [81]	13.7
HFC-134a [79,80]	5.0
HC-290 [81]	0.05
HFC-404A [7]	16.7
HFC-410A [79,81]	10.7

4.3.9 End of Life Emissions

The final component accounted for in the indirect emissions is the emissions generated by the disposal of the unit. Material disposal emissions include all emissions up to the production of recycled material. For metals and plastics this includes the shredding of the material [4, 7, 83-84]. For refrigerants this includes energy required to recover the refrigerant. These emissions may be included in the manufacturing emissions if the material is produced from recycled materials. A public records search was conducted to determine the amounts of emissions were generated by shredding metals and plastics. The results are shown for each material in Table 14-Table 17. Most sources did not distinguish between types of metals or plastics. The

values of 0.07 kg CO_{2e}/kg for metal and 0.01 kg CO_{2e}/kg were selected from the available sources.

Table 14: Aluminum EOL Emissions

Source	Emissions Value
GREEN-MAC-LCCP [6]	0.01 kg/MJ Total EOL energy = 10.1 MJ
AHRI LCCP [3]	0.170 lb CO_2/lb
ORNL LCCP [9, 17]	0.170 lb CO_2/lb
Metals (EPA) [57]	1.93 [$MTCO_2e$/short ton]
Methods for Estimating GHG Emission Reductions from Recycling (CA. EPA) [41]	0.6 [$MTCO_2e$/short ton]

Table 15: Steel EOL Emissions

Source	Emissions Value
GREEN-MAC-LCCP [6]	0.01 kg/MJ Total EOL energy = 10.1 MJ
AHRI LCCP [3]	0.170 lb CO2/lb
ORNL LCCP [9, 17]	0.170 lb CO_2/lb
Metals [EPA] [57]	0.63 [MTCO2e/short ton]
Methods for Estimating GHG Emission Reductions from Recycling (CA. EPA) [41]	0.4 [MTCO2e/short ton]

Table 16: Copper EOL Emissions

Source	**Emissions Value**
GREEN-MAC-LCCP [6]	0.01 kg/MJ Total EOL energy = 10.1 MJ
AHRI LCCP [3]	0.170 lb CO_2/lb
ORNL LCCP [9, 17]	0.170 lb CO_2/lb
Metals [EPA] [57]	0.16 [$MTCO_2e$/short ton]

Table 17: Plastics EOL Emissions

Source	Emissions Value
GREEN-MAC-LCCP [6]	0.01 kg/MJ Total EOL energy = 0.158 MJ
AHRI LCCP [3]	0.015 lb CO_2/lb
ORNL LCCP [9, 17]	0.015
Plastics [EPA] [51]	0.13 [$MTCO_2$/Short ton]
Methods for Estimating GHG Emission Reductions from Recycling (CA. EPA) [41]	0.37 [$MTCO_2e$/short ton]

Chapter 5 : Residential Heat Pump Evaluation

This section is dedicated to determining ways to improve LCCP using different refrigerants and advanced VCC options. A residential heat pump sample problem is evaluated.

5.1 Residential Heat Pump Sample Problem

A residential heat pump was evaluated in five locations in the continental USA, representing different climatic conditions. The cities evaluated are: Miami, FL, Phoenix, AZ, Atlanta, GA, Seattle, WA and Chicago, IL. The heat pump has the characteristics shown in Table 18. The heat pump modeled is Goodman SSZ16-0361A [85]. The unit is a single speed compressor unit with a fixed fan speed and a resistance heater for backup heat. The heat pump performance characteristics were evaluated according to AHRI Standard 210/240 (2008) [16]. The values used are shown in Table 18.

Table 18: Residential Heat Pump Characteristics

Capacity	11 kW
Refrigerant	R-410A
Charge	6 kg
Lifetime	15 years
Unit Mass	115 kg
Annual Leakage Rate	4%
EOL Leakage Rate	15%

5.1.1 Direct Emissions Calculation

The residential heat pump uses the refrigerant R-410A. The GWP value of this refrigerant is found in Table 3. The standard assumptions for the leakage rates are found in Table 4. The breakdown of the calculation is shown in Table 19. The direct emissions remain the same for all locations evaluated. Adaptive GWP for R-410A was assumed to be zero because of the lack of available data.

Table 19: Direct Emissions Results

Annual Leakage Emissions (kg CO_2e)	6,926.4
End of Life Emissions (kg CO_2e)	1,731.6
Adp. GWP Emissions (kg CO_2e)	Not Available

5.1.2 Indirect Emissions Calculation

The indirect emission calculation was broken down into three parts: energy consumption calculation, material manufacturing emissions, and the end of life disposal emissions.

Energy Consumption Calculation

The energy consumption calculation was performed using the AHRI Standard 210/240 [16] for Residential Heat Pumps and the TMY03 data [54] for the five locations. The local conditions were evaluated using the temperature bin method. The standard temperature bins and resulting bin hours for the cities are shown in Table 21. Each city was evaluated at each bin for the amount of energy required to provide cooling and heating. That value was then multiplied by the number of hours in the bin. This calculated value was multiplied by the regional energy generation

emissions rate to determine the total amount of emission from energy consumption per year that the unit generates. The NERC interconnection used for each city is shown in Table 22.

Table 20: AHRI Standard 210/240 Performance Data

Cooling or Heating	Test Number	Capacity (W)	Total Power (W)
Cooling	A Test	10,140	2,550
Cooling	B Test	10,474	2,378
Heating	H1 Test	10,082	2,500
Heating	H2 Test	8,382	2,370
Heating	H3 Test	6,154	2,310

Table 21: Temperature Bin Hours for U. S. Cities from AHRI Std 210/240 (2008)

Cooling Temperature Bins (°C)	Miami, FL	Phoenix, AZ	Atlanta, GA	Chicago, IL	Seattle, WA
18.2 <°C ≤ 21.1	778	711	944	767	505
21.1 <°C ≤ 23.8	1,327	586	977	538	285
23.8 <°C ≤ 26.6	2,511	744	879	531	155
26.6 <°C ≤ 29.3	2,312	922	703	428	72
29.3 <°C ≤ 32.1	838	817	424	160	17
32.1 <°C ≤ 34.9	54	619	127	26	0
34.9 <°C ≤ 37.7	6	614	13	1	0
Above 37.7	0	750	0	0	0
Heating Bins (°C)	**Miami, FL**	**Phoenix, AZ**	**Atlanta, GA**	**Chicago, IL**	**Seattle, WA**
15.6 <°C ≤ 18.2	480	929	1,066	848	1,001
12.7 <°C ≤ 15.6	276	730	795	677	1,479
10 <°C ≤ 12.7	146	670	751	641	1,613
7.2 <°C ≤ 10	25	329	562	528	1,352
4.4 <°C ≤ 7.2	7	268	626	567	1,296
1.6 <°C ≤ 4.4	0	71	369	773	652
(-1.2) <°C ≤ 1.6	0	0	221	759	264
(-4.0) <°C ≤ (- 1.2)	0	0	197	473	63
(-6.6) <°C ≤ (-4.0)	0	0	86	322	6
(-9.5) <°C ≤ (-6.6)	0	0	20	382	0
(-12.3) <°C ≤ (-9.5)	0	0	8	157	0
(-15.1) <°C ≤ (-12.3)	0	0	1	108	0
(-17.9) <°C ≤ (-15.1)	0	0	0	83	0
(-20.6) <°C ≤ (-17.9)	0	0	0	41	0
(-23.4) <°C ≤ (-20.7)	0	0	0	23	0
(-26.2) <°C ≤ (-23.4)	0	0	0	0	0
(-28.3) <°C ≤ (-26.2)	0	0	0	0	0
Below (-28.3)	0	0	0	0	0

Table 22: Annual Energy Consumption

Location	Miami, FL	Phoenix, AZ	Atlanta, GA	Chicago, IL	Seattle, WA
NERC Interconnection	Eastern	Western	Eastern	Eastern	Western
Annual Cooling Energy Consumption (kWh)	8,228	8,924	3,700	1,946	559
Cooling Season Emissions (kg CO_2e)	6,483	5,301	2,916	1,534	332
Heating Climate Region	I	II	III	IV	V
Annual Heating Energy Consumption (kWh)	211	1,162	3,352	8,265	4,075
Heating Season Emissions (kg CO_2e)	166	691	2,641	6,513	2,420
Total Energy Consumption Emissions (kg CO_2e)	99,745	89,868	83,358	120,699	41,289

Material Manufacturing Emissions

The material manufacturing emissions are calculated using the mass of the unit and the percent composition of the unit shown in Table 6 and the material manufacturing emissions rates from Table 12. This calculation uses the standard virgin manufacturing emissions for the materials and refrigerant.

Table 23: Manufacturing Emissions

Steel Manufacturing (kg CO_2e)	95
Aluminum Manufacturing (kg CO_2e)	174
Copper Manufacturing (kg CO_2e)	66
Plastic Manufacturing (kg CO_2e)	74
Total Manufacturing Emissions (kg CO_2e)	409

End of Life Emissions

The end of life disposal of the unit assumes that the unit is shredded for recycling. This is calculated using the emission rates in Table 24. The unit weight was taken and multiplied by the percentage of metal and plastic. This amount was then multiplied by the recycling emissions factor for the material.

Table 24: EOL Emissions

Metal EOL (kg CO_2e)	6.2
Plastic EOL (kg CO_2e)	0.4
Total EOL Emissions (kg CO_2e)	6.6

5.1.3 Total Lifetime Emissions

The direct and indirect emissions are summed for the total emissions generated over the lifetime of the unit. Table 25 shows the total emissions generated using the LCCP equation shown in Equation 1. The most influential category for all of the locations is the energy consumption of the unit over its lifetime.

Table 25: LCCP Total Lifetime Emissions

Results	Miami, FL	Phoenix, AZ	Atlanta, GA	Chicago, IL	Seattle WA
LCCP Total Lifetime Emission (kg CO_2e)	108,819	98,941	92,431	129,772	50,362
Total Direct Emission (kg CO_2e)	8,658	8,658	8,658	8,658	8,658
Annual Refrigerant Leakage (kg CO_2e)	6,926	6,926	6,926	6,926	6,926
EOL Refrigerant Loss (kg CO_2e)	1,732	1,7312	1,7312	1,732	1,732
Adaptive GWP (kg CO_2e)	-	-	-	-	-
Total Indirect Emissions (kg CO_2e)	100,161	90,283	83,773	121,114	41,704
Energy Consumption (kg CO_2e)	99,745	89,868	83,358	120,700	41,289
Equipment Manufacturing (kg CO_2e)	409	409	409	409	409
Equipment EOL (kg CO_2e)	6.6	6.6	6.6	6.6	6.6
Refrigerant Manufacturing (kg CO_2e)	103	103	103	103	103

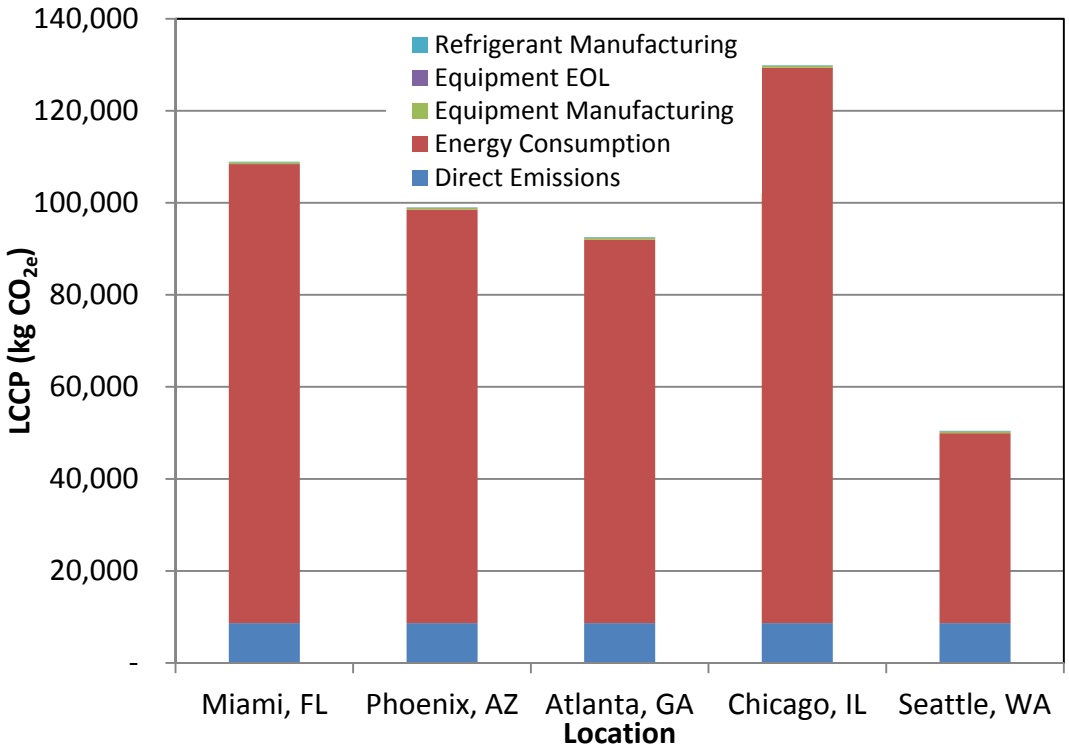

Figure 12: LCCP Residential HP Comparison

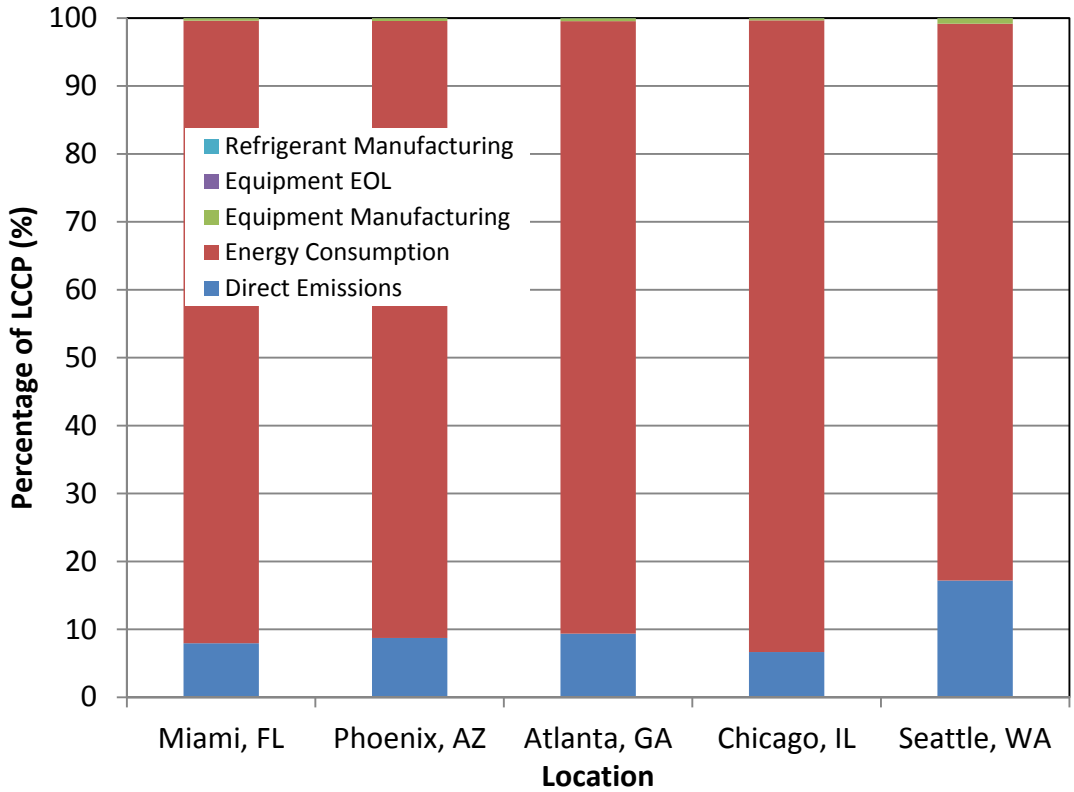

Figure 13: Percentage of LCCP versus Location for Residential Heat Pump Sample Problem

5.1.4 Specific LCCP

Specific LCCP was calculated for each location. The total emissions were divided by the cooling and heating provided by the unit. The results are shown in Table 26. Chicago, IL has the highest specific LCCP followed by Atlanta. The lowest specific LCCP occurs at Phoenix, AZ.

Table 26: Specific LCCP

Results	Miami, FL	Phoenix, AZ	Atlanta, GA	Chicago, IL	Seattle WA
Specific LCCP (kg CO_2e/kWh)	0.224	0.174	0.251	0.302	0.229

5.2 Sensitivity Study

5.2.1 Baseline

The sensitivity study was conducted using the performance data and physical characteristics of an 11 kW (3 ton) residential heat pump located in Atlanta, GA. The energy consumption was calculated using the IIR Residential Heat Pump LCCP excel tool [86]. Goodman SSZ16-0361A unit was used for this study. The AHRI Standard 210/240 data used is shown below in Table 27. Annual leakage was assumed to be 4%, end of life leakage 15% and the manufacturing emissions from R-410A were used for the baseline calculation. The unit weighs 115 kg with a charge of 6 kg. The unit lifetime was assumed to be fifteen years. This same unit was used as the residential heat pump baseline for the evaluation of advanced cycle option. The charge amount and the unit weight were held constant for all scenarios. The energy efficiency was varied from 90% to 110%. The annual refrigerant leakage was varied

from 0% to 50% of the charge. It was assumed that the unit was recharged annually and that there was no performance degradation caused by the reduction in charge. The end of life refrigeration loss was varied from 0% to 100%. Each parameter was varied for GWP values of 10, 100, 500, 1,000 and 3,000. The results were plotted and evaluated.

Table 27: AHRI Standard 210/240 Performance Data for Sensitivity Studies

Cooling or Heating	Test Number	Capacity (W)	Total Power (W)
Cooling	A Test	10,140	2,550
Cooling	B Test	10,474	2,378
Heating	H1 Test	10,082	2,500
Heating	H2 Test	8,382	2,370
Heating	H3 Test	6,154	2,310

A baseline comparison was created using the given GWP values. It demonstrates that the primary factor in the LCCP calculation is the energy consumption over the lifetime of the unit. Table 28 shows the emissions generated for a range of GWP values. Table 29 shows the percentage of the total emissions for each component of LCCP for a range of GWP values. Figure 15 shows the percentages for each category of the total emissions graphically. Figure 14 shows the total emissions for each GWP value broken down by emissions category. The energy consumption comprises of 85.7% for GWP of 3,000 to 99.5% for a GWP of 10. For all GWP values end of life emissions contributed a very small percentage of the overall total, approximately 0.01%. When GWP values drop below 300, the contribution of direct emission also drops below one percent of the total.

Table 28: Total Emissions for Sample GWP Values

Category	GWP 10	GWP 100	GWP 500	GWP 1,000	GWP 3,000
Total Emissions (kg CO_2e)	83,818	84,223	86,023	88,273	97,273
Total Direct Emission (kg CO_2e)	45	450	2,250	4,500	13,500
Annual Refrigerant Leakage (kg CO_2e)	36	360	1,800	3,600	10,800
EOL Refrigerant Loss (kg CO_2e)	9	90	450	900	2,700
Adaptive GWP (kg CO_2e)	-	-	-	-	-
Total Indirect Emissions (kg CO_2e)	83,773	83,773	83,773	83,773	83,773
Energy Consumption (kg CO_2e)	83,358	83,358	83,358	83,358	83,358
Equipment Manufacturing (kg CO_2e)	409	409	409	409	409
Refrigerant Manufacturing (kg CO_2e)	6.5	6.5	6.5	6.5	6.5
Equipment EOL (kg CO_2e)	103	103	103	103	103

Table 29: LCCP Baseline Comparison Percentages

Item	GWP 10	GWP 100	GWP 500	GWP 1,000	GWP 3,000
Total Direct Emission	0.05%	0.53%	2.62%	5.10%	13.88%
Ref. Leakage	0.04%	0.43%	2.09%	4.08%	11.10%
Ref. Loss at EOL	0.01%	0.11%	0.52%	1.02%	2.78%
Adp. GWP	-	-	-	-	-
Total Indirect Emissions	99.95%	99.47%	97.38%	94.90%	86.12%
Energy Consumption	99.45%	98.97%	96.90%	94.43%	85.69%
Equipment Mfg	0.49%	0.49%	0.48%	0.46%	0.42%
Equipment EOL	0.01%	0.01%	0.01%	0.01%	0.01%
Refrigerant Mfg	0.12%	0.12%	0.12%	0.12%	0.11%

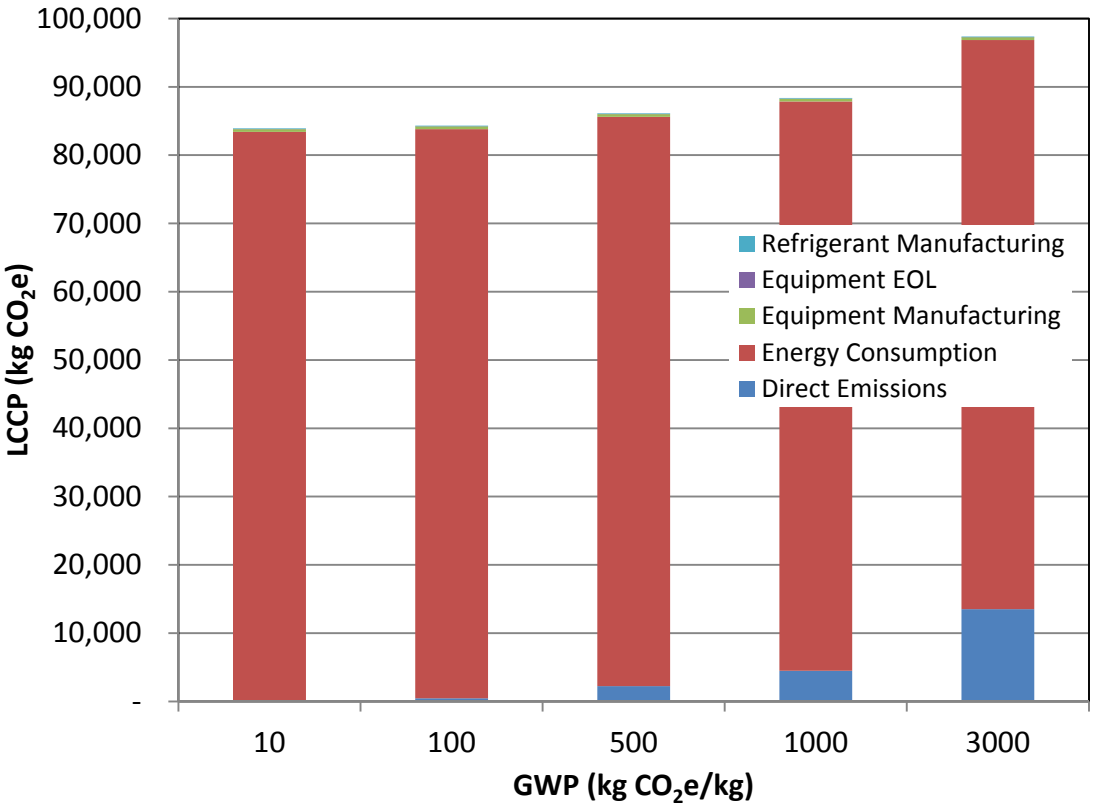

Figure 14: LCCP Baseline Sensitivity Study Total Emissions

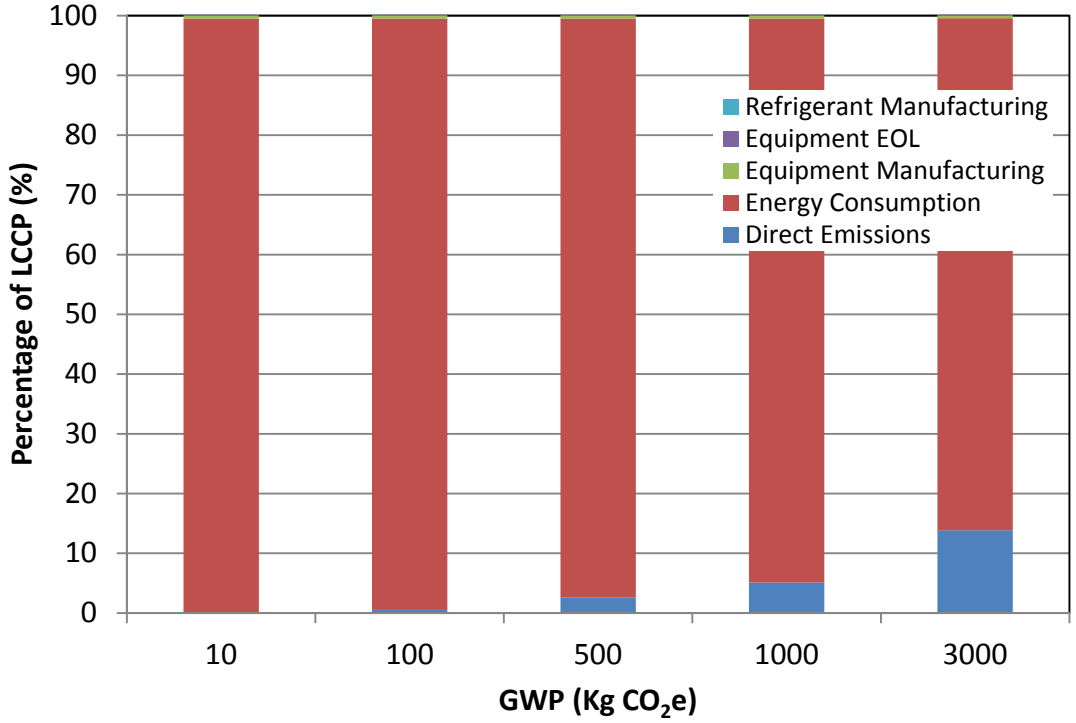

Figure 15: LCCP GWP Sensitivity Study Percentage of Total Emissions

5.2.2 Energy Consumption

When the energy consumption was varied, the baseline energy consumption value was increased above 100% to simulate a less efficient system and decreased below 100% to simulate a more efficient system. Similar trends were observed in the baseline comparison. The results of the study are shown graphically in Figure 16. Energy consumption remains the most influential factor in the LCCP equation for all scenarios. The percentage of energy consumption of the total emissions varied from 84.35% to 99.5%. The refrigerant manufacturing emissions and end of life emissions provided negligible contributions to the total emissions.

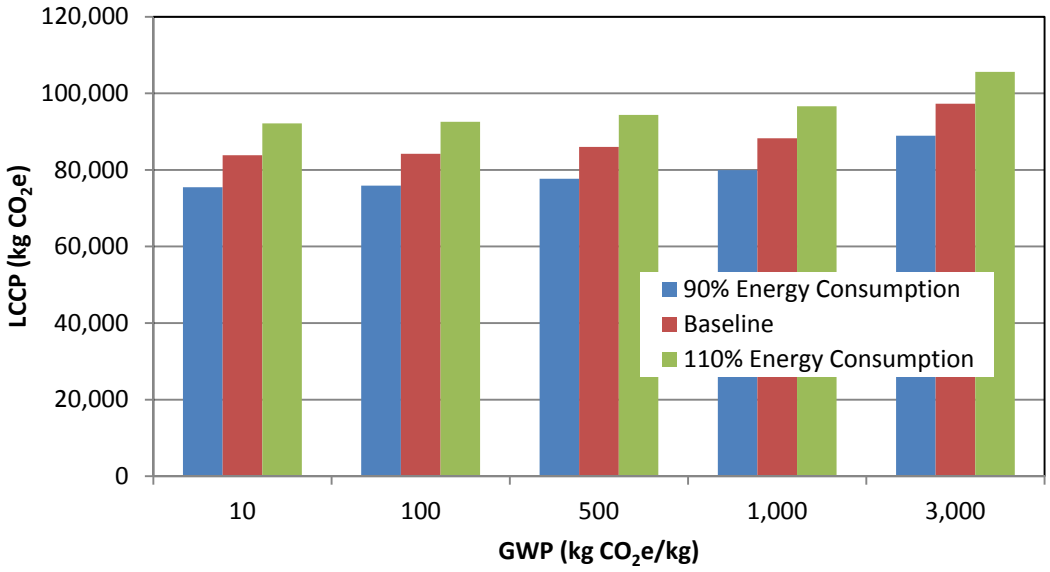

Figure 16: Energy Consumption Sensitivity Study

The energy consumption was then plotted against the total emissions generated by the unit and a range of GWP values from 10 to 3,000. The results are displayed in Figure 17. When the energy consumption of the unit is varied from 90% to 110% of the baseline system the total emissions increase by 8,336 kg CO_2e for all

GWP values. The percentage of the total emissions changed from 99.45% to 99.5% for a GWP of 10 and from 85.7% to 86.82% for a GWP of 3,000.

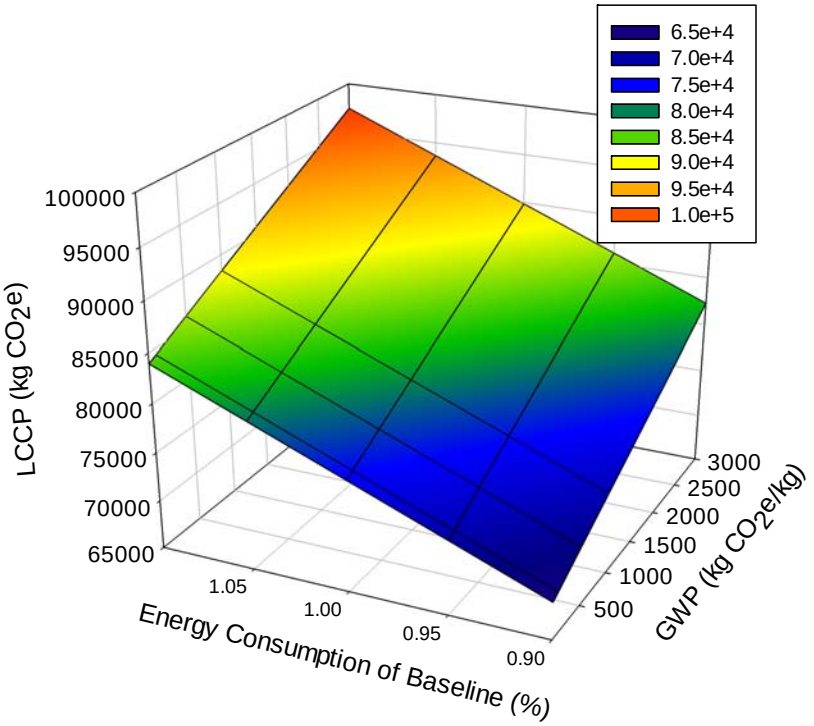

Figure 17: Energy Efficiency Sensitivity Study 3-D Graph

5.2.3 Annual Leakage Rate

When the annual leakage rates are varied from 0% to 50%, the GWP of the refrigerant plays an increasingly influential role in the total emissions. When high GWP refrigerants are used, it is vital to minimize the amount of refrigerant leaked from the unit. The percentage of the total emissions from annual leakage increases linearly. The results are shown graphically in Figure 18. The percentage of the total varied from 0% to 0.43% for a GWP of 10 and from 0% to 55.53% for a GWP of 3,000.

The increased annual leakage rates also impacts the refrigerant manufacturing emissions. For a GWP of 10 this rises to 0.65% of total emissions when the ALR is increased to 50% and for GWP of 3,000 this increases to 0.25% of the total.

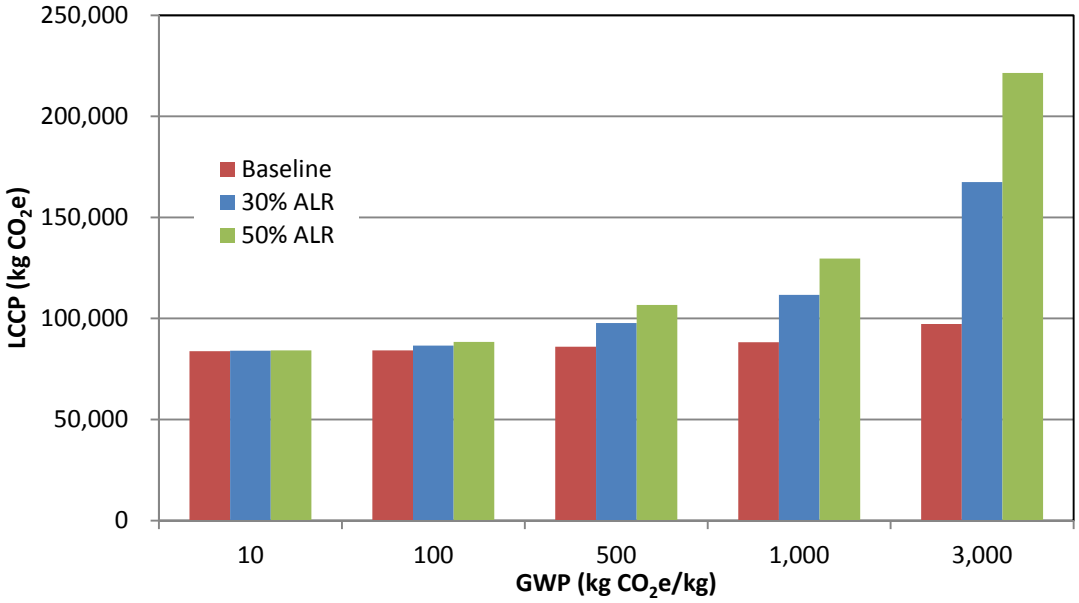

Figure 18: Annual Leakage Rate Sensitivity Study

The annual refrigerant leakage rate was varied from 0% to 50% and was then plotted against the total emissions generated by the unit and a range of GWP values from 10 to 3,000 as shown in Figure 19. The higher the GWP value the more of an impact the annual leakage rate has on the total emissions. This impact is reflected in the emissions generated by the annual leakage rate of the refrigerant and the emissions from the manufacturing of the refrigerant. As the refrigerant annual leakage rate is increased the amount of refrigerant required during the lifetime of the system also increases dramatically. The total emissions varied by 450 kg CO_2e for a refrigerant with a GWP of 10 and 135,000 kg CO_2e for a refrigerant with a GWP of 3,000.

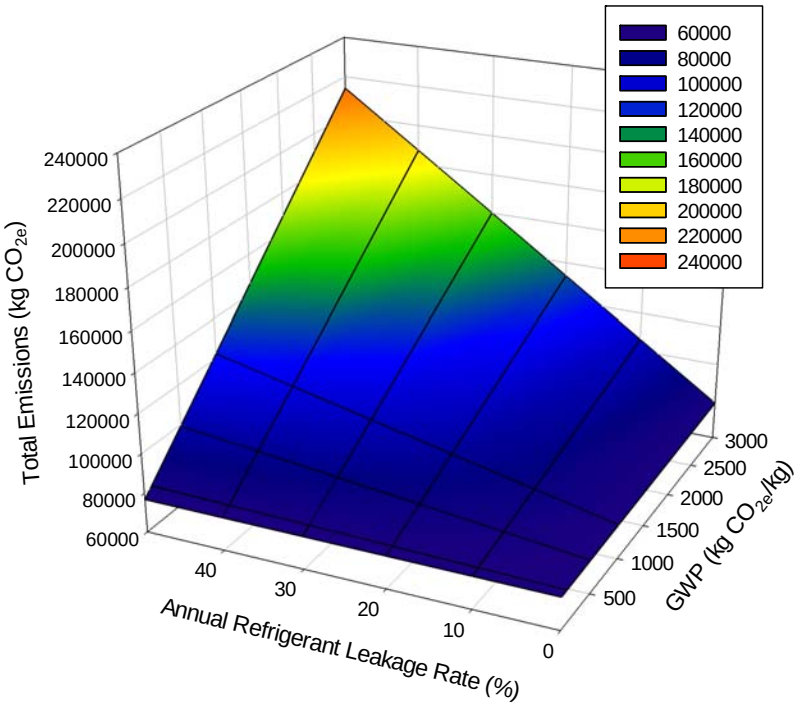

Figure 19: Annual Leakage Rate Sensitivity Study 3-D Graph

5.2.4 End of Life Leakage

The end of life leakage rates were varied from 0% to 100% of the charge for the specified GWP values. All other variable were held constant. When the end of life leakage rates were varied from 0% to 100%, the GWP of the refrigerant plays an increasingly influential role in the total emissions. When high GWP refrigerants are used, it is vital to minimize the amount of refrigerant leaked from the unit. The percentage of the total emissions from end of life leakage increases linearly. The results are shown graphically in Figure 20. The percentage of the total varied from 0% to 0.07% for a GWP of 10 and from 0% to 16% for a GWP of 3,000.

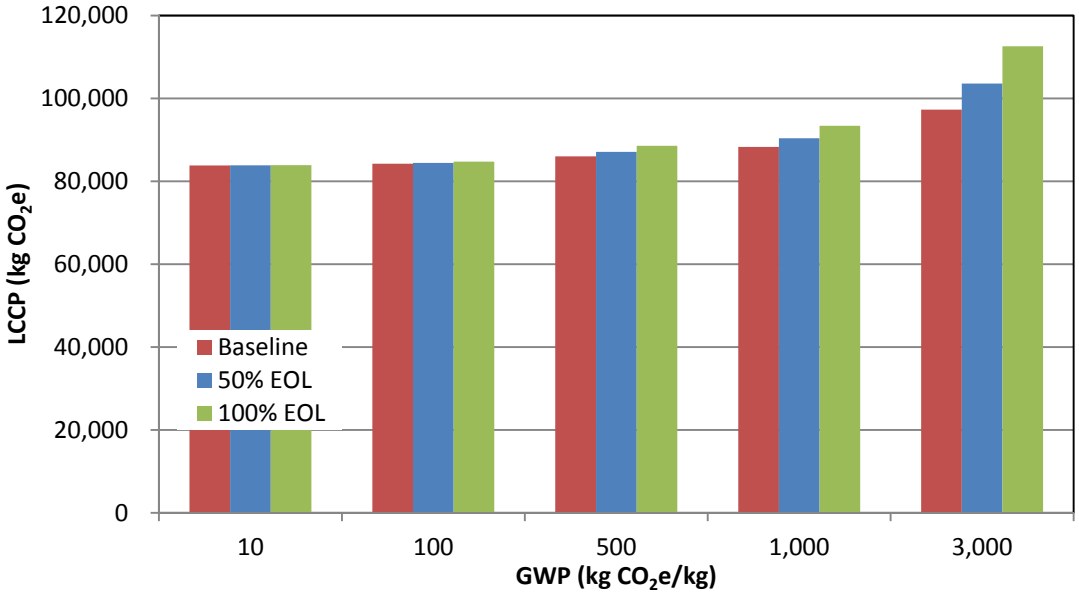

Figure 20: End of Life Leakage Sensitivity Study

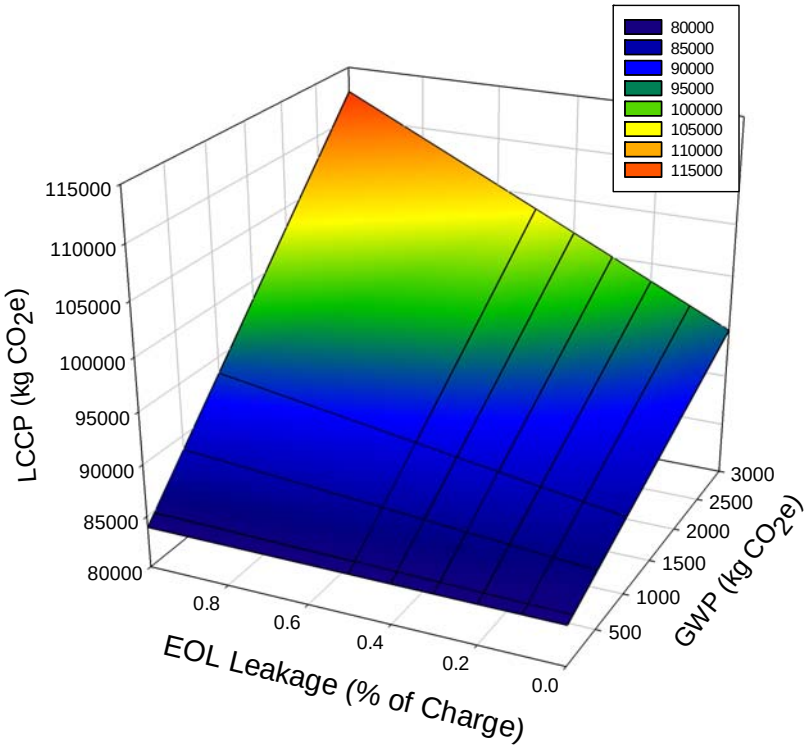

Figure 21: End of Life Leakage Sensitivity Study 3-D

5.2.5 Manufacturing Emissions

The manufacturing emissions were varied from the baseline to 1000%. All other values were held constant. The mass of the unit was assumed to be 115 kg. The results are shown in Figure 22. The manufacturing emissions were 408.7 kg CO_2e for the baseline case. This constituted 0.49% of the total emissions for a GWP 10. The percentage decreased linearly to 0.36% for a GWP of 3,000. When the manufacturing emissions were multiplied by a factor of ten the percentage of the total for GWP of 10 increased to 5.37% and to 4.65% for GWP of 3,000.

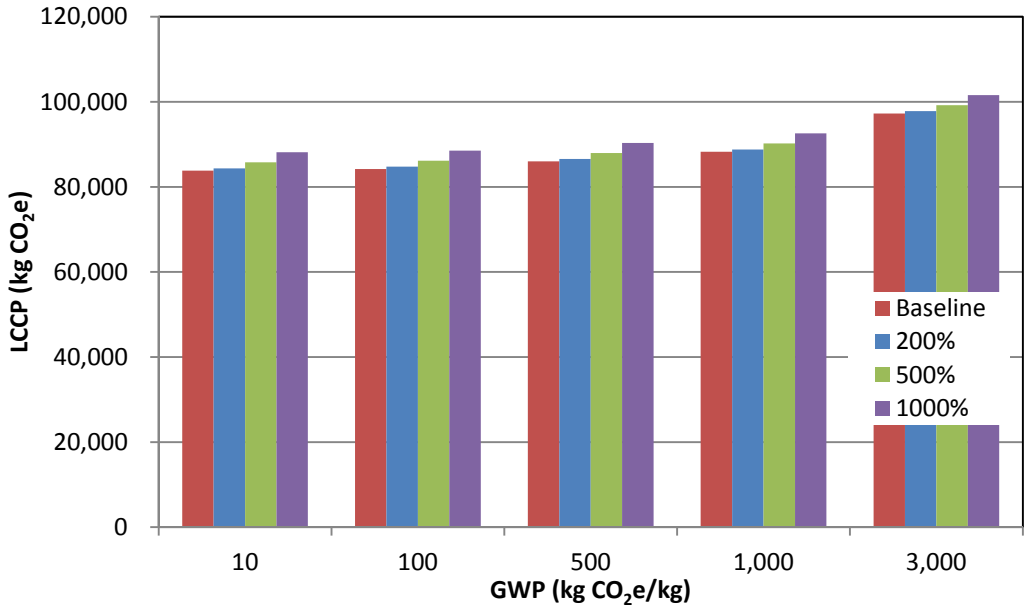

Figure 22: Manufacturing Emissions Sensitivity Study

The results of this sensitivity study were also plotted on a 3-D graph to show the combined impact of GWP and manufacturing emissions. The result is shown in Figure 23. The increase remains constant for all GWP values.

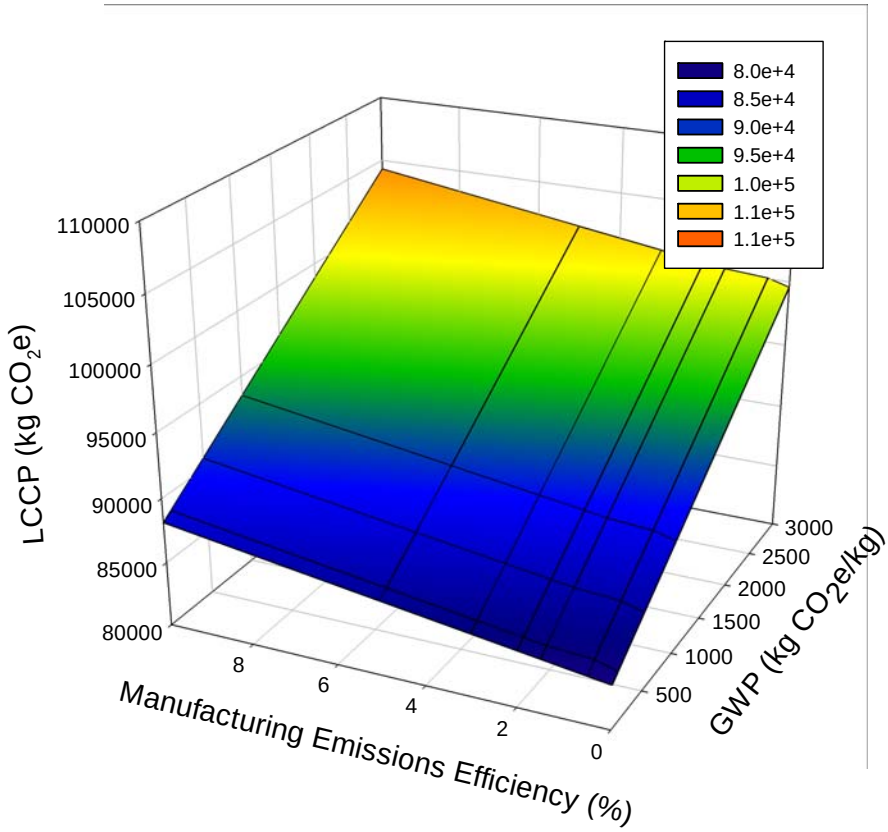

Figure 23: Manufacturing Emissions Sensitivity Study 3-D

5.3 Excel Tool Development

An excel tool was built for a single speed compressor, single speed fan residential heat pump system [86]. The inputs are in SI units. The system includes six built in refrigerants: HFC-32, HFC-1234yf, HFC-134a, R-290, HFC-404A, HFC-410A, L-41b, DR-5. The calculation is performed at five locations in five different climate zones including: Miami, FL, Phoenix, AZ, Atlanta, GA, Chicago, IL and Seattle, WA. The material manufacturing can be set to either virgin material or a mix of recycled and virgin materials. The tool uses ARHI 210/240 standard for energy consumption calculation. The inputs are shown in Figure 24.

.

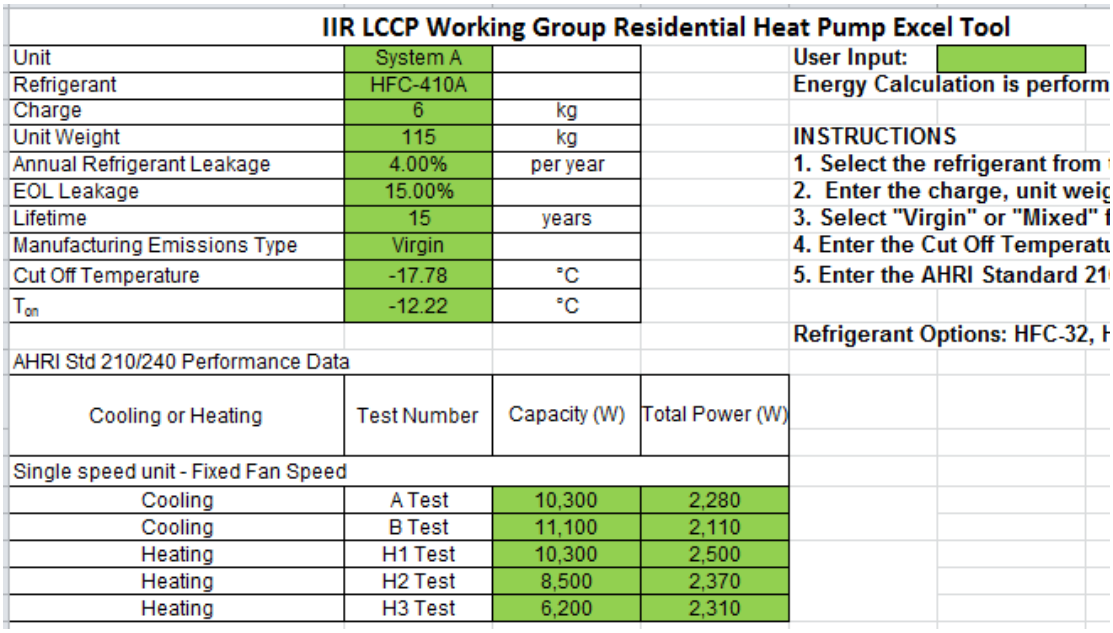

IIR LCCP Working Group Residential Heat Pump Excel Tool				
Unit	System A			User Input:
Refrigerant	HFC-410A			Energy Calculation is perform
Charge	6	kg		
Unit Weight	115	kg		INSTRUCTIONS
Annual Refrigerant Leakage	4.00%	per year		1. Select the refrigerant from
EOL Leakage	15.00%			2. Enter the charge, unit weig
Lifetime	15	years		3. Select "Virgin" or "Mixed"
Manufacturing Emissions Type	Virgin			4. Enter the Cut Off Temperatu
Cut Off Temperature	-17.78	°C		5. Enter the AHRI Standard 21
T_{on}	-12.22	°C		
				Refrigerant Options: HFC-32, H
AHRI Std 210/240 Performance Data				
Cooling or Heating	Test Number	Capacity (W)	Total Power (W)	
Single speed unit - Fixed Fan Speed				
Cooling	A Test	10,300	2,280	
Cooling	B Test	11,100	2,110	
Heating	H1 Test	10,300	2,500	
Heating	H2 Test	8,500	2,370	
Heating	H3 Test	6,200	2,310	

Figure 24: IIR LCCP Excel Tool Inputs

The tool shows the breakdown of the different LCCP components in table and graph form. The results are also shown as a percentage of the total. The results page is shown in Figure 25.

The weather data can be easily changed for a different city in the same climate zone. The tool also provides a graphical representation of the results as shown in Figure 26 and Figure 27.

LCCP Results					
Location	Miami, FL	Phoenix, AZ	Atlanta, GA	Chicago, IL	Seattle, WA
Total Lifetime Emission (kg CO_{2e})	94,219.43	88,792.67	84,993.57	123,766.95	48,804.08
Total Direct Emission (kg CO_{2e})	8,658.00	8,658.00	8,658.00	8,658.00	8,658.00
Annual Refrigerant Leakage (kg CO_{2e})	6,926.40	6,926.40	6,926.40	6,926.40	6,926.40
EOL Refrigerant Leakage (kg CO_{2e})	1,731.60	1,731.60	1,731.60	1,731.60	1,731.60
Adp. GWP (kg CO_{2e})	-	-	-	-	-
Total Indirect Emissions (kg CO_{2e})	85,561.43	80,134.67	76,335.57	115,108.95	40,146.08
Energy Consumption (kg CO_{2e})	85,146.26	79,719.49	75,920.40	114,693.78	39,730.91
Equipment Mfg (kg CO_{2e})	408.71	408.71	408.71	408.71	408.71
Equipment EOL (kg CO_{2e})	6.46	6.46	6.46	6.46	6.46
Refrigerant Mfg (kg CO_{2e})	102.72	102.72	102.72	102.72	102.72

Expanded Energy Consumption Results					
Location	Miami, FL	Phoenix, AZ	Atlanta, GA	Chicago, IL	Seattle, WA
Electricity Generation Region	Eastern Interconnection	Western Interconnection	Eastern Interconnection	Eastern Interconnection	Western Interconnection
Annual Cooling Energy Consumption (kWh)	6,995.97	7,830.47	3,146.52	1,644.95	465.66
Annual Cooling Emissions (kg CO_{2e})	5,512.83	4,651.30	2,479.45	1,296.22	276.60
Heating Climate Region	I	II	III	IV	V
Annual Heating Energy Consumption (kWh)	207.60	1,116.73	3,276.53	8,058.41	3,993.47
Heating Emissions (kg CO_{2e})	163.59	663.34	2,581.91	6,350.03	2,372.12

Percentage of Composition					
Location	Miami, FL	Phoenix, AZ	Atlanta, GA	Chicago, IL	Seattle, WA
Total Direct Emission	9.19%	9.75%	10.19%	7.00%	17.74%
Annual Refrigerant Leakage	7.35%	7.80%	8.15%	5.60%	14.19%
EOL Refrigerant Leakage	1.84%	1.95%	2.04%	1.40%	3.55%
Adp. GWP	-	-	-	-	-
Total Indirect Emissions	90.81%	90.25%	89.81%	93.00%	82.26%
Energy Consumption	90.37%	89.78%	89.32%	92.67%	81.41%
Equipment Mfg	0.43%	0.46%	0.48%	0.33%	0.84%
Equipment EOL	0.01%	0.01%	0.01%	0.01%	0.01%
Refrigerant Mfg	0.11%	0.12%	0.12%	0.08%	0.21%

Figure 25: IIR LCCP Excel Tool Results

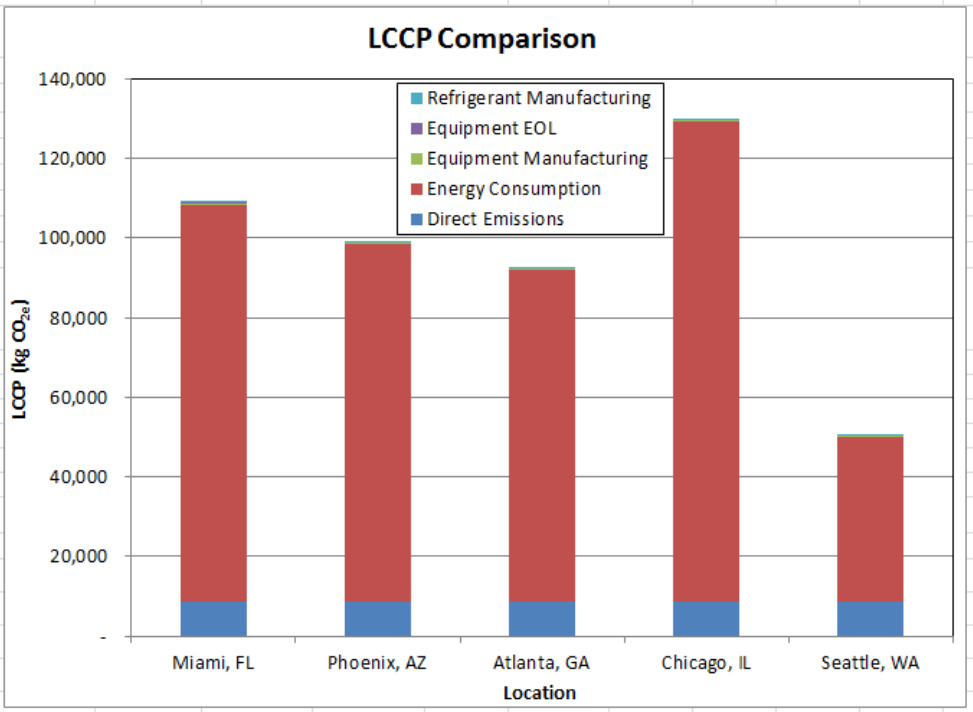

Figure 26: IIR LCCP Tool Total Emissions Chart

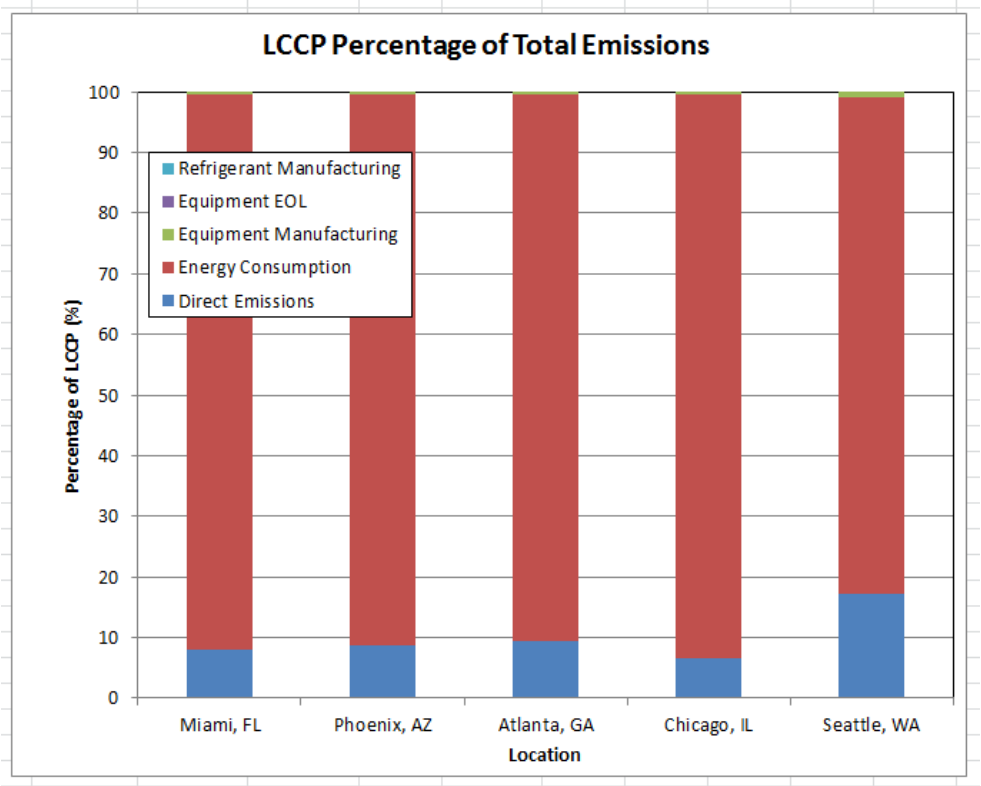

Figure 27: Percentage of LCCP

Validation

The results of the tool were compared with the results of the AHRI LCCP tool. All values were within 5%.

Chapter 6 : Improving LCCP with the Use of Advanced Cycle Options

Advanced cycle options aim to improve the performance of the basic VCC. These technologies can be categorized into three categories: subcooling cycles, expansion loss recovery cycles, and multi-stage cycles. Three different cycles were modeled and then the results were incorporated into the LCCP calculation presented in Chapter 4. The cycle models used are accepted models and assumptions from literature.

6.1 Modeling Approach

The basic VCC and the four advanced cycles were modeled in Engineering Equation Solver (EES). The assumptions for each cycle are detailed in this section. The ambient and room conditions were held constant for all the cycles. The test conditions from the AHRI 210/240 Standard were used to compare the performance of the cycles. The test conditions used are shown in Table 30.

Table 30: AHRI 210/240 Standard Test Conditions

Test	Outdoor Dry Bulb [°C]	Outdoor Wet Bulb [°C]	Indoor Dry Bulb [°C]	Indoor Wet Bulb [°C]
A	35	23.9	26.7	19.4
B	27.8	18.3	26.7	19.4
H1	8.33	6.11	21.1	15.6
H2	1.67	0.56	21.1	15.6
H3	-8.33	-9.44	21.1	15.6

6.1.1 Basic Vapor Compression Cycle

The basic VCC was modeled using EES as a four component cycle with a compressor, condenser, thermal expansion valve and a condenser. The system schematic is shown in Figure 28. System information from the Goodman SZ14-0361B system [87] and AREP #20 [88] experimental set up were used in the model. The experimental results in AREP #20 were used to validate the basic cycle model [88].

Table 31: Basic VCC Modeling Assumptions

Compressor Efficiency	(0.9-0.0467*PR)*.95
Isentropic Efficiency	0.9-0.0467*PR
Volumetric Efficiency	1-0.04*PR
Motor Efficiency	0.90
Condenser Air Flow Rate	0.59 m^3/s
Evaporator Air Flow Rate	0.63 m^3/s
Compressor RPM	3,500
Compressor Displacement	27.4 cc/rev

The pressures and the subcooling and superheating values were taken from the experimental tests performed in AREP #20. Each test result included the measured pressures and degrees of subcooling and superheating. These values are listed in Table 32.

Table 32: Basic VCC Modeling Pressure and Temperature Assumptions

AHRI 210/240 Test	A	B	H1	H2	H3
Low Pressure (kPa)	1099	1082.7	835.8	710.2	521.7
High Pressure (kPa)	2608.8	2201.1	2304.5	2160.1	1943.3
Subcooling (°C)	3	3	9	10	10
Superheating (°C)	2	2	5	5	5

The cycle was modeled as a simple four component VCC, with a compressor, condenser, expansion device and an evaporator. The model configuration is shown in

Figure 28. It was assumed that there was no pressure drop across the condenser or evaporator. The unit used a thermal expansion valve for cooling applications and an orifice for heating.

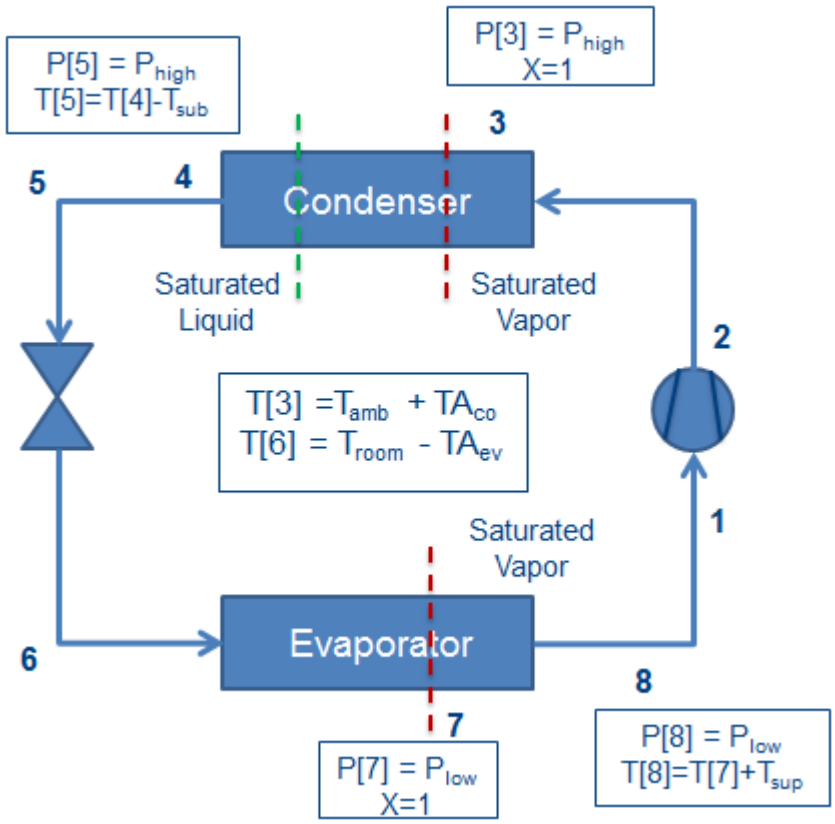

Figure 28: Basic VCC Model Configuration

The approach temperatures, the temperature difference between the ambient and the condenser and the temperature difference between the evaporator and the room temperature, were determined using the test conditions shown in Table 30. The pinch point method was used to the model to calculate these values. The approach temperature for the condenser and evaporator was calculated using the following equations:

$$T[3] = T_{amb} - TA_{co} \tag{4}$$

$$T[6] = T_{room} - TA_{ev} \quad (5)$$

Where T[3] is saturated vapor at high pressure in the condenser and T[6] is the vapor released from the expansion device. The values were then used for all the other cycle models for that respective test.

The compressor was modeled using the efficiency equations presented in Table 33 and the assumed system characteristics including compressor displacement and RPM from AREP #20.

Isenthalpic expansion was assumed in the expansion valve for both heating and cooling conditions. The system uses a thermal expansion valve for cooling and an orifice for heating.

It was assumed that the condenser fan has a flow rate of 0.59 m^3/s and the evaporator has a flow rate of 0.63 m^3/s. The values were obtained from the AREP #20 report and the specifications of the Goodman unit used. The fan work was modeled using the following equation where the volume flow rate is in m^3/s.

$$W_{fan} = 0.775 * \dot{V}_{air} \quad (6)$$

The system performance of the unit was calculated in terms of COP. The total work of the unit was summed including the work of the fans and the compressor. The capacity in cooling mode was calculated using the evaporator and the capacity in heating mode was calculated using the condenser.

$$Q_{evap} = MFR_{ref}(h_8 - h_6)\,; Q_{cond} = MFR_{ref}(h_2 - h_5) \quad (7)$$

$$W_{total} = W_{compressor} + W_{cond,fan} + W_{evap,fan} \quad (8)$$

$$COP_{cooling} = Q_{evap}/W_{total};\ COP_{heat} = Q_{cond}/W_{total} \quad (9)$$

6.1.2 Suction Line Heat Exchanger Cycle

The suction line heat exchanger cycle was modeled using EES. The cycle configuration is shown in Figure 29. The assumptions listed in Table 33 were used in the model. The approach temperatures were determined in basic VCC model and were used in the SLHX model. The efficiency assumptions from the basic VCC model were also used. The SLHX itself was assumed to have an efficiency of 0.7.

Table 33: SLHX Cycle Model Assumptions

Compressor Efficiency	(0.9-0.0467*PR)*.95
Isentropic Efficiency	0.9-0.0467*PR
Volumetric Efficiency	1-0.04*PR
Motor Efficiency	0.9
SLHX Effectiveness	0.7
Condenser Air Flow Rate	0.59 m^3/s
Evaporator Air Flow Rate	0.63 m^3/s
Compressor RPM	3,500
Compressor Displacement	0.0000274 m^3/rev

Table 34: SLHX Cycle Model Pressure Assumptions

Test	A	B	H1	H2	H3
Low Pressure (kPa)	1,099.0	1,082.7	835.8	710.2	521.7
High Pressure (kPa)	2,608.8	2,201.1	2,304.5	2,160.1	1,943.3
Subcooling (°C)	3	3	9	10	10
Superheating (°C)	2	2	5	5	5
TA_{ev} (°C)	16.3	16.9	7.0	5.3	4.4
TA_{co} (°C)	8.0	8.2	16.8	14.2	10.0

The SLHX was assumed to be located between the condenser and the expansion valve for the high pressure side and between the evaporator and the compressor for the low pressure side. The other components in the system remained the same as the basic VCC.

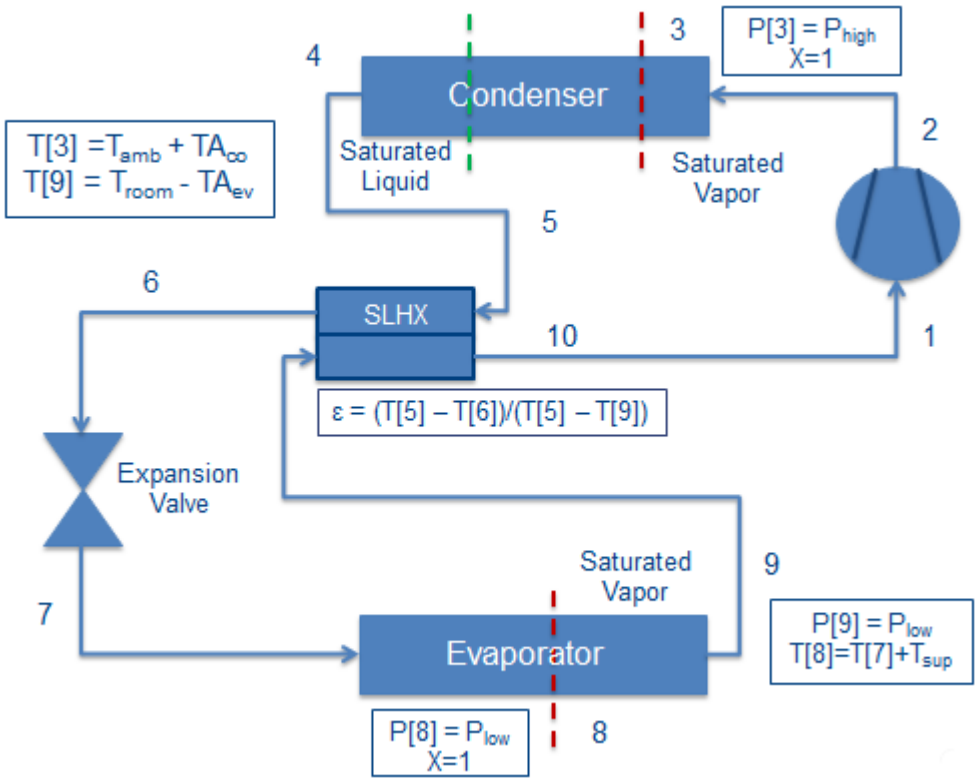

Figure 29: SLHX Cycle Model Configuration

The suction line heat exchanger was modeled using its effectiveness using the following equations. The assumed pressures and approach temperatures were used to determine the enthalpies at the state points.

$$\varepsilon_{SLHX} = (T_5 - T_6)/(T_5 - T_9) \tag{10}$$

$$h_{10} - h_9 = h_5 - h_6 \tag{11}$$

The other components in the system were modeled the same way as the basic VCC. The system performance was also calculated in the same way as the basic VCC model.

6.1.3 Expander Cycle

The expander cycle was modeled using EES. The cycle configuration is shown in Figure 30. The assumptions listed in Table 35 and Table 36 were used in the model. The same pressures and degrees of subcooling and superheating used in the basic cycle were used in the expander cycle. The approach temperatures calculated from the basic VCC were also applied to the expander cycle. The expander was assumed to have an effectiveness of 70%. The expander was mechanically connected to the compressor. The linkage was assumed to have an efficiency of 95%.

Table 35: Expander Cycle Modeling Assumptions

Compressor Efficiency	(0.9-0.0467*PR)*0.95
Isentropic Efficiency	0.9-0.0467*PR
Volumetric Efficiency	1-0.04*PR
Compressor Motor Efficiency	0.8
Expander Efficiency	0.7
Expander Mechanical Efficiency	0.95
Condenser Air Flow Rate	0.59 m^3/s
Evaporator Air Flow Rate	0.63 m^3/s
Compressor RPM	3,500
Compressor Displacement	27.4 cc/rev

Table 36: Expander Cycle Model Pressure Assumptions

Test	A	B	H1	H2	H3
Low Pressure (kPa)	1,099	1,082.7	835.8	710.2	521.7
High Pressure (kPa)	2,608.8	2,201.1	2,304.5	2,160.1	1,943.3
Subcooling (°C)	3	3	9	10	10
Superheating (°C)	2	2	5	5	5
TA_{ev} (°C)	16.3	16.9	7.0	5.3	4.4
TA_{co} (°C)	8.0	8.2	16.8	14.2	10.0

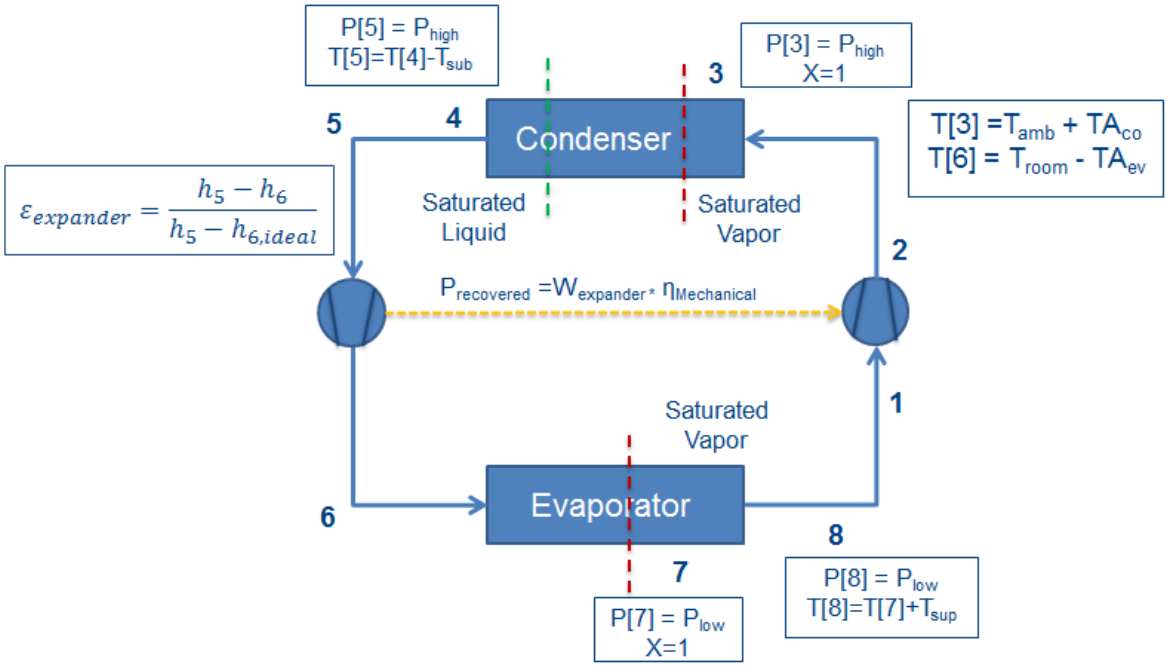

Figure 30: Expander Cycle Model Configuration

The expander was modeled as a compressor in reverse. An enthalpy balance was used to determine the conditions of the exiting vapor.

$$\varepsilon_{expander} = (h_5 - h_6)/(h_5 - h_{6,ideal}) \tag{12}$$

The performance of the system was calculated by taking the work done by the compressor and the fans and subtracting the work recovered from the expander. The work of the expander was multiplied by a generator efficiency to account for losses as mechanical work is converted back to electricity.

$$W_{total} = W_{compressor} + W_{fan,cond} + W_{fan,evap} - W_{expander}\eta_{mechanical} \tag{13}$$

The other components of the cycle were modeled the same was as they were in the basic VCC model.

6.1.4 Ejector Cycle

The ejector cycle was modeled in EES. The ejector was treated as the expansion device in the cycle. The pressures, the degrees of subcooling and superheating, and the approach temperatures that were determined in the basic cycle were used in this model. The assumptions are listed in Table 37 and Table 38.

Table 37: Ejector Cycle Modeling Assumptions

Compressor Efficiency	(0.9-0.0467*PR)*0.95
Isentropic Efficiency	0.9-0.0467*PR
Volumetric Efficiency	1-0.04*PR
Motor Efficiency	0.9
Condenser Air Flow Rate	0.59 m^3/s
Evaporator Air Flow Rate	0.63 m^3/s
Compressor RPM	3,500
Compressor Displacement	27.4 cc/s
Ejector Motive Nozzle Efficiency	0.5
Ejector Suction Nozzle Efficiency	0.5
Ejector Diffuser Efficiency	0.5

Table 38: Ejector Cycle Pressure and Temperature Modeling Assumptions

Test	A	B	H1	H2	H3
Low Pressure (kPa)	1,099.0	1,082.7	835.8	710.2	521.7
High Pressure (kPa)	2,608.8	2,201.1	2,304.5	2,160.1	1,943.3
Subcooling (°C)	3	3	9	10	10
Superheating (°C)	2	2	5	5	5
TA_{ev}	16.3	16.9	7.0	5.3	4.4
TA_{co}	8.0	8.2	16.8	14.2	10.0

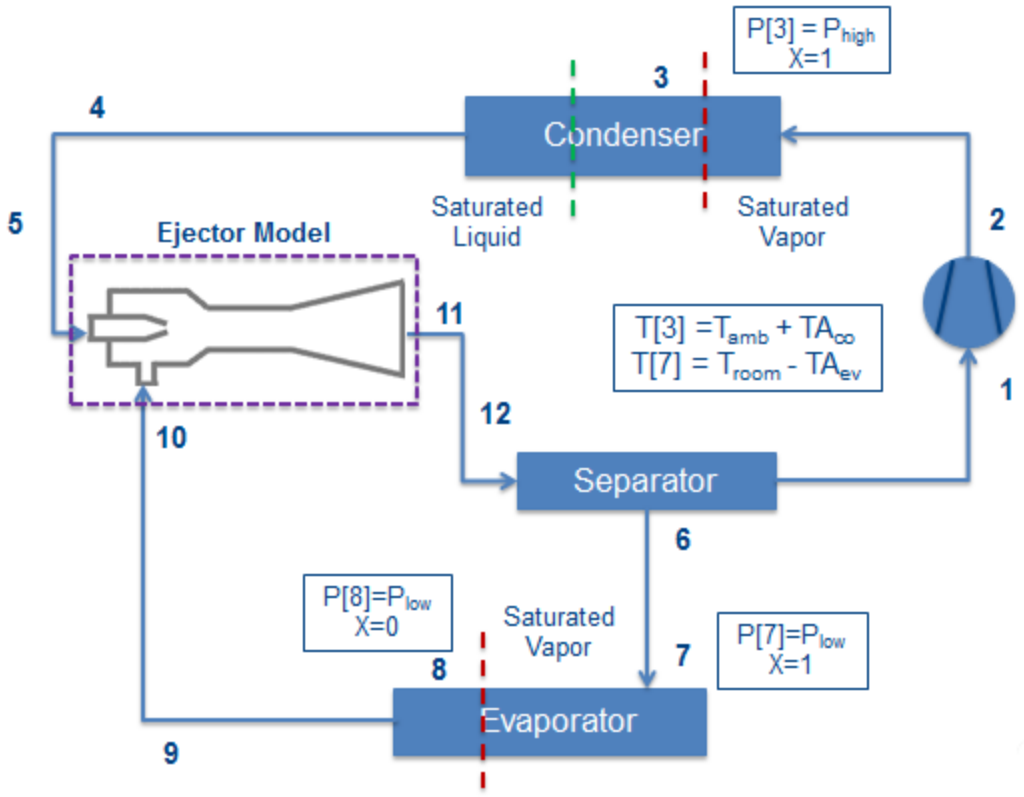

Figure 31: Ejector Cycle Model Configuration

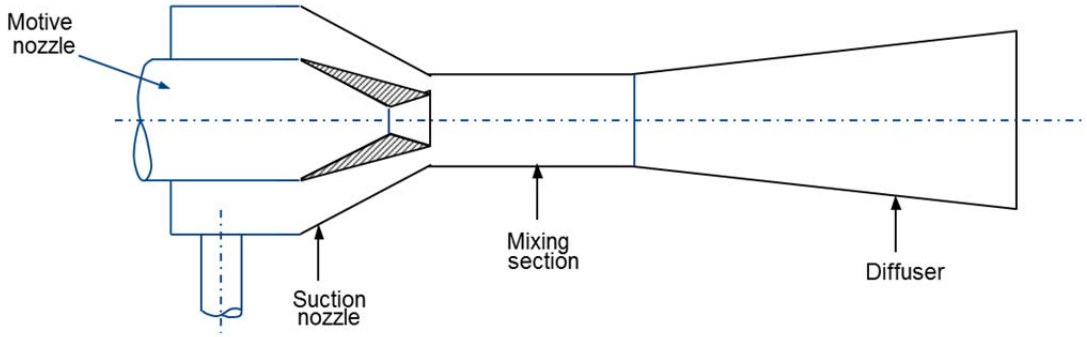

Figure 32: Ejector Components [32]

The ejector itself was modeled in four sections: the motive nozzle, the suction nozzle, the mixing section and the diffuser. The sections of the ejector are shown in Figure 32. The expansion in the motive nozzle of the ejector was modeled using an enthalpy balance. The expansion in this section of the nozzle is assumed to be isentropic for

the ideal case. The real enthalpy value of the exiting stream was calculated using the efficiency equation shown below.

$$\eta_{motive} = (h_5 - h_{m,real})/(h_5 - h_{m,ideal}) \quad (14)$$

The $h_{m,real}$ was then used to determine the velocity, u_m, of the motive stream at the inlet of the mixing section. The specific volume of the stream is determined using the enthalpy and the assumed pressure. The properties are used to determine a_m.

$$u_{m,real} = \sqrt{2 * (h_5 - h_{m,real}) * 1000} \quad (15)$$

$$a_m = v_m/u_{m,real} * (1 + w) \quad (16)$$

The suction nozzle of the ejector was modeled similarly. This part of the ejector accepts the vapor refrigerant that exits the evaporator. The expansion process in the suction nozzle is also considered to be isentropic in the ideal case.

$$\eta_{suction} = (h_{10} - h_{s,real})/(h_{10} - h_{s,ideal}) \quad (17)$$

$$u_{s,real} = \sqrt{2 * (h_{10} - h_{s,real}) * 1000} \quad (18)$$

$$a_s = \frac{v_s}{u_s} * \frac{w}{(1 + w)} \quad (19)$$

A system of equations was used to solve for the properties in the mixing and diffuser sections. The diffuser is modeled as an ideal isentropic process. The efficiency is then used to solve for the real conditions.

$$(1 + w)h_{dis.ideal} = h_3 + w * h_{10} \quad (20)$$

$$\eta_{dis} = (h_{dis,real} - h_{mix})/(h_{dis,ideal} - h_{mix}) \quad (21)$$

The properties of the motive and the suction nozzles and the diffuser are combined in the mixing section of the ejector. The pressure drop across the ejector is

assumed to be 10 Pa. The specific volume of the mixture is calculated using a property call function in EES.

$$\left(P_{10} - \Delta P_{ej}\right)(a_m + a_s)1000 + \frac{1}{(1+w)}u_m + \frac{w}{(1+w)}u_s = P_m(a_m + a_s) * 1000 + u_{mix} \quad (22)$$

$$h_3 * 1000 + w * h_{10} * 1000 = (1+w)\left(h_{mix} * 1000 + {}^1/_2\, u_{mix}{}^2\right) \quad (23)$$

$$(a_m + a_s) * \frac{u_{mix}}{v_{mix}} = 1 \quad (24)$$

The performance of system is evaluated using the same method as the basic VCC. The heat moved by the condenser determines the heating capacity and the heat moved by the evaporator determines the cooling capacity.

6.1.5 Vapor Injection Flash Tank Cycle

The vapor injection flash tank cycle was modeled in EES. A two stage compression process was assumed in the cycle. The pressures and approach temperatures determined in the basic cycle model were used in this model. The cycle was assumed to have a two stage compressor.

Table 39: Vapor Inject Flash Tank Cycle Modeling Assumptions

Compressor Efficiency	(0.9-0.0467*PR)*0.95
Isentropic Efficiency	0.9-0.0467*PR
Volumetric Efficiency	1-0.04*PR
Motor Efficiency	0.9
Condenser Air Flow Rate	0.59 m^3/s
Evaporator Air Flow Rate	0.63 m^3/s
Compressor RPM	3,500
Compressor Displacement	27.4 cc/s
Vapor Injection Compression	2 stage compressor

Table 40: Vapor Injection Flash Tank Cycle Modeling Assumptions

Test	A	B	H1	H2	H3
Low Pressure (kPa)	1,099.0	1,082.7	835.8	710.2	521.7
High Pressure (kPa)	2,608.8	2,201.1	2,304.5	2,160.1	1,943.3
Subcooling (°C)	3	3	9	10	10
Superheating (°C)	2	2	5	5	5
TA_{ev}	16.3	16.9	7.0	5.3	4.4
TA_{co}	8.0	8.2	16.8	14.2	10.0

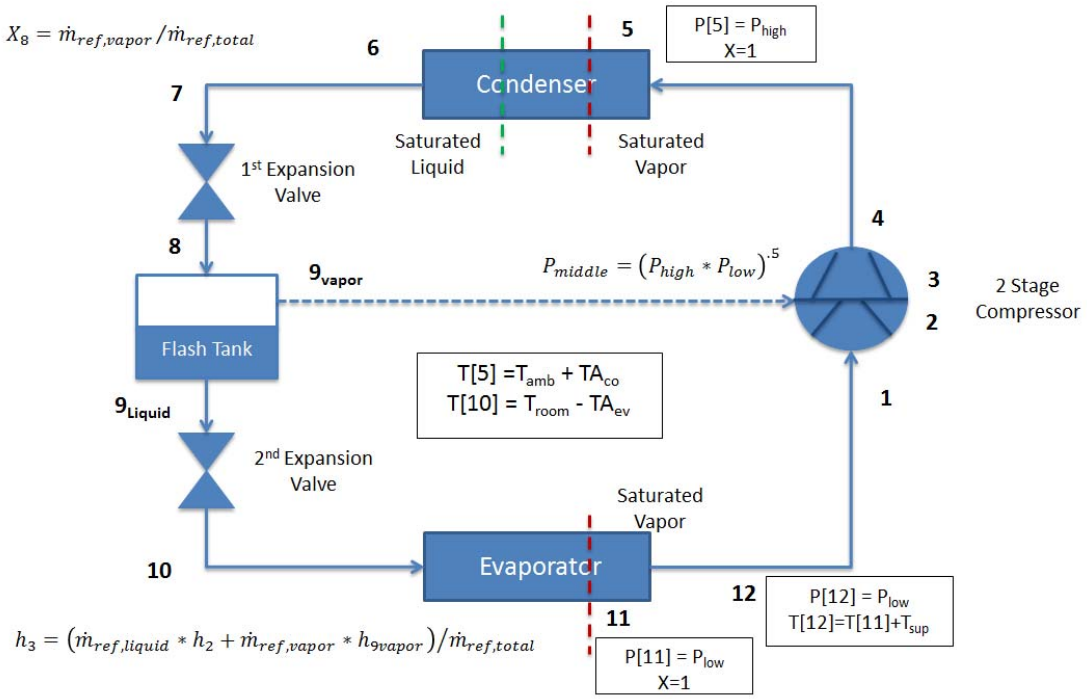

Figure 33: Flash Tank Vapor Injection Model Configuration

The compressor in the vapor injection system is assumed to be a two stage compressor with the vapor being injected at the middle pressure. The isentropic efficiency and motor efficiencies were applied to each stage. The middle pressure was calculated using a ratio of the high and low pressure.

$$P_{middle} = (P_{high} * P_{low})^{.5} \quad (25)$$

The amount of vapor that was separated was calculated using a mass and enthalpy balance. The enthalpy of state point 9_{vapor} was calculated using the middle pressure and a quality of 1.

$$h_3 = \left(\dot{m}_{ref,liquid} * h_2 + \dot{m}_{ref,vapor} * h_{9vapor}\right)/\dot{m}_{ref,total} \quad (26)$$

$$X_8 = \dot{m}_{ref,vapor}/\dot{m}_{ref,total} \quad (27)$$

The capacity of the condenser was calculated using the total mass flow rate of the refrigerant and the capacity of the evaporator was calculated using the mass flow rate of the liquid refrigerant, $\dot{m}_{ref,liquid}$.

6.2 LCCP Comparison Approach

The effects of the cycles were then evaluated on their effect on the LCCP of the cycle option. Parametric studies were performed for each of the cycles for each of the temperatures bins shown in Table 5. The capacities and power consumption was calculated for each bin. A ratio was used to calculate the prorated power consumption of the advanced cycle unit.

$$\frac{Advanced\ Cycle\ Capacity}{Advanced\ Cycle\ Power\ Consumption} = \frac{Basic\ VCC\ Capacity}{Advanced\ Cycle\ Prorated\ Power\ Consumption} \quad (28)$$

From the prorated power consumption, the percent change between the advanced cycle and the basic cycle was calculated. The percent change in energy consumption for each bin was then applied to the energy consumption of the basic VCC model. The LCCP for each cycle was then calculated using the IIR LCCP excel tool and compared to the basic VCC results and each other.

6.3 Modeling Results

6.3.1 Basic Vapor Compression Cycle

The model was then compared for the AHRI 210/240 standard test conditions with the results shown in Table 41.

Table 41: Basic VCC Modeling Results

AHRI Std Test	A	B	H1	H2	H3
Q_{eva} (kW)	9.70	10.45	7.97	6.85	4.98
Q_{cond} (kW)	11.49	11.88	9.60	8.38	6.36
W_{tot} (kW)	2.80	2.43	2.63	2.53	2.36
$COP_{cooling}$	3.47	4.31	3.03	2.70	2.11
$COP_{heating}$	4.11	4.90	3.65	3.31	2.69
TA_{ev} (°C)	16.3	16.9	7.0	5.3	4.4
TA_{co} (°C)	8.0	8.2	16.8	14.2	10.0
MFR (kg/s)	0.068	0.060	0.044	0.037	0.026

The results of the model were compared to the experimental data generated by AREP #20. AREP #20 used the ASHRAE Std. 116-1995. This standard requires a different set of tests than AHRI Std. 210/240. Several of them require the same conditions and the results are listed in Table 42. The H2 test was not performed so placeholders have been inserted. The difference in capacity and the difference in power consumption between the model and the unit data were determined for each test. A negative value indicates the results are less than the unit data. A positive value indicates that the results are higher than the unit data.

The capacities demonstrate the correct trends. The capacity decreases as the test conditions become more extreme. The capacity of test A is lower than that of test B as well as H3 is much lower than H1. The mass flow rate correctly increases with

the temperature and the power consumption also increases with the higher mass flow rate.

The model results show good agreement for all tests. The largest disagreement occurs in the heating tests. The heating tests, especially H3 are more difficult to perform than the cooling tests leading to more unreliable data. However, the model predicted the performance of the unit within 6.4%.

Table 42: AREP #20 Experimental Data versus Basic VCC Model Results

AHRI Std Test	A	B	H1	H2	H3
% Difference Capacity	-0.8%	-1.0%	-6.4%	-	6.0%
% Difference Power	1.0%	0.2%	3.1%	-	0.9%

Property diagrams were generated for the cycle. The temperature-entropy diagram and pressure-enthalpy diagram were created for the cycle. Both diagrams demonstrate the appropriate patterns.

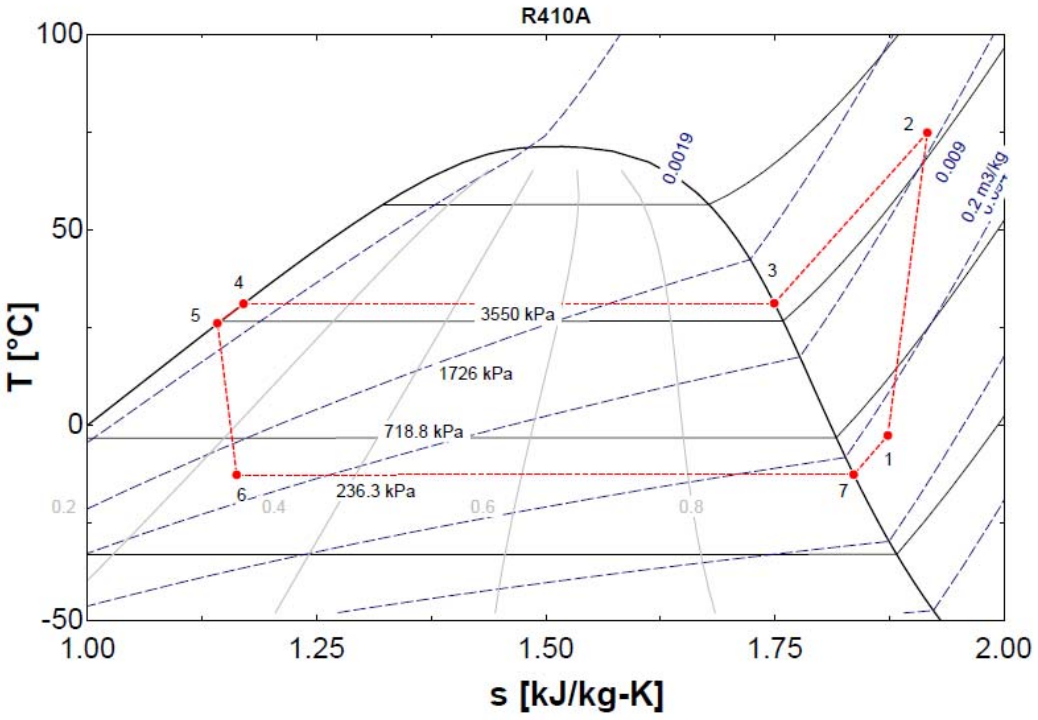

Figure 34: Basic VCC Model in T-s Diagram

The cycle in the T-s diagram shows the sloped line from state 1 to 2 correctly including the compressor efficiency. The first part of the condenser removes the majority of the heat which is demonstrated by state points 2-4. State point 5 represents the inlet to the expansion device. The line to state point 6 represents the expansion of the refrigerant. State points 6 and 7 represent the evaporator.

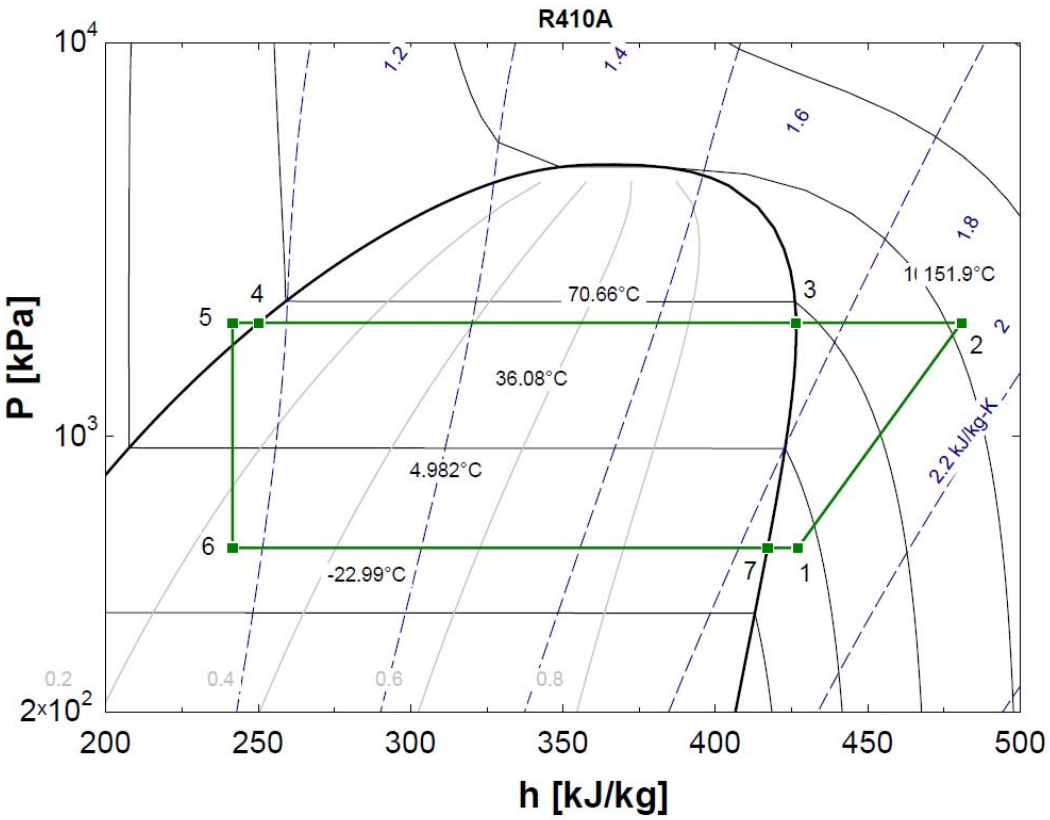

Figure 35: Basic VCC Model in P-h diagram

The P-h diagram also shows the correct pattern. It shows the two pressure levels without pressure drops through the evaporator and condenser. The isenthalpic expansion through the expansion device is shown between state points 5 and 6.

The UA values were calculated for both the evaporator and condenser in heating and cooling modes. The UA values decreased slightly as the temperatures increased for the cooling mode and as temperatures decreased in heating mode. The same trend is observed in the capacity of the unit itself. The UA values are shown in Figure 36 and Figure 37.

.

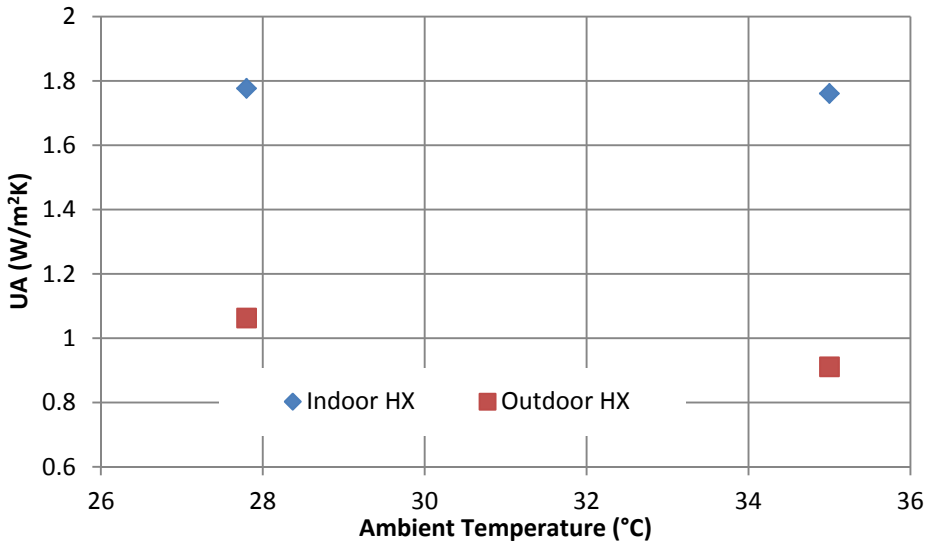

Figure 36: Basic VCC Model Cooling UA Comparison

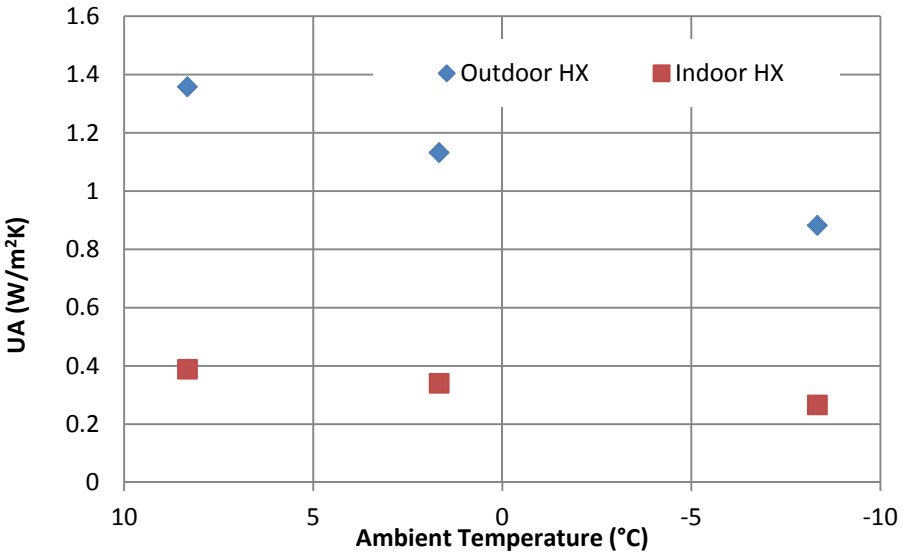

Figure 37: Basic VCC Model Heating UA Comparison

6.3.2 Suction Line Heat Exchanger

The EES model was used to determine the performance of a SLHX cycle at the AHRI Std. 210/240 test conditions. The results are shown in Table 43.

Table 43: SLHX Model Results

AHRI Std. Test	A	B	H1	H2	H3
Q_{eva} (kW)	9.71	10.34	7.89	6.72	4.91
Q_{cond} (kW)	11.42	11.71	9.45	8.23	6.22
W_{tot} (kW)	2.82	2.44	2.64	2.54	2.37
$COP_{cooling}$	3.45	4.24	3.00	2.66	2.07
$COP_{heating}$	4.05	4.81	3.58	3.24	2.62
MFR (kg/s)	0.050	0.052	0.038	0.031	0.223

The mass flow rate of the SLHX cycle shows the correct trend by decreasing slightly from the MFR in the basic cycle for each cycle. The mass flow rate was the highest in the more temperature test conditions. As the tests became more extreme the capacity of the unit decreased for both heating and cooling.

Property plots were generated for the cycle. The temperature-entropy diagram clearly shows in the impact of the SLHX. It is show between points 5 and 6 and between points 9 and 1. The SLHX transfers heat to the compressor inlet stream ensuring that only superheated vapor enters into the compressor. The pressure-enthalpy diagram demonstrates the correct pattern. The SLHX extends the processes further into the liquid and vapor zones.

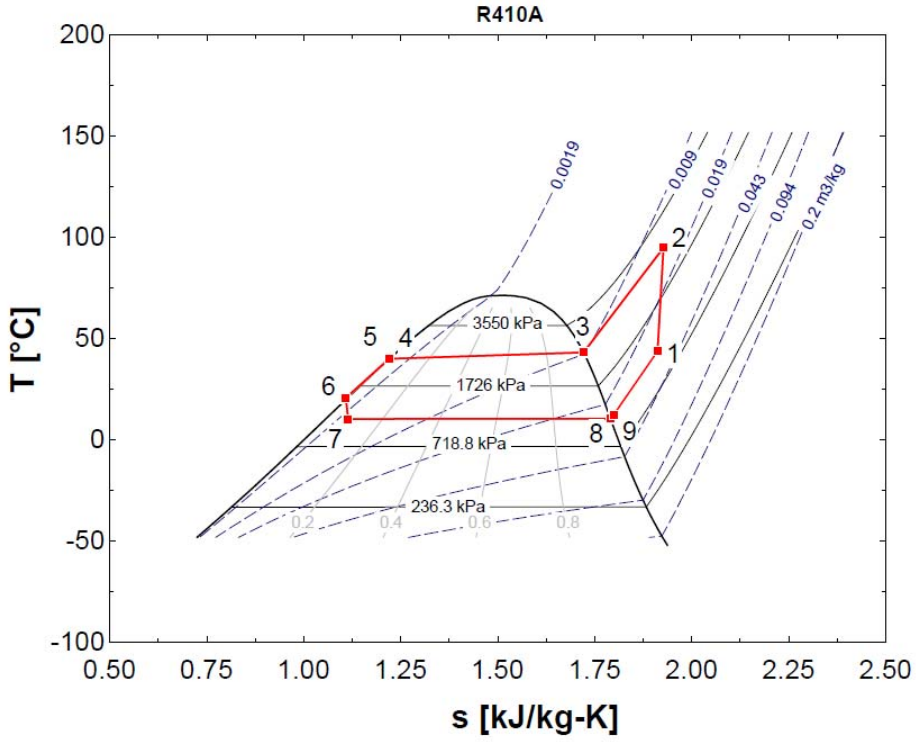

Figure 38: SLHX Cycle in T-s Diagram

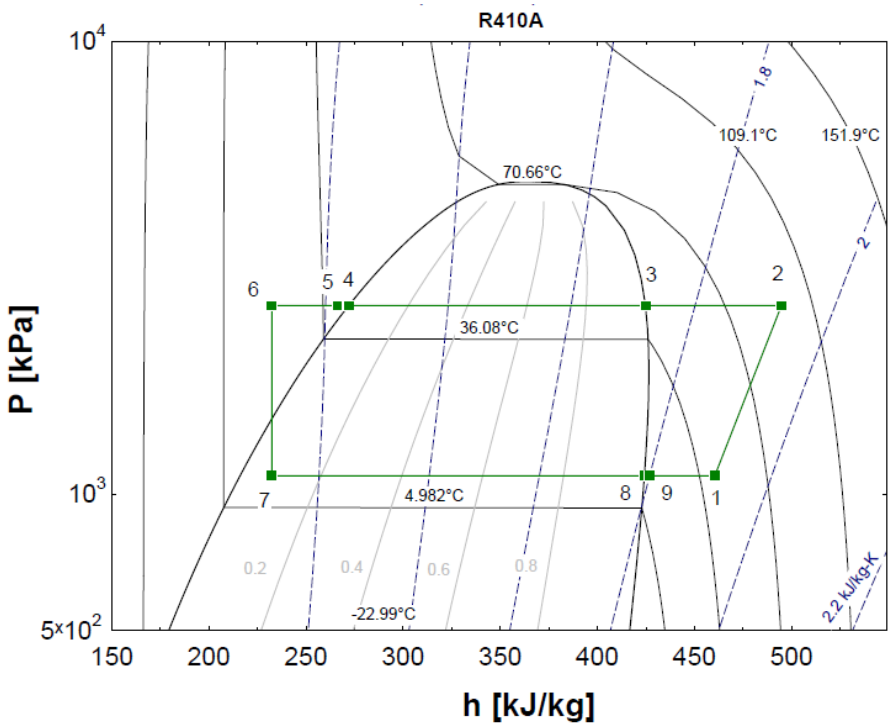

Figure 39: SLHX Cycle in P-h Diagram

The results of the SLHX model were then compared the results of the basic VCC model. The comparison is shown in Table 44. The capacities of the unit increased by 0.1% for Test A and decreased for all of the other cycles. The power consumption increased slightly for all of the tests.

Table 44: SLHX Model Results versus Basic VCC Model Results

AHRI Std Test	A	B	H1	H2	H3
% Difference Capacity	0.1%	-1.1%	-1.5%	-1.8%	-2.2%
% Difference Power	0.7%	0.4%	0.5%	0.5%	0.4%

The model demonstrates that a SLHX is ineffective for the refrigerant R-410A. The capacity of the system decreases while in general the power consumption increases. This would require a bigger system to still maintain the same capacity as the basic VCC.

6.3.3 Expander Cycle Modeling Results

The results from the expander cycle model are shown in Table 45. The cycle was modeled for the test conditions detailed in AHRI Std. 210/240.

Table 45: Expander Cycle Modeling Results

AHRI Std. Test	A	B	H1	H2	H3
Q_{eva} (kW)	9.87	10.56	8.07	6.96	5.06
Q_{cond} (kW)	11.40	11.81	9.51	8.29	6.29
W_{tot} (kW)	2.64	2.32	2.53	2.40	2.28
$COP_{cooling}$	3.74	4.55	3.20	2.84	2.22
$COP_{heating}$	4.32	5.09	3.76	3.40	2.75
MFR (kg/s)	0.060	0.060	0.043	0.037	0.026

The results of the model demonstrate the expected results. The mass flow rate decrease with temperature. The values are also reduced from the basic VCC in cooling tests where the capacity of the cycle increased. The power consumption followed the same pattern as basic VCC. For the cooling tests, the higher the ambient temperature, the more power was required. For the heating tests, the power requirement was reduced as the temperature dropped.

Property plots for the expander cycle were constructed. Temperature-entropy plots and pressure-enthalpy plots were generated. The plots are shown in Figure 40 and Figure 41.

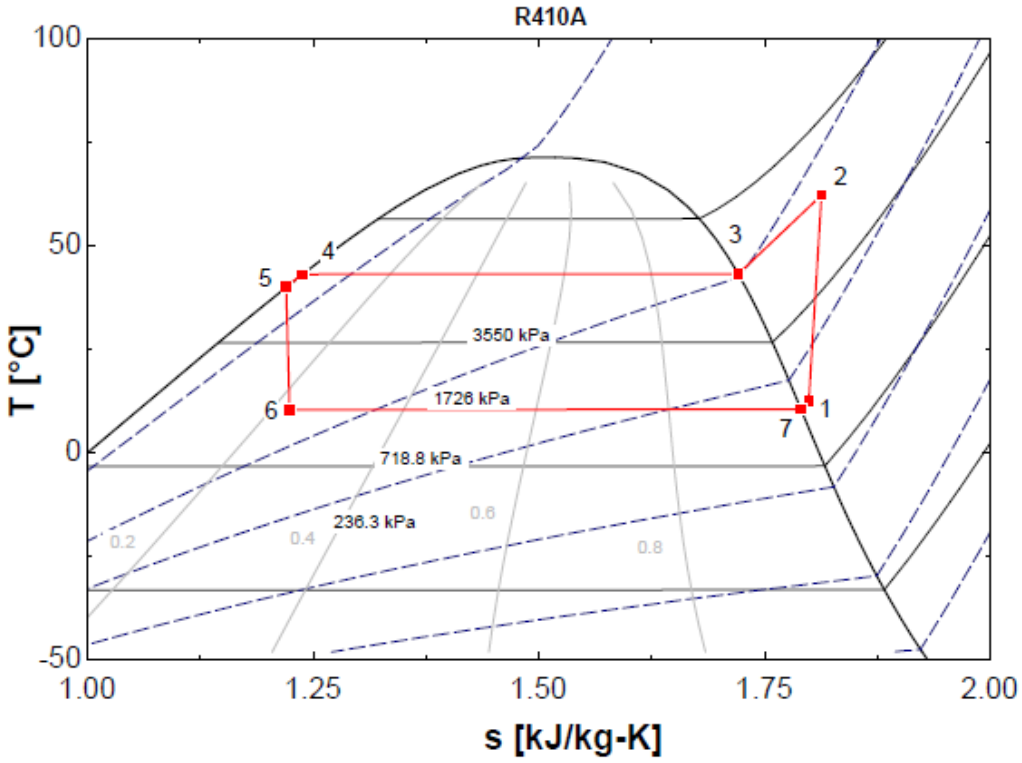

Figure 40: Expander Model in T-s Diagram

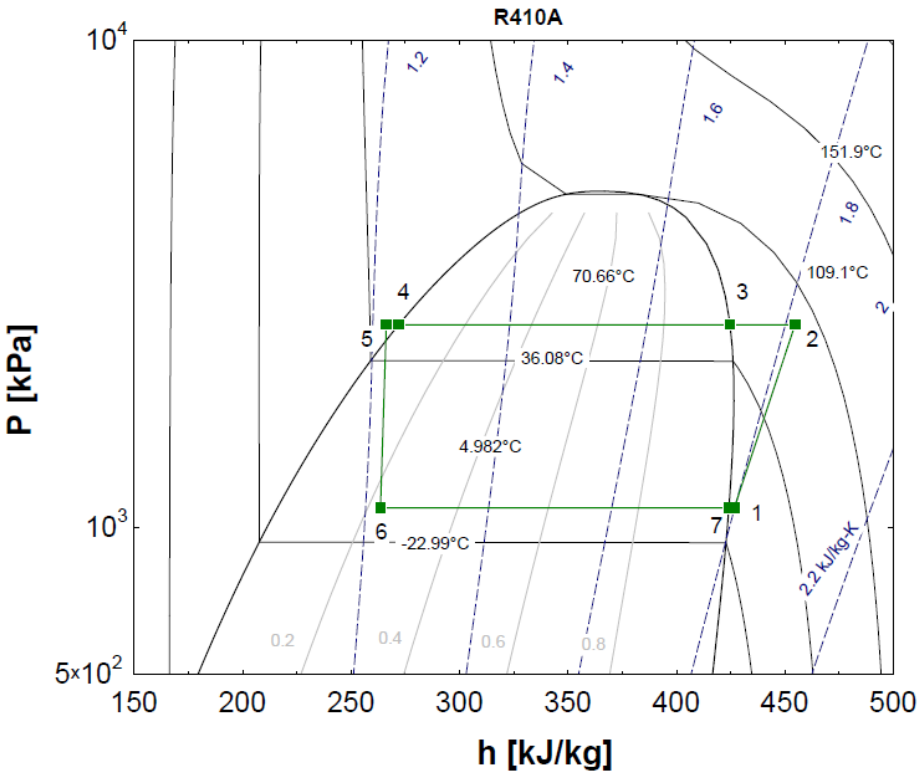

Figure 41: Expander Cycle in P-h Diagram

The T-s diagram and the P-h diagram show the expected cycle paths. The use of similar assumptions for the components of the expander cycle compared to the basic cycle resulted in similar plots.

The results of the expander cycle model were then compared to the results from the basic VCC model. The capacity of the cycle increased slightly and the power consumption was reduced by the use of the expander for the cooling cases. The capacity of the unit decreased approximately 1% for all heating cases and the power decreased from 3.9% for Test H1 to 5.1% for Test H2.

Table 46: Expander Cycle Model versus Basic VCC Model

AHRI Std. Test	A	B	H1	H2	H3
% Difference Capacity	1.7%	1.1%	-0.9%	-1.1%	-1.1%
% Difference Power	-5.7%	-4.3%	-3.9%	-5.1%	-3.3%

The expander cycle is effective in reducing the energy consumption of the unit as modeled. The decreased power consumption of the unit compensates for the small decrease in capacity in the heating tests.

6.3.4 Ejector Cycle Modeling Results

The EES ejector cycle modeling results are shown in Table 47: Ejector Cycle Modeling Results are shown in Table 47. The cycle was modeled for the test conditions detailed in AHRI Std. 210/240.

Table 47: Ejector Cycle Modeling Results

AHRI Std Test	A	B	H1	H2	H3
Q_{eva} (kW)	10.24	10.87	7.95	6.79	5.01
Q_{cond} (kW)	12.22	12.45	9.75	8.51	6.55
W_{tot} (kW)	2.68	2.28	2.51	2.41	2.24
$COP_{cooling}$	3.82	4.77	3.17	2.82	2.37
$COP_{heating}$	4.56	5.46	3.89	3.53	2.92
MFR (kg/s)	0.062	0.0616	0.046	0.0385	0.0276

The capacity results show the correct pattern. The capacities decrease as the test conditions become more extreme. The power consumption of the cycle also follows the same pattern as the basic cycle. It increases as the ambient temperature increases for both cooling and heating tests.

A pressure-enthalpy plot was created for the cycle. The plot follows the correct pattern shown by Park et al. [14] in their review of the performance of ejector cycles.

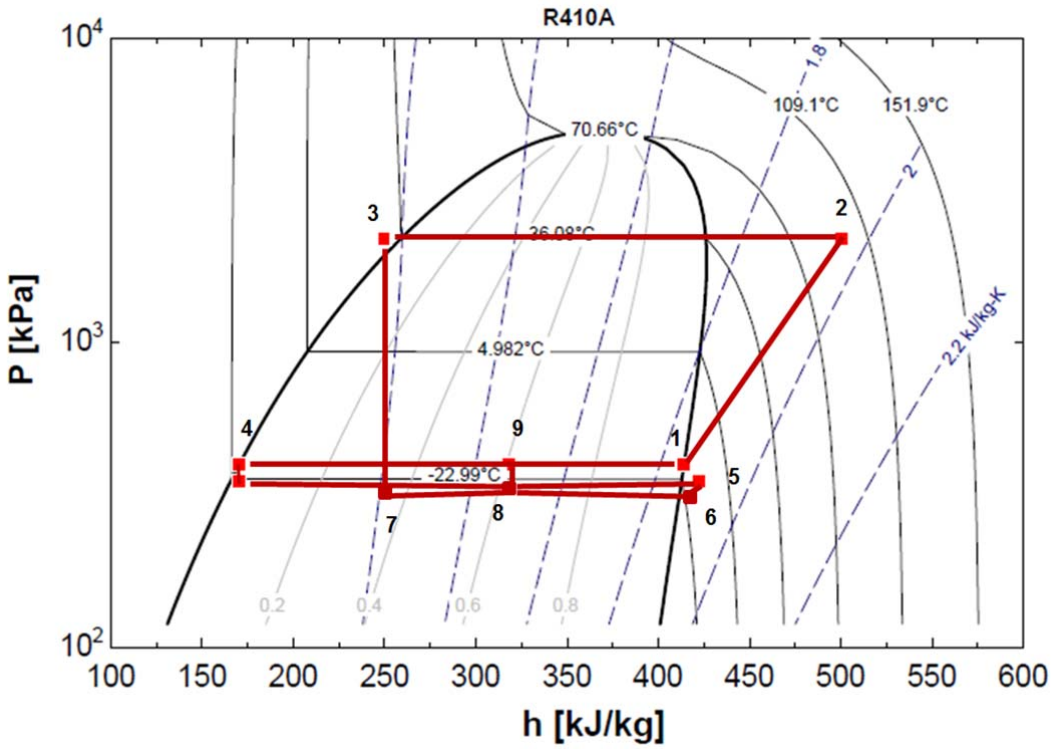

Figure 42: Ejector Cycle in P-h Diagram

The modeling results were compared to the results from the basic VCC model. Power consumption dropped between 4.2% and 5.9%. The capacity increased for all test conditions. The more extreme test conditions exhibited a large increase.

Table 48: Ejector Cycle Model Results versus Basic VCC Model Results

AHRI Std. Test	A	B	H1	H2	H3
% Difference Capacity	5.5%	4.0%	1.6%	1.5%	3.0%
% Difference Power	-4.2%	-5.9%	-4.6%	-4.7%	-5.1%

This cycle is effective in reducing the power consumption of a unit for all of the standard test conditions. The capacity increase is larger in conjunction with the decrease in power consumption make the cycle is more effective at the extreme conditions of A and H3.

6.3.5 Vapor Injection Flash Tank Cycle Modeling Results

The VI-FT modeling results are shown in

Table **49**. The results showed the appropriate trends. The capacities decreased as the test conditions became more extreme for both heating and cooling.

Table 49: VI-FT Cycle Modeling Results

AHRI Std Test	A	B	H1	H2	H3
Q_{eva} (kW)	11.63	11.86	9.11	7.89	5.99
Q_{cond} (kW)	13.44	13.28	10.75	9.44	7.37
W_{tot} (kW)	2.92	2.49	2.69	2.58	2.41
$COP_{cooling}$	3.98	4.76	3.35	3.01	2.46
$COP_{heating}$	4.60	5.33	3.95	3.60	3.02
MFR (kg/s)	0.0627	0.062	0.046	0.039	0.029

The cycle was then placed onto the T-s diagram and the P-h diagram. The cycle showed the expected pattern as compared to the work conducted by Wang et al. [35].

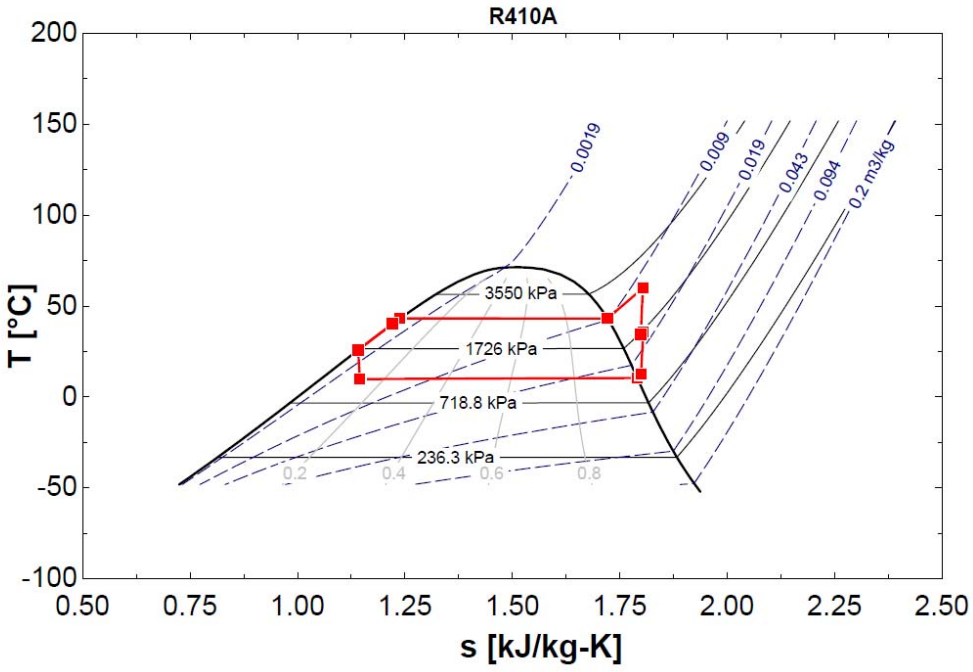

Figure 43: VI-FT Cycle in T-s Diagram

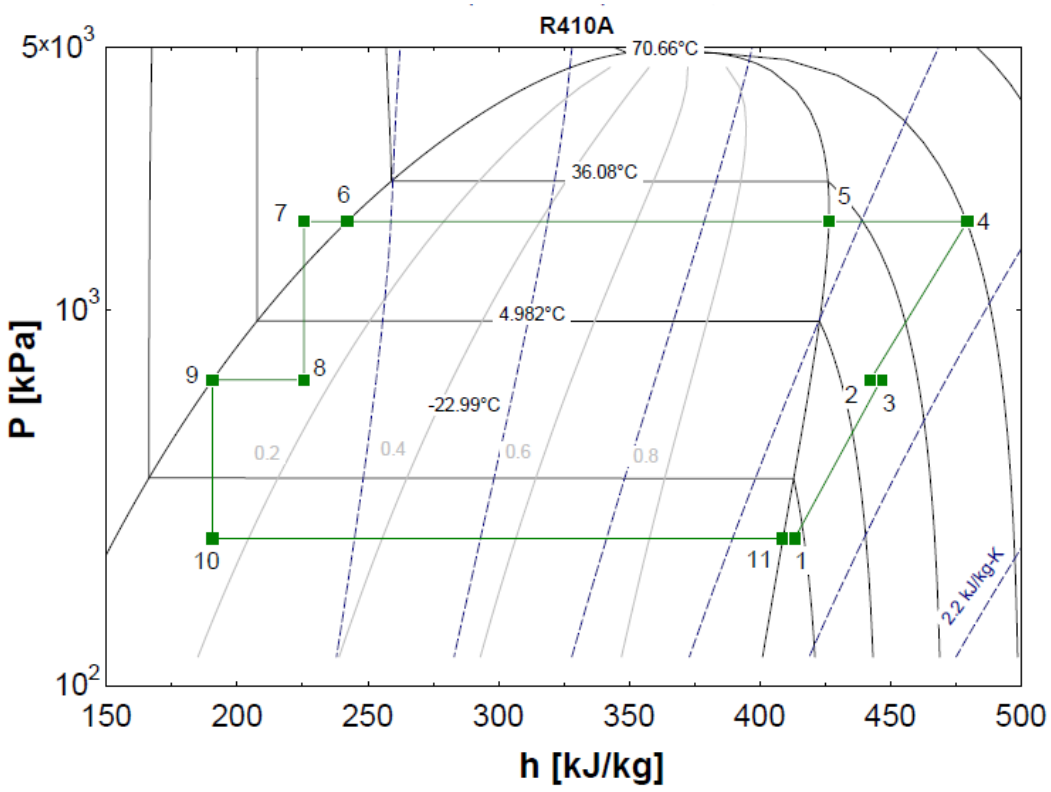

Figure 44: VI-FT Cycle in P-h Diagram

The results of the VI-FT model were then compared to the results of the basic VCC model. The comparison is shown in Table 50. The capacity was increased from 12.0% for H1 to 19.8% for Test A. The power consumption increased between 2.0% to 4.5%.

Table 50: VI-FT Model Results versus Basic VCC Model Results

AHRI Std Test	A	B	H1	H2	H3
% Difference Capacity	19.8%	13.5%	12.0%	12.6%	15.9%
% Difference Power	4.5%	2.8%	2.2%	2.0%	2.0%

The comparison shows the expected results. The VI-FT cycle increases the capacity of the system significantly and also increase the amount of power consumed. The power consumption is compensated for by the large increase in capacity for all of the test conditions. The increased capacity allows a smaller system to be constructed than the basic VCC.

6.3.6 Advanced Cycle Option Comparison

The results of all the advanced cycle options were compared to determine their effectiveness for the unit being evaluated. Each advanced cycle option was compared to the baseline VCC model for each of the test conditions. The results of the comparison are shown in Table 51 and graphically in Figure 45 and Figure 46. A negative value indicates a drop in capacity or a drop in power consumption compared to the baseline value. A positive value indicates an increase in power consumption or capacity as compared to the baseline value.

Table 51: Advanced Cycle Options Performance versus Baseline Model

Cycle Option	AHRI Std 210/240 Test	A	B	H1	H2	H3
Baseline Model vs. Experimental	% Difference Capacity	-0.8%	-1.0%	-10.6%	-	6.0%
	% Difference Power	1.0%	0.2%	3.1%	-	0.9%
Baseline Model Vs. SLHX	% Difference Capacity	0.1%	-1.1%	-0.9%	-1.8%	-2.2%
	% Difference Power	0.7%	0.4%	0.5%	0.5%	0.4%
Baseline Model vs. Expander	% Difference Capacity	1.7%	1.1%	-0.9%	-1.1%	-1.1%
	% Difference Power	-5.7%	-4.3%	-3.9%	-5.1%	-3.3%
Baseline Model vs. Ejector	% Difference Capacity	5.5%	4.0%	1.6%	1.5%	3.0%
	% Difference Power	-4.2%	-5.9%	-4.6%	-4.7%	-5.1%
Baseline Model vs. Vapor Injection	% Difference Capacity	19.8%	13.5%	12.0%	12.6%	15.9%
	% Difference Power	4.5%	2.8%	2.2%	2.0%	2.0%

The vapor injection cycle demonstrated the largest increase in capacity of the cycles modeled. It increased between 19.8% in Test A and 12.0% in Test H1. The expander cycle showed small increases in capacity for the cooling tests and small decreases in capacity for the heating tests. The ejector cycle showed increases in capacity and decreases in power consumption for all tests. The SLHX cycle capacity remained the same or dropped.

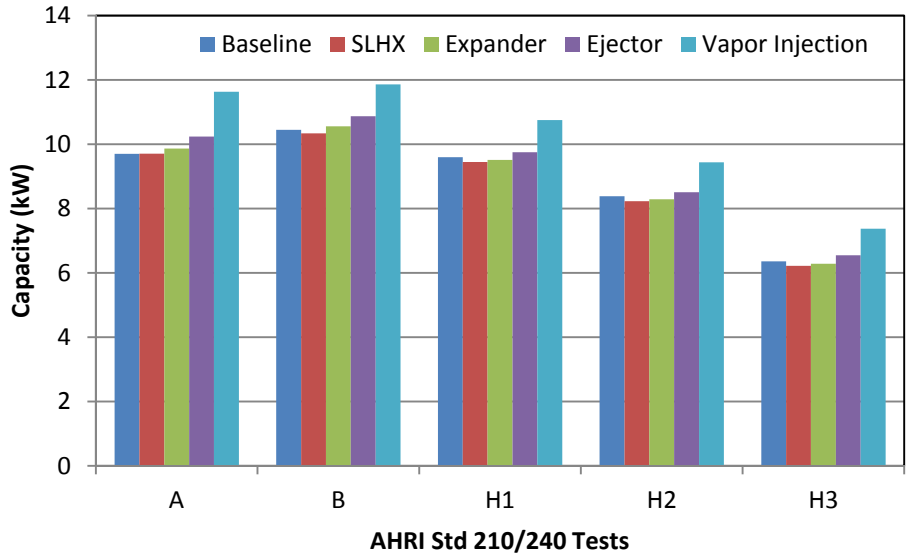

Figure 45: Advanced Cycle Options Capacity Change

The both the expander and ejector cycles showed the most dramatic drop in power consumption for the cycles modeled. The power consumption decreased by 4.2% to 5.9% for the ejector cycle and 3.3% to 5.7% for the expander cycle. The SLHX cycle and the vapor injection increased the power consumption of the unit.

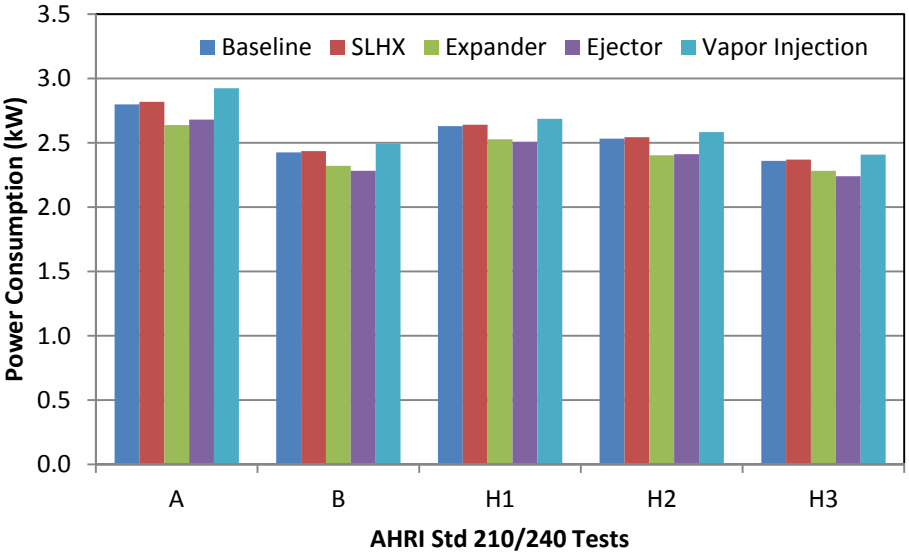

Figure 46: Advanced Cycle Options Power Consumption Change

From the cycle modeling and comparison, the suction line heat exchanger was shown to be ineffective with the unit modeled using R-410A as a refrigerant. The cycle increases the power consumption while decreasing capacity. The expander cycles, the ejector cycles and the vapor injection cycle are effective in reducing the energy consumption of the unit. The vapor injection cycle does this through an increase in capacity and the expander and ejector cycles do this through a decrease in power consumption.

6.4 LCCP Comparison Results

6.4.1 Basic VCC Cycle's LCCP Results

The basic VCC model results were input into the IIR Residential Heat Pump LCCP tool. The assumptions used for this analysis are shown in Table 52.

Table 52: Advanced Cycle Option LCCP Assumptions

Capacity	11 kW
Refrigerant	R-410A
Charge	6 kg
Lifetime	15 years
Unit Mass	115 kg
Annual Leakage Rate	4%
EOL Leakage Rate	15%

The cycle was evaluated in five cities in different climate zones within the United States. The results are show in Table 53 and the energy calculation results are shown in Table 54.

Table 53: Basic VCC Model LCCP Results

Location	Miami, FL	Phoenix, AZ	Atlanta, GA	Chicago, IL	Seattle, WA
LCCP Total Lifetime Emission (kg CO_2e)	99,151	97,040	82,980	133,397	51,290
Total Direct Emission (kg CO_2e)	8,658	8,658	8,658	8,658	8,658
Annual Refrigerant Leakage (kg CO_2e)	6,926	6,926	6,926	6,926	6,926
EOL Refrigerant Leakage (kg CO_2e)	1,732	1,732	1,732	1,732	1,732
Adp. GWP (kg CO_2e)	-	-	-	-	-
Total Indirect Emissions (kg CO_2e)	90,493	88,382	74,322	124,739	42,632
Energy Consumption (kg CO_2e)	90,078	87,967	73,907	124,324	42,217
Equipment Mfg (kg CO_2e)	409	409	409	409	409
Equipment EOL (kg CO_2e)	6.46	6.46	6.46	6.46	6.46
Refrigerant Mfg (kg CO_2e)	103	103	103	103	103

Table 54: Basic VCC Model Energy Calculation Results

Location	Miami, FL	Phoenix, AZ	Atlanta, GA	Chicago, IL	Seattle, WA
Electricity Generation Region	Eastern	Western	Eastern	Eastern	Western
Annual Cooling Energy Consumption (kWh)	7,385.18	8,612.40	3,320.12	1,724.78	480.50
Annual Cooling Emissions (kg CO_2e)	5,819.52	5,115.76	2,616.25	1,359.13	285.41
Heating Climate Region	I	II	III	IV	V
Annual Heating Energy Consumption (kWh)	235.61	1,260.47	2,932.59	8,793.29	4,257.66
Heating Emissions (kg CO_2e)	185.66	748.72	2,310.88	6,929.11	2,529.05

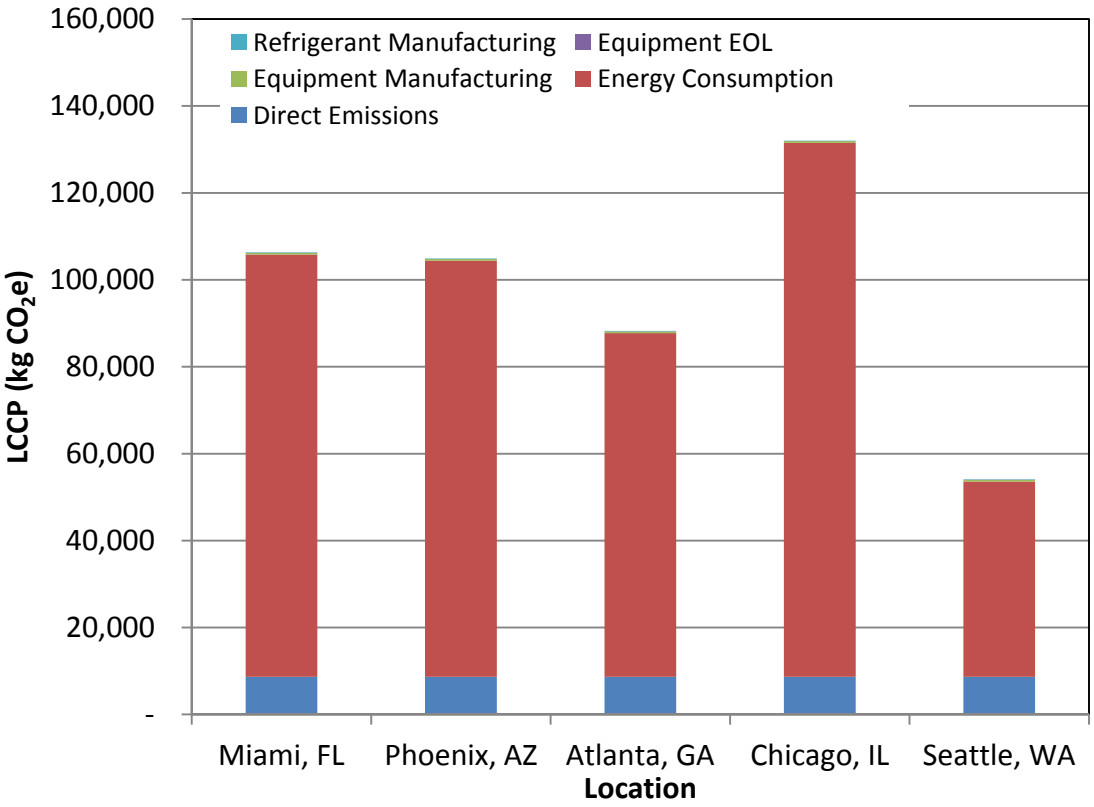

Figure 47: Basic VCC Model LCCP Results

Since the modeling results under estimate the unit's heating capacity at the H3 test, the LCCP tool energy consumption calculation assumes that the lack of capacity is compensated for by an electric resistance heater. The resistance heater is much less efficient than the heat pump forcing the emissions of the unit higher than the unit data indicates.

6.4.2 Advanced Cycle LCCP Results

Each advanced cycle option was evaluated using the LCCP tool developed for the IIR working group. The performance of each of the cycles was calculated for each temperature bin. The prorated power consumption was determined using Equation 28. The From the prorated power consumption, the percentage difference between the

advanced cycle and the basic VCC model was calculated. The results are shown in Table 55 for each of the cycles.

Each cycle's performance varied greatly over the temperature range. The vapor injection cycle and the ejector's performance improved as the temperature became more extreme. The ejector's performance improved more in the cooling conditions than the vapor injection cycle; however, the vapor injection cycle's performance improved more dramatically in the heating conditions. The SLHX cycle's performance improved in cooling mode as the temperature increased, but deteriorated as the temperature dropped in heating mode.

Table 55: Advanced Cycle Options Prorated Power Consumption

Temperature Bin (°C)	SLHX	Expander	Ejector	Vapor Injection
18.3-21.1	1.54%	-2.74%	-11.08%	-5.12%
21.1-23.8	1.52%	-3.66%	-10.35%	-6.68%
23.9–26.6	1.68%	-4.29%	-10.02%	-7.90%
26.7-29.3	1.52%	-5.16%	-9.62%	-9.43%
29.4–32.1	1.20%	-5.94%	-9.40%	-10.78%
32.2-34.9	0.91%	-6.60%	-9.21%	-12.06%
35–37.7	0.39%	-7.54%	-9.18%	-13.54%
37.8-40	-0.18%	-8.38%	-9.23%	-15.06%
Heating Temperature Bins (°C)	SLHX	Expander	Ejector	Vapor Injection
15.6-18.2	2.00%	-3.00%	-5.59%	-7.65%
12.8-15.5	2.06%	-2.91%	-5.76%	-7.98%
10-12.7	2.08%	-2.90%	-5.94%	-8.39%
7.2-9.9	2.11%	-2.87%	-6.11%	-8.77%
4.4-7.1	2.16%	-2.81%	-6.43%	-9.17%
1.7-4.3	2.29%	-2.52%	-6.02%	-9.22%
(-1.1)-1.6	2.37%	-2.43%	-6.42%	-9.76%
(-3.9)-(- 1.2)	2.44%	-2.33%	-6.81%	-10.43%
(-6.7)-(-4.0)	2.56%	-2.19%	-7.29%	-11.14%
(-9.4) - (-6.6)	2.61%	-2.11%	-7.88%	-12.04%
(-12.2) - (-9.5)	2.68%	-2.07%	-8.28%	-12.79%
(-15) - (-12.3)	2.78%	-1.96%	-8.69%	-13.64%
(-17.8)-(-15.1)	2.85%	-1.84%	-9.16%	-14.56%
(-20.6) - (-17.9)	2.87%	-1.74%	-9.74%	-15.65%
(-23.3) - (-20.7)	3.01%	-1.57%	-10.36%	-16.90%
(-26.1) - (-23.4)	3.05%	-1.46%	-11.11%	-18.39%
(-28.3) - (-26.2)	3.13%	-1.21%	-12.04%	-20.14%
(-28.4) and Below	3.34%	-0.87%	-13.05%	-22.24%

The change in energy consumption was then applied to the energy consumption of the baseline cycle in the IIR LCCP excel tool for each advanced cycle option in each of the five different climate zones in the U.S. The unit assumptions in Table 52 were used to describe the unit. The other components of LCCP were held constant for this calculation. In Table 56, a negative value indicates a reduction in

LCCP from the baseline VCC model and a positive value indicates an increase in LCCP from the baseline VCC model.

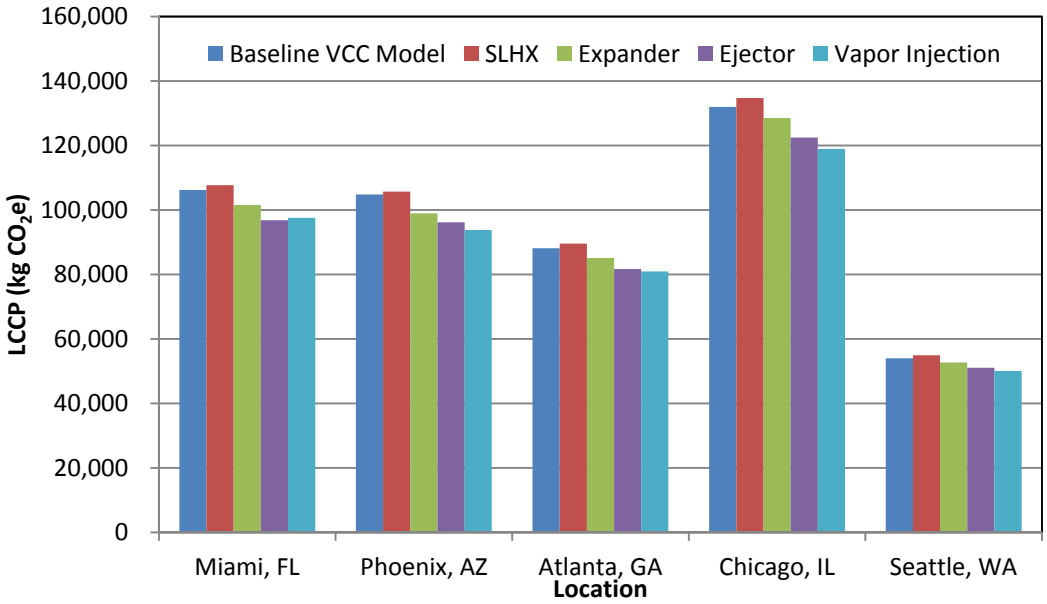

Figure 48: Advanced Cycle Option LCCP Results Comparison

Chicago, IL shows the largest decrease in LCCP. There is a decrease of 2.6% for expander cycle, 7.2% for ejector cycle and a 9.9% decrease for the vapor injection cycle. This city's LCCP was the most heavily dependent on energy consumption, especially heating. Seattle, WA showed the smallest reduction in LCCP because of its mild climate. The energy consumption of the unit is a much smaller percentage of the total emissions.

Table 56: LCCP Reduction Achieved by Advanced Cycle

Cycle	Miami, FL	Phoenix, AZ	Atlanta, GA	Chicago, IL	Seattle, WA
SLHX	1.4%	0.8%	1.6%	2.1%	1.7%
Expander	-4.4%	-5.6%	-3.5%	-2.6%	-2.4%
Ejector	-8.8%	-8.2%	-7.3%	-7.2%	-5.4%
VI-FT	-8.2%	-10.5%	-8.2%	-9.9%	-7.3%

The ejector cycle was slightly more effective in reducing LCCP for Miami, FL because Miami's climate is dominated by cooling hours in the extreme temperature bins. In these bins, the ejector cycle has a slight advantage over the vapor injection cycle. For all other locations the vapor injection cycle achieved the highest reduction in LCCP.

The expander cycle, the ejector cycle and the vapor injection cycle were effective in reducing the LCCP of the unit in all locations. The vapor injection cycle was the most effective of the options evaluated. The expander cycle reduced the LCCP of the unit by the smallest amount. The suction line heat exchanger cycle was not effective in reducing LCCP for the unit modeled.

Chapter 7 : Recommendations for LCCP Minimization

Another avenue to be considered in reducing LCCP is combining the benefits of advanced cycle options with low GWP refrigerants. Both of these options are necessary to achieve more significant reductions in LCCP.

7.1 Applying Low GWP refrigerants to Advanced Cycles Approach

A range of GWP values that are representative what the refrigerants are currently available were chosen for this study. These GWP values were substituted for the basic VCC and each advanced cycle option for all five locations. The results of each cycle were evaluated as compared to the baseline cycle. As a baseline, the basic VCC model's GWP values were substituted for the selected range of values. The percentage difference between the LCCP of the baseline VCC with R-410A as a refrigerant was determined.

7.2 Applying Low GWP refrigerants to Advanced Cycles Results

The reduction in LCCP for each cycle for the range of GWP values was determined. The results varied greatly depending on the location.

Miami, FL were compared to the baseline VCC with R-410A as the refrigerant. When the GWP of the refrigerant is reduced to 10 and the vapor injection cycle is used, a 16.2% decrease in LCCP can be achieved. The ejector cycle is slightly more effective in Miami, FL because of its more dramatic improvement in the high temperature bins than the vapor injection cycle.

Table 57: % Difference in LCCP versus Baseline VCC for Miami, FL

GWP	10	100	500	1000
Baseline VCC	-8.0%	-7.6%	-5.9%	-3.8%
SLHX	-6.6%	-6.2%	-4.6%	-2.4%
Expander	-12.4%	-12.1%	-10.4%	-8.2%
Ejector	-16.9%	-16.5%	-14.8%	-12.7%
VI	-16.2%	-15.8%	-14.1%	-12.0%

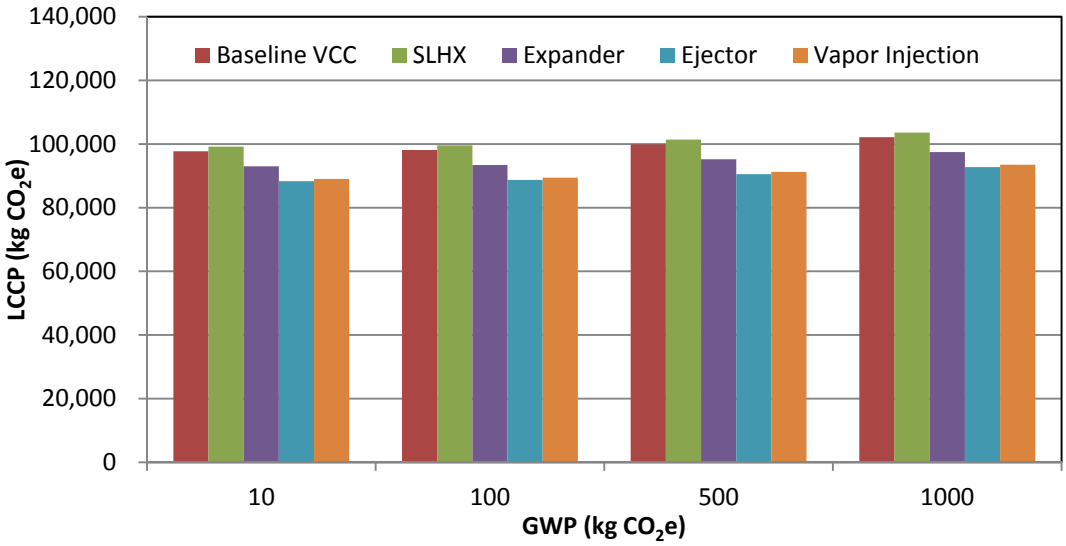

Figure 49: Comparison of LCCP for Low GWP and Advanced Cycle Options in Miami

The results for Phoenix, AZ were compared to the baseline VCC with R-410A as the refrigerant. When the GWP of the refrigerant is reduced to 10 and the vapor injection cycle is used, an 18.6% decrease in LCCP can be achieved.

Table 58: % Difference in LCCP versus Baseline VCC for Phoenix, AZ

GWP	10	100	500	1000
Baseline VCC	-8.1%	-7.7%	-6.0%	-3.9%
SLHX	-7.3%	-6.9%	-5.2%	-3.0%
Expander	-13.7%	-13.3%	-11.6%	-9.5%
Ejector	-16.3%	-16.0%	-14.2%	-12.1%
VI	-18.6%	-18.2%	-16.5%	-14.4%

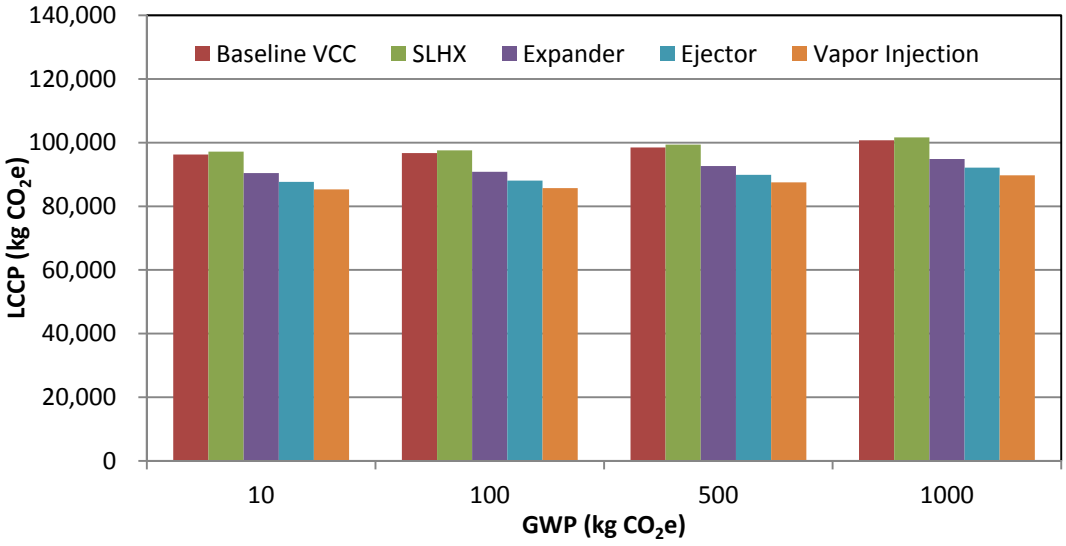

Figure 50: Comparison of LCCP for Low GWP and Advanced Cycle Options for Phoenix

The results for Atlanta, GA were compared to the baseline VCC with R-410A as the refrigerant. When a refrigerant with a GWP of 10 is combined with the vapor injection cycle a 17.8% decrease in the LCCP can be achieved.

Table 59: % Difference in LCCP versus Baseline VCC for Atlanta, GA

GWP	10	100	500	1000
Baseline VCC	-9.7%	-9.2%	-7.2%	-4.6%
SLHX	-8.0%	-7.6%	-5.5%	-3.0%
Expander	-13.1%	-12.7%	-10.6%	-8.1%
Ejector	-17.0%	-16.5%	-14.5%	-11.9%
VI	-17.8%	-17.4%	-15.3%	-12.8%

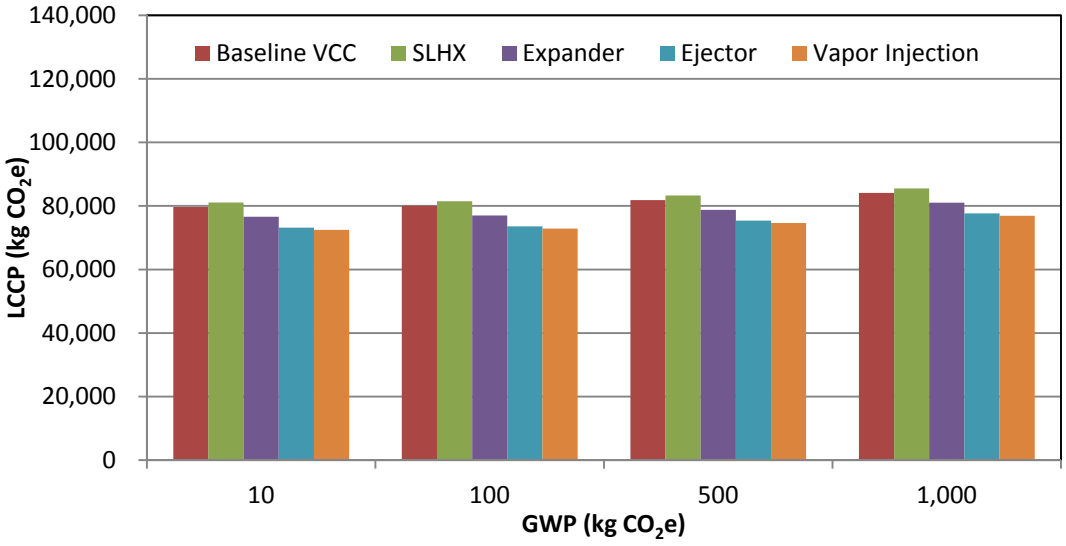

Figure 51: Comparison of LCCP for Low GWP and Advanced Cycle Options in Atlanta

The results for Atlanta, GA were compared to the baseline VCC with R-410A as the refrigerant. When a refrigerant with a GWP of 10 is combined with the vapor injection cycle a 16.3% decrease in the LCCP can be achieved.

Table 60: % Difference in LCCP versus Baseline VCC for Chicago, IL

GWP	10	100	500	1000
Baseline VCC	-6.5%	-6.1%	-4.8%	-3.1%
SLHX	-4.3%	-4.0%	-2.6%	-0.9%
Expander	-9.0%	-8.7%	-7.3%	-5.6%
Ejector	-13.6%	-13.3%	-12.0%	-10.3%
VI	-16.3%	-16.0%	-14.6%	-12.9%

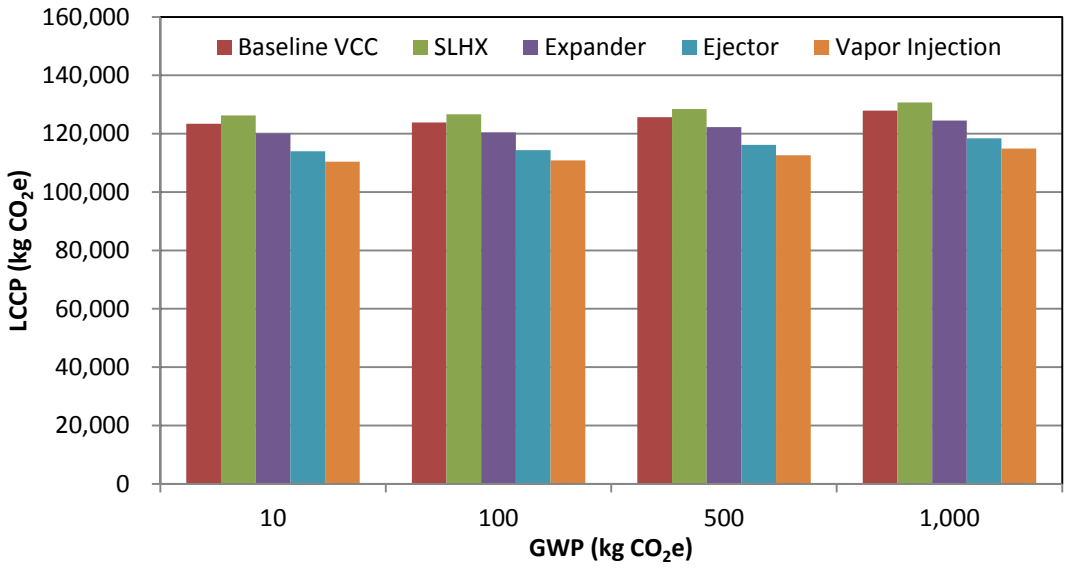

Figure 52: Comparison of LCCP for Low GWP and Advanced Cycle Options in Chicago

The results for Seattle, WA were compared to the baseline VCC with R-410A as the refrigerant. When a refrigerant with a GWP of 10 is combined with the vapor injection cycle a 23.0% decrease in the LCCP can be achieved.

Table 61: % Difference of LCCP versus Baseline VCC for Seattle, WA

GWP	10	100	500	1000
Baseline VCC	-15.8%	-15.0%	-11.7%	-7.5%
SLHX	-14.0%	-13.3%	-9.9%	-5.8%
Expander	-18.2%	-17.4%	-14.1%	-9.9%
Ejector	-21.2%	-20.5%	-17.1%	-13.0%
VI	-23.0%	-22.3%	-18.9%	-14.8%

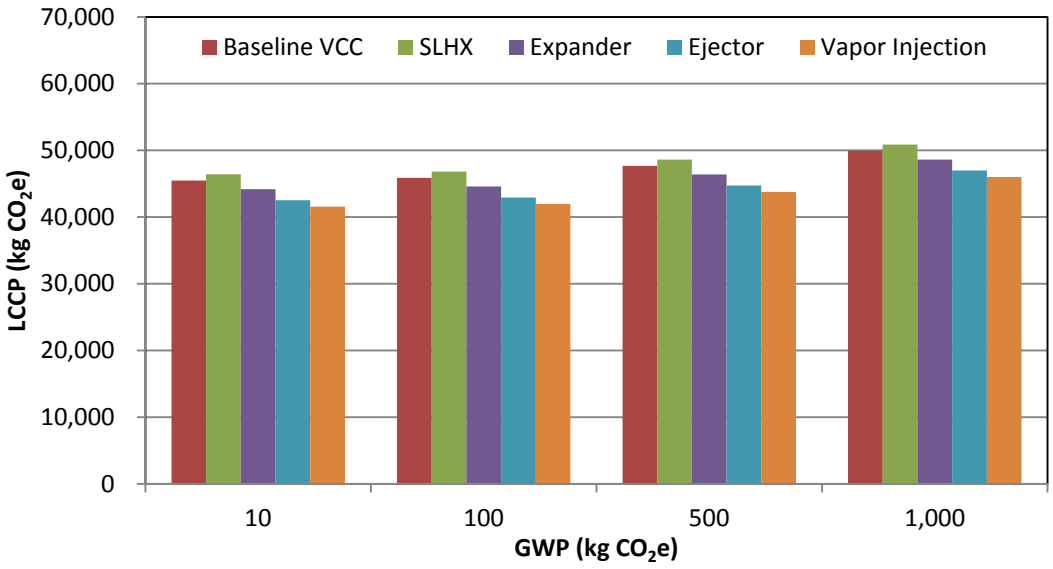

Figure 53: Comparison of LCCP for Low GWP and Advanced Cycle Options in Seattle

The combination of the use of low GWP refrigerant and the use of advanced cycle is effective in reducing LCCP of the unit modeled by up to 23%. Since, heating and cooling comprise of 54% of the energy usage in residential buildings [1], this would dramatically reduce the electricity demand for these buildings from current levels.

7.3 DOE Energy Reduction Goals

The U. S. Department of Energy set a goal of reducing residential energy consumption by 40% from 2010 levels by 2025 [89]. To reach this goal for heating and cooling of the home, a combination of energy efficiency and reduction in GWP of the refrigerants used must be undertaken. The current technology can achieve 16 - 23% decrease in energy used for space conditioning using a refrigerant with a GWP of 10 and the vapor injection cycle depending on the location of the unit. This is

approximately half way to the target if a proportional decrease is achieved in all other categories of residential energy use.

A study was conducted to determine the amount of reduction that is needed to achieve this 40% decrease in LCCP for household HVAC units. The same unit used as a baseline for the advanced cycle modeling was used for this analysis. The GWP values and the energy consumption values were varied for each location. The results are shown in Figure 54 through Figure 58 for each of the locations previously analyzed.

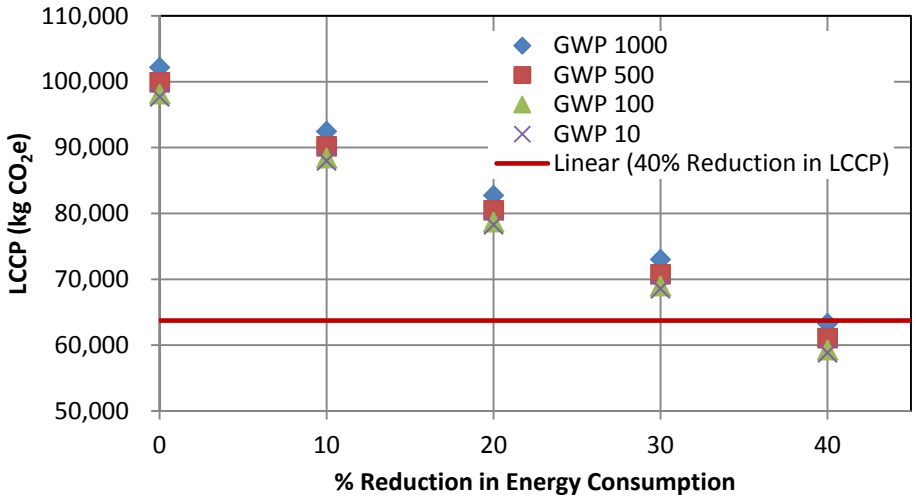

Figure 54: LCCP Reduction Comparison for Miami

In Miami, FL, energy consumption and GWP both need to be reduced dramatically to achieve the desired goal of 40% reduction in LCCP. Energy consumption decreases of 39.5%, 37.4%, 35.4%, and 35% are required for GWP values of 1,000, 500, 100, and 10, respectively. The required energy consumptions reduction is approximately four times what was modeled for the vapor injection cycle.

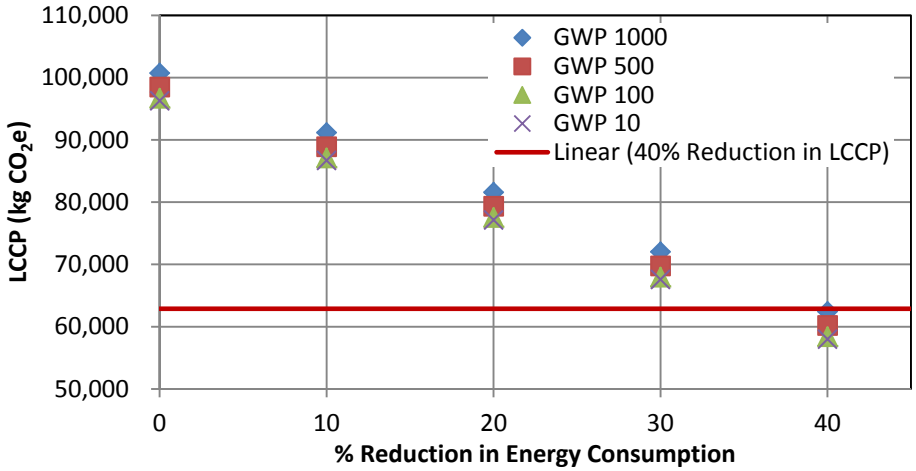

Figure 55: LCCP Reduction Comparison for Phoenix

In Phoenix, AZ, similar results to Miami, FL were observed. The energy consumption and GWP both need to be reduced dramatically to achieve the desired goal. Energy consumption decreases of 39.7%, 37.2%, 35.3%, and 34.8% are required for GWP values of 1,000, 500, 100, and 10, respectively. These decreases are approximately 3.5 to 4 times the energy consumption decrease achieved by the most effective advanced cycle option, vapor injection.

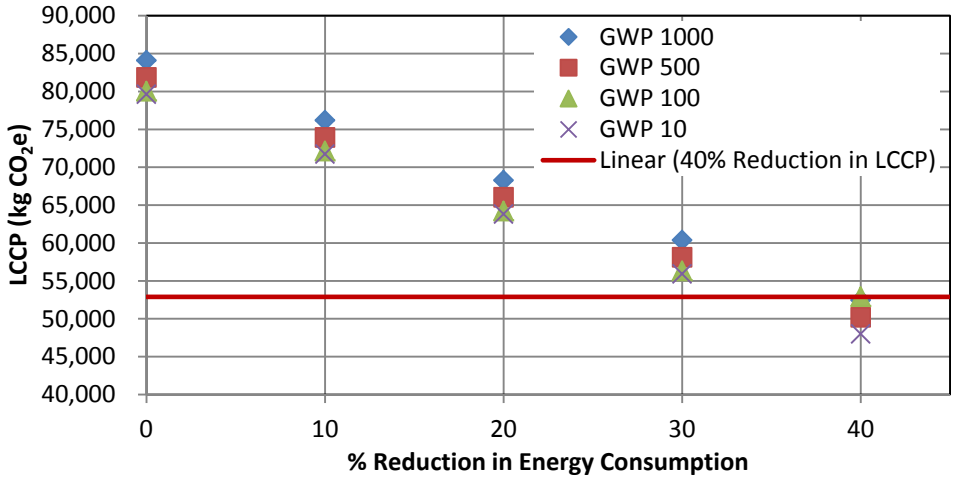

Figure 56: LCCP Reduction Comparison for Atlanta

In Atlanta, GA, energy consumption decreases of 39.5%, 36.6%, 34.7%, and 33.8% are required for GWP values of 1,000, 500, 100, and 10 respectively. These decreases are much higher than those that can be achieved with the advanced cycles evaluated in Chapter 6.

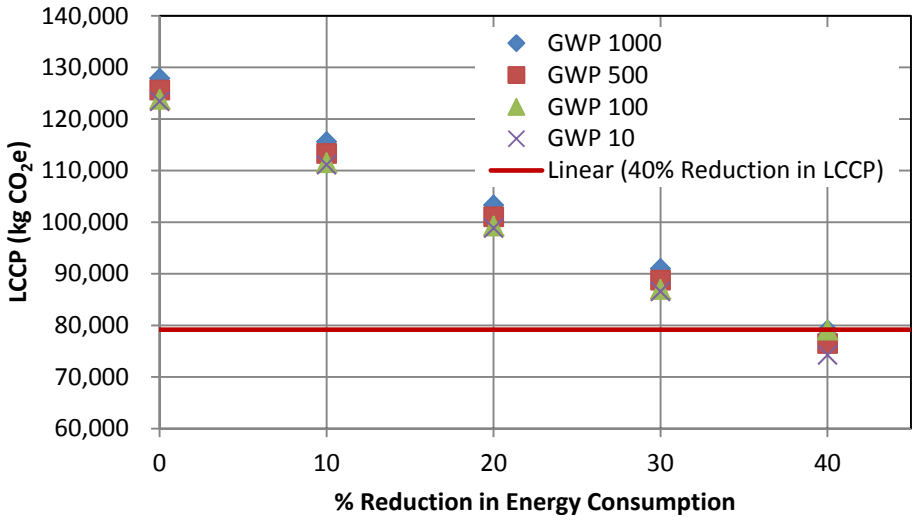

Figure 57: LCCP Reduction Comparison for Chicago

Similar results to Miami and Atlanta were calculated in Chicago, IL. Energy consumption decreases of 39.7%, 37.8%, 36.4%, and 36% are required for GWP values of 1,000, 500, 100, and 10, respectively.

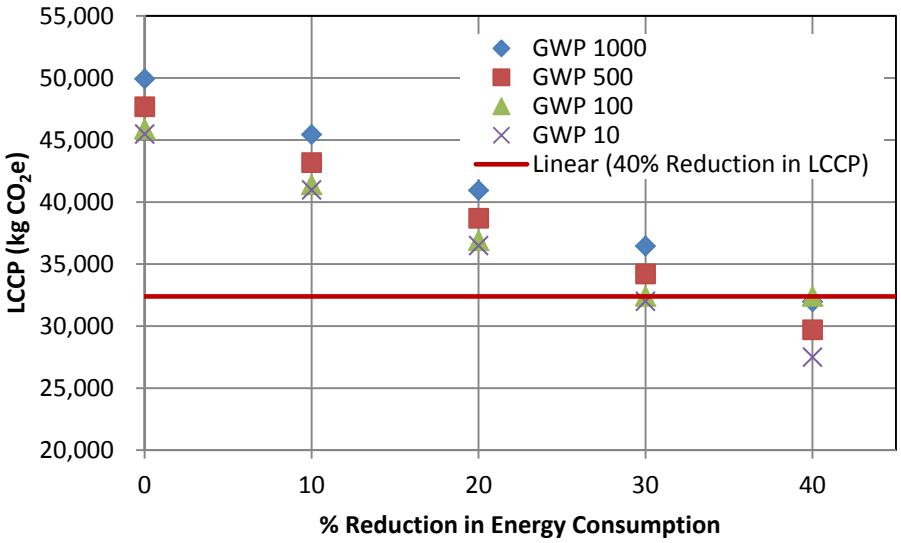

Figure 58: LCCP Reduction Comparison for Seattle

In Seattle, WA, energy consumption decreases of 38.1%, 34.1%, 30%, and 29.9% are required for GWP values of 1,000, 500, 100, and 10, respectively. These lower reductions were achieved in Seattle because of the city's mild climate. Direct emissions have much more influence on the LCCP total in Seattle than they do in Chicago or Phoenix. However the required energy consumption reduction is still approximately three times what can be achieved using the vapor injection cycle as modeled.

Table 62: % Energy Consumption Reduction versus GWP Value Required for 40% LCCP Reduction

GWP (kg CO_2e)	Miami, FL	Phoenix, AZ	Atlanta, GA	Chicago, IL	Seattle, WA
1000	39.5	39.7	39.5	39.7	38.1
500	37.4	37.2	36.6	37.8	34.1
100	35.4	35.3	34.7	36.4	30
10	35	34.8	33.8	36	29.9

The results of this analysis are summarized in Table 62. The minimum amount the energy consumption must be reduced by is 29.9% in Seattle for a refrigerant with a GWP of 10. The highest amount the energy consumption must be reduced by is 39.5% from the baseline VCC using R-410A using a refrigerant with a GWP of 1,000. A combination of reduction in GWP and reduction in energy consumption is essential to meet the DOE proposed goal of 40% reduction in residential energy consumption. More efficient cycle than those currently is necessary to achieve this goal.

Chapter 8 Conclusions

Summary of Accomplishments

The work described in this thesis resulted in a number of accomplishments. They are enumerated below:

- A harmonized equation for LCCP was developed which combined the efforts of previous researchers.
- Traceable data sources were established for all aspects of the LCCP calculation using governmental agency, trade organizations and other researchers.
- Sensitivity studies were conducted on all aspects of LCCP including leakage rates, energy consumption, and manufacturing emissions rates.
- Energy consumption was determined to be the most influential component of LCCP followed by the annual leakage rates.
- An Excel based tool was developed for single speed residential heat pump calculations. The tool evaluates the unit in five different climate zones in the United States using the developed equation and the AHRI 210/240 Std. for the energy calculation.
- The LCCP Guideline was published by IIR in January 2016.
- An IIR Informational Note was developed to inform IIR members about the LCCP Guideline and recommendations for the use of LCCP

- A paper for the 2016 Purdue conference was written and accepted about the development and use of LCCP.
- Four advanced cycles and the basic VCC were modeled using Engineering Equation Solver. The advanced cycles included: the suction line heat exchanger cycle, the expander cycle, the ejector cycle and the vapor injection flash tank cycle.
- The expander cycle, the ejector cycle and the vapor injection flash tank cycle were determined to be effective in reducing LCCP with vapor injection being the most effective.
- The LCCP reduction that can be achieved with the combination of advanced cycle options and low GWP options were calculated
- The GPW and energy consumption reductions required to achieve the DOE goal of 40% reduction in residential energy consumption were calculated.

Conclusions

The LCCP guideline was published by IIR in January 2016 and is available on their website. An excel tool was created for residential heat pumps using AHRI Std 210/240 for five climate zones in the United States. This tool will be further expanded to include international locations and standards. An informatory note for IIR was developed about the use of the LCCP guideline and recommendations on reducing a system's LCCP.

For the residential heat pump case study, it can be concluded that energy consumption is the main contributor to total lifetime emissions. When the calculation

is done for a more temperate the climate, such as Seattle, WA, direct emissions will have a larger impact on the system however energy consumption will still have the most impact. From this study it was determined that the most effective way to reduce emissions is to increase the energy efficiency of the unit.

Further sensitivity studies were conducted on the unit. The annual leakage percentages, the energy consumption, the manufacturing emissions were varied individually over a range of GWP values. Energy consumption was the most influential component of LCCP followed by annual leakage rate. The energy consumption becomes more dominant the lower the GWP value is.

Four advanced vapor compression cycles were modeled and analyzed. The expander cycle, ejector cycle and the vapor injection cycles show significant improvement in LCCP for residential heat pump applications while the suction line heat exchanger is not effective using R410A. The expander cycle reduces energy consumption by 3.3 to 5.5%. The ejector cycle reduces energy consumption by 4.2 to 5.1% and increases capacity by 1.5 to 5.5%. The vapor injection cycle increases capacity by 12 to 19.6%. This increase in capacity reduces the size of the unit needed to cool the same space. This results in a decrease of 10.5% for Phoenix and a 9.9% decrease for Chicago, IL for LCCP. The vapor injection was the most effective cycle. It reduced the LCCP of Chicago IL by 15.9% and 15.3% for Miami, FL.

The advanced cycles modeled were combined with low GWP refrigerants to determine the reduction in LCCP. The use of a refrigerant with a GWP of 10 combined with the vapor injection cycle yielded 16.2%- 23% reduction in LCCP depending on the location of the unit. This falls short of the DOE goal of 40%

reduction in electricity usage in residential buildings. The unit modeled would require between 39% - 29% reduction in energy consumption depending on the location in addition to the use of a refrigerant with a GWP of ten to attain this goal with a proportional decrease in all other categories of residential energy usage. Additional research into advanced cycles and refrigerant options is necessary to achieve the DOE goal.

Bibliography

1. U.S. Energy Information Administration, “Annual Energy Outlook 2015 with Projections to 2040.” April 2015.
2. International Institute of Refrigeration Working Group on LCCP Evaluation. http://www.iifiir.org/medias/medias.aspx? INSTANCE= EXPLOITATION &PORT AL _ID = portal_model_instance__WP_LCCP_Evaluation.xml.
3. ADL (A.D. Little, Inc), 1999: Global Comparative Analysis of HFC and Alternative Technologies for Refrigeration, Air Conditioning, Foam, Solvent, Aerosol Propellant, and Fire Protection Applications. Final Report to the Alliance for Responsible Atmospheric Policy, August 23, 1999, Acorn Park, Cambridge, Massachusetts, USA.
4. Zhang, M., Muehlbauer, J., Aute, V. and Radermacher, R., 2011, Life Cycle Climate Performance Model for Residential Heat Pump System, Air-Conditioning, Heating and Refrigeration Technology Institute, Inc. (AHRTI).
5. Sand, J.R., S.K. Fischer and V.D. Baxter, 1997: Energy and Global Warming Impacts of HFC Refrigerants and Emerging Technologies, U.S. Department of Energy and AFEAS, Arlington, Va, USA.
6. Papasavva, S., Hill, W. R. and Andersen, S. O., 2010. GREEN-MAC-LCCP: A Tool for Assessing the Life Cycle Climate Performance of MAC Systems. Environmental Science & Technology, 44(19), pp. 7666-7672.
7. GREEN-MAC-LCCP program, version 3b (http://www.epa.gov/cppd/mac/compare.htm). Accessed October 2014.

8. Abdelaziz, O., Fricke, B. and Vineyard, E., 2012, "Development of Low Global Warming Potential Refrigerant Solutions for Commercial Refrigeration Systems using a Life Cycle Climate Performance Design Tool. 14th International Refrigeration and Air Conditioning Conference", Purdue University, West Lafayette, Indiana.
9. Oak Ridge National Laboratory (ORNL), and the University of Maryland College Park (UMCP), 2013. LCCP Desktop Application v1 Engineering Reference. (http://info.ornl.gov/sites/publications/Files/Pub49128.pdf).
10. UNEP/TEAP report, 1999. "The Implications to the Montreal Protocol of the Inclusion of HFCs and PFCs in the Kyoto Protocol".
11. Kyoto Protocol to the United Nations Framework Convention on Climate Change, 1997.
12. EN 378 European Standard "Refrigerating systems and heat pumps-Safety and environmental requirements". 2012.
13. McQuiston, F. C., and Parker, J., *Heating, Ventilating and Air-Conditioning*, 6th ed., John Wiley and Sons, ISBN 0-471-47015-5.
14. Park, C., Lee, H., Hwang, Y., Radermacher, R., 2015. Recent advances in vapor compressions cycle technologies. Int. J. Refrigeration 60, 118-134.
15. U.S. Energy Information Administration. "International Energy Outlook 2013." July 2013.
16. ANSI/AHRI Standard 210/240 with Addenda 1 and 2 Standard for Performance Rating of Unitary Air-Conditioning & Air-Source Heat Pump Equipment , 2008.

17. Beshr, M., Aute, V., Fricke B., and Radermacher, R. “An Evaluation of the Environmental Impact of Commercial Refrigeration Systems Using Alternative Refrigerants.” 3rd IIR International Conference on Sustainability and the Cold Chain, London, 2014.
18. Beshr, M., ORNL Life Cycle Climate Performance—V1.0, http://lccp.umd.edu/ornllccp/ , 2014.
19. Pac Calc Pro, http://en.ipu.dk/Indhold/refrigeration-and-energy-technology/Pack%20Calculation%20Pro/Pack%20Calculation%20Pro.aspx.
20. Hwang, Y., Jin, D., and Radermacher, R., 2007, “Comparison of R-290 and two HFC blends for walk-in refrigeration systems.” Int. J. of Refrigeration 30, pg. 633-641.
21. Chen, W. 2008, “A comparative study on the performance and environmental characteristics of R410A and R22 residential air conditioners.” Applied Thermal Engineering 28, pg. 1-7.
22. Beshr, M., Aute, V., Sharma, V., Abdelaziz, O., Fricke, B., and Radermacher, R., 2015, “A comparative study on the environmental impact of supermarket refrigeration systems using low GWP refrigerants.” Int. J. of Refrigeration 56, pg. 154-164.
23. Li , G., 2015, “Comprehensive investigations of life cycle climate performance of packaged air source heat pumps for residential application.” Renewable and Sustainable Energy Reviews 43, pg. 702-710.
24. ASHRAE, 2013 ASHRAE Handbook: Fundamentals. 2013.

25. Alabdulkarem, A., Eldeeb, R., Hwang, Y., Aute, V., and Radermacher, R., 2015, "Testing, simulation and soft-optimization of R410A low-GWP alternatives in heat pump system." Int. J. Refrigeration 60, pg. 106-117.
26. Hermes, C., 2015, "Refrigerant charge reduction in vapor compression refrigeration cycles via liquid-to-suction heat exchange." IIR 52, pg 93-99.
27. Fernandez, N., Hwang, Y., Radermacher, R., 2010, "Comparison of CO2 heat pump water heater performance with baseline cycle and two high COP cycles." Int. J. Refrigeration 33, pg. 635-644.
28. Preissner, M., 2001, *Carbon Dioxide Vapor Compression Cycle Improvements with Focus on Scroll Expanders.* Unpublished Phd dissertation. University of Maryland, College Park, Maryland.
29. She, X., Yin, Y., Zhang, X., 2014, "A proposed subcooling method for vapor compression refrigeration cycle based on expansion power recovery." Int. J. Refrigeration 43, pg. 50-61.
30. Moles, F., Navarro-Esbrı´, J., Peris, B., et al., 2014, Theoretical energy performance evaluation of different single stage vapour compression refrigeration configurations using R1234yf and R1234ze(E) as working fluids
31. Yang, J., Mab, Y., Liu, S., 2007, "Performance investigation of transcritical carbon dioxide two-stage compression cycle with expander." Energy 33, pg.237-245.
32. Naduvath, M., 1999, *Investigation of Single and Two-Phase Flow Ejectors.* Unpublished Phd Dissertation, University of Maryland, College Park, MD.

33. Wang, X., Yu, J., Zhou, M., Lv, X., 2014, Comparative studies of ejector-expansion vapor compression refrigeration cycles for applications in domestic refrigerator-freezers." Energy 70, pg. 635-642.
34. Li, H., Cao, F., Bu, X., Wang, L., and Wang, X., 2014, "Performance characteristics of R1234yf ejector-expansion refrigeration cycle." Applied Energy 121, pg. 96–103.
35. Wang, X., Hwang, Y., and Radermacher, R., 2009, "Two-stage heat pump system with vapor-injected scroll compressor using R410A as a refrigerant." Int. J. Refrigeration 32, pg 1442–1451.
36. Xu, X., Hwang, Y., Radermacher, R., 2011. Rrefrigeration injection of heat pumping/air-conditioning systems: literature review and challenges and discussions. Int. J. Refrigeration 34, 402-215.
37. Redón, A., Navarro-Peris, E., Pitarch, M., Gonzálvez-Macia, J., Corberán, J., 2013, "Analysis and optimization of subcritical two-stage vapor injection heat pump systems." Applied Energy 124, pg. 231–240.
38. Shuxue, X., Guoyuan, M., Qi, L., and Zhongliang, L., 2013, "Experiment study of an enhanced vapor injection refrigeration/heat pump system using R32." Int. J. of Thermal Sciences 68, pg. 103-109.
39. Xu, X., Hwang, Y., Radermacher, R., 2013. Performance comparison of R-410A and R-32 in vapor injection cycles. Int. J. Refrigeration 36, 892-903.
40. He, Y., Cao, F., Jin, L., Wang, X., Xing, Z., 2015, "Experimental study on the performance of a vapor injection high temperature heat pump." Int. J. of Refrigeration 60, pg. 1-8.

41. Baek, C., Heo, J., Jung, J., Lee, E., and Kim, Y., 2014, "Effects of vapor injection techniques on the heating performance of a CO2 heat pump at low ambient temperatures." Int. J. of Refrigeration 43, pg. 26-35.
42. International Institute of Refrigeration Working Group on LCCP Evaluation. *Guideline for Life Cycle Climate Performance*. 2016.
43. U.S. Energy Information Administration, "Glossary", http://www.eia.gov/tools/glossary/index.cfm?id=G, 2015.
44. Intergovernmental Panel on Climate Change (IPCC), 2014, Fifth Assessment Report: Climate Change, Geneva, Switzerland.
45. Intergovernmental Panel on Climate Change (IPCC), 2007, Fourth Assessment Report: Climate Change, Geneva, Switzerland.
46. Baral, A, Minjares, R., and Urban, R., Upstream Climate Impacts from Production of R-134a and R-1234yf refrigerants used in Mobile Air Conditioning Systems. International Council on Clean Transportation, Aug. 2013.
47. UNEP, 2003c: 2002 Report of the Refrigeration, Air Conditioning and Heat Pumps Technical Options Committee – 2002 Assessment. [L. Kuijpers (ed.)]. UNEP Ozone Secretariat, Nairobi, Kenya.
48. U.S. EPA, "Complying with the Section 608 of the Refrigerant Recycling Act." http://www.epa.gov/Ozone/title6/608/608fact.html
49. International Organization for Standardization (ISO), www.iso.org/home.htm.
50. American Society of Heating, Refrigerating and Air-Conditioning Engineers, https://www.ashrae.org/home.

51. Air Conditioning, Heating, and Refrigeration Institute (AHRI), http://www.ahrinet.org/site/1/Home.
52. EN 14825 (2013) Air conditioners, liquid chilling packages and heat pumps, with electrically driven compressors, for space heating and cooling. Testing and rating at part load conditions and calculation of seasonal performance.
53. International Weather for Energy Calculations Version 2.0, 2012 ASHRAE, Atlanta GA.
54. NREL - National Solar Radiation Data Base - TMY3 Data, January 2011 (http://rredc.nrel.gov/solar/old_data/nsrdb/1991-2005/tmy3/).
55. Wilcox, S. and W. Marion. 2008. User's Manual for TMY3 Data Sets, NREL/TP-581-43156. April 2008. Golden, Colorado: [National Renewable Energy Laboratory.
56. Energy Data Sources, U. S. Department of Energy, Feb. 2014 http://apps1.eere.energy.gov/buildings/energyplus/weatherdata_sources.cfm.
57. International Energy Agency, http://data.iea.org/ieastore/product.asp?dept_id=101&pf_id=305.
58. Deru, M. and Torcellini, P., 2007, Source Energy and Emission Factors for Energy Use in Buildings, Technical Report NREL/TP-550-38617.
59. International Energy Administration. "Worldwide Trends in Energy Use and Efficiency, 2008" 2008.
60. Ecometrica (2011). Electricity-specific emission factors for grid electricity.
61. Steel's Contribution to a Low Carbon Future: WorldSteel Position Paper. 2014 World Steel Association.

62. IPCC TEAP, “IPCC/TEAP Special Report: Safeguarding the Ozone Layer and the Global Climate System.” 2009.

63. Simonsen, M., 2009, “Energy Requirements and CO2 Emissions from Manufacturing and Maintenance of Locomotives and Trains”. (http://vfp1.vestforsk.no/sip/pdf/Jernbane/Train Manufacturing.pdf)

64. Wyns, Tomas, “The Low Carbon Future of European Steel Sector.” Presentation to European Union Parliament Sep. 2012. Center for Clean Air Policy. http://ccap.org/resource/the-low-carbon-future-of-the-european-steel-sector/.

65. Chang-ping, Hu et. al. “Emissio Mitigation of CO2 in Steel Industry: Current Status and Future Scenarios.” Journal of Iron and Steel Research International. 2006, 13(6) pg 38-42.

66. Chunbao (Charles) XU, Da-qiang CANG, A Brief Overview of Low CO2 Emission Technologies for Iron and Steel Making, Journal of Iron and Steel Research, International, Volume 17, Issue 3, March 2010, Pages 1-7, ISSN 1006-706X, http://dx.doi.org/10.1016/S1006-706X(10)60064-7. (http://www.sciencedirect.com/science/article/pii/S1006706X10600647).

67. California Environmental Protection Agency. “Method for Estimating Greenhouse Gas Emission Reductions from Recycling.” November 14, 2011.

68. U.S. Energy Requirements for Aluminum Production BCS Report prepared for DOE, Feb 2007.

69. U. S. Department of Energy. “Energy and Environmental Profile of the U. S. Aluminum Industry.” Prepared by Energetics Inc. July 1997.

70. International Aluminum Institute, “Global Life Cycle Inventory Data for the Primary Aluminum Industry: 2010 Data. World Aluminum, August 2013.
71. “Aluminum the Element of Sustainability: A North American Aluminum Industry Sustainability Report.” The Aluminum Association, September 2011.
72. International Copper Study Group. “The World Copper Factbook 2014.” 2014 http://copperalliance.org/wordpress/wp-content/uploads/2012/01/ICSG-Factbook-2014.pdf
73. “The Environmental Profile of Copper Products: A Cradle to Gate Life-Cycle Assessment for Copper Tube, Sheet and Wire Produced in Europe.”, European Copper Institute Copper Alliance, 2012.
74. U. S. Environmental Protection Agency. “Streamlined Life-Cycle Greenhouse Gas Emission Factors for Copper Wire.” June, 2005.
75. International Copper Association, Ltd. “Copper.” 2000.
76. Franklin Associates report prepared for the American Chemistry Council , July 2014, “Cradle-To-Gate Life Cycle Inventory of Nine Plastic Resins and Four Polyurethane Precursors”.
77. EPA “Plastics” U. S. Environmental Protection Agency, Waste Reduction Model Version 13. June 2014.
78. PlasticsEurope. Eco-profiles of the European Plastics Industry: HDPE bottles. March 2005 http://lca.plasticseurope.org/main2.htm.
79. Banks, R. and Sharratt, P., “Environmental Impacts of the Manufacture of HFC-134a.” 07 Nov. 1996.

80. Spatz, M.W., Motta, S.F.Y., 2004. “An evaluation of options for replacing HCFC-22 in medium temperature refrigeration systems”. International Journal of Refrigeration, Volume 27, Issue 5, pp. 475-483.
81. Hill, W., Papasavva, S., 2005. “Life Cycle Analysis Framework; a Comparison of HFC-134a, HFC-134a Enhanced, HFC-152a, R744, R744 Enhanced, and R290 Automotive Refrigerant Systems”. SAE Technical Series Paper, 2005-01-1511, Society of Automotive Engineers, Warrendale, PA.
82. “IIR-LCCP-EmissionsDatabase_Version1.exp” University of Maryland Department of Mechanical Engineering ACTA Consortium. 2014.
83. EPA, “Metals.” U. S. Environmental Protection Agency, Waste Reduction Model Version 13. June 2014.
84. EPA “Plastics” U. S. Environmental Protection Agency, Waste Reduction Model Version 13. June 2014.
85. Goodman, “SSZ16 High Efficiency Split System Heat Pump Product Specifications,” 2014.
86. International Institute of Refrigeration Working Group on LCCP, *IIR LCCP Working Group Calculation Tool*, 2016.
87. Goodman, “SSZ14 High Efficiency Split System Heat Pump Product Specifications,” 2015.
88. Akabdulkarem, A., Hwang, Y., and Radermacher, R., “Test Report #20 System Drop-In Tests of Refrigerants R-32, D2Y-60, and L-41a in Air Source Heat Pump.” Prepared for AHRI Low-GWP AREP. AHRI, 2013.Amrane, K., Overview of AHRI Research on Low-GWP Refrigerants, 2013

89. U. S. Dept. of Energy, Residential Building Integration.

http://energy.gov/eere/buildings/residential-buildings-integration.